

University of Alberta

**A STUDY OF THE GAS-LIQUID REACTION SYSTEM OF
HYDROGEN SULFIDE AND SULFURIC ACID**

By

HUI WANG



A thesis submitted to the Faculty of Graduate Studies and Research in partial fulfillment
of the requirements for the **Doctor of Philosophy**

in

Chemical Engineering

Department of Chemical and Materials Engineering

Edmonton, Alberta

Spring 2003

National Library
of Canada

Acquisitions and
Bibliographic Services

395 Wellington Street
Ottawa ON K1A 0N4
Canada

Bibliothèque nationale
du Canada

Acquisitons et
services bibliographiques

395, rue Wellington
Ottawa ON K1A 0N4
Canada

Your file *Votre référence*
ISBN: 0-612-82178-1
Our file *Notre référence*
ISBN: 0-612-82178-1

The author has granted a non-exclusive licence allowing the National Library of Canada to reproduce, loan, distribute or sell copies of this thesis in microform, paper or electronic formats.

The author retains ownership of the copyright in this thesis. Neither the thesis nor substantial extracts from it may be printed or otherwise reproduced without the author's permission.

L'auteur a accordé une licence non exclusive permettant à la Bibliothèque nationale du Canada de reproduire, prêter, distribuer ou vendre des copies de cette thèse sous la forme de microfiche/film, de reproduction sur papier ou sur format électronique.

L'auteur conserve la propriété du droit d'auteur qui protège cette thèse. Ni la thèse ni des extraits substantiels de celle-ci ne doivent être imprimés ou autrement reproduits sans son autorisation.

Canada

University of Alberta

Library Release Form

Name of Author: *Hui Wang*

Title of Thesis: *A Study of the Gas-Liquid Reaction System of Hydrogen
Sulfide and Sulfuric Acid*

Degree: *Doctor of Philosophy*

Year of Degree Granted: *2003*

Permission is hereby granted to the University of Alberta Library to produce single copies of this thesis and to lend or sell such copies for private, scholarly or scientific research purpose only.

The author reserves all other publication and other rights in association with the copyright in the thesis, and except before provided, neither the thesis nor any substantial portion thereof may be printed or otherwise reproduced in any material form whatever without the author's prior written permission.



614 Blackshire Crescent,
Saskatoon, Saskatchewan
S7V 1B4
CANADA

University of Alberta

Faculty of Graduate Studies and Research

The undersigned certify that they have read, and recommend to the Faculty of Graduate Studies and Research for acceptance, a thesis entitled *A Study of the Gas-Liquid Reaction System of hydrogen Sulfide and Sulfuric Acid* submitted by **HUI WANG** in partial fulfillment of the requirements of the degree of **Doctor of Philosophy** in **Chemical Engineering**.



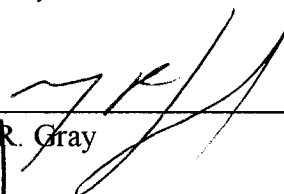
Dr. K. T. Chuang (Supervisor)



Dr. I. G. Dalla Lana (Supervisor)



Dr. R. B. Jordan



Dr. M. R. Gray



Dr. J. M. Shaw



Dr. A. K. Dalai (External)

Date:

January 3/03

DEDICATION

*Dedicated to
my parents
with much love, affection and deep gratitude*

*and to
my wife Jinxian;
and my daughters Doris Ruixue and Amy Ruiyun*

ABSTRACT

Thermodynamics and mass-balance studies indicate the following reaction scheme for the H₂S-sulfuric acid gas-liquid system from room temperature to 120°C:



The measured stoichiometry of the two reactions depends on the acid concentration. Under appropriate conditions the two reactions may occur stoichiometrically such that they remove H₂S and recover sulfur without any sulfur emission. The possible chemical reactions between sulfuric acid (from 80 to 96 wt%) and other components likely present in sour gases requiring sulfur removal, *i.e.*, methane, ethylene, CO, CO₂, COS, CS₂, mercaptan and thiophene, were investigated.

The kinetics for each of the two reactions was studied separately by measuring the total pressure-drop rate in a closed and constant-volume batch reactor enabling an initial-rate analysis. Reaction (1) under acid concentrations from 88 to 100 wt% behaves first order with respect to the pressure of H₂S. The reaction order with respect to sulfuric acid cannot be expressed in terms of an integer. The temperature (20-60°C) dependence of the global rate constant fits the Arrhenius equation. A formula correlating the rate constant with acid concentration and temperature is determined based on the kinetics measurements and an empirical rate equation is proposed. Reaction (2) in presence of sulfuric acid solution (from 30 to 60 wt%) is first order with respect to the pressure of H₂S and to the concentration of SO₂ in the solution, respectively. Its rate constant also depends on the temperature (20-60°C) in accordance with the Arrhenius equation but it is

independent of the concentration of sulfuric acid solution, which merely provides a liquid medium for the reaction. The rate function for the second reaction may be extrapolated to acid concentrations larger than 60 wt%. Both reactions are found occurring at the interface between gas and liquid.

The reaction rate equations obtained provide a basis for the simulation of the overall reaction rate in a batch reactor. The behaviors of the reactions in a packed column reactor are also studied. And the structure of the technology using these reactions is suggested.

ACKNOWLEDGEMENTS

While Edmonton, with a mysterious white world in winter and picture-like green river valley in summer, is a beautiful city to live in, University of Alberta, with tremendous opportunities for learning, is a wonderful place for a graduate student to stay. Especially, I have thoroughly enjoyed the atmosphere of study and research created by people in Department of Chemical and Materials Engineering and in Faculty of Graduate Studies and Research.

First and foremost, I would like to thank my supervisors, Dr. K. T. Chuang and Dr. I. G. Dalla Lana, for their encouraging guidance and kind patience, which have kept me on course and provided me with an excellent environment for chemical engineering research.

I also would like to thank Dr. A. E. Mather, Dr. R. E. Hayes, and Dr. S. E. Wanke for beneficial discussions with them in thermodynamics, reaction kinetics and even foreign literature translation.

I am very grateful for the Memorial Graduate Scholarship named after Captain Thomas Farrell Greehalgh, who graduated from this department and died of wounds he received in the action in Sogel, Germany during World War Two when he served in the Canadian Army as a Royal Canadian Engineer.

My thanks are due to my group-mates, past and present, for their friendship and kind help and caring in every aspect. I thank Dr. Q. Zhang, in particular, for his helpful ideas and beneficial discussions when we worked together. I also thank Mr. Z. G. Han and Mr. H. Zhang for their help with MATLAB simulations.

I appreciate the work provided by support staff in the department, including but not limited, Ms. A. Koenig, Mr. B. Barton, Ms. A. Brereton, Mr. W. Boddez, Mr. R. Copper, Mr. J. Gibeau, Ms. S. Markin, and Mr. B. Scott.

I acknowledge Professor S. Lynn from University of California, Berkeley for giving me full reference to his student's dissertation.

My wife, Jinxian, has been a great source of emotional support. Her love and patience and enthusiasm always strengthened me when I was exhausted and, sometimes, defeated. Her sacrifices as a graduate student's wife and hard work to support our family deserve recognition and appreciation. My debt to her is enormous, and my most grateful thanks are due to her. My thanks are also due to my two lovely daughters, Doris and Amy, who always bring love and joy to my life as a graduate student. I have a very deep sense of gratitude to my parents for all they have done for me and to my mother-in-law for her understanding and support.

This work was supported financially by the National Science and Engineering Research Council of Canada and Alberta Oilsands Technology and Research Authority.

TABLE OF CONTENTS

Chapter 1	Introduction	1
1.1	Introduction to Sulfur Removal and Recovery Technologies	1
1.2	Advantages of Technology to be Developed	2
1.3	Properties of Sulfuric Acid, Hydrogen Sulfide and Sulfur Dioxide	3
1.3.1	Sulfuric acid	3
1.3.2	Hydrogen sulfide	4
1.3.3	Sulfur dioxide	7
1.4	Research Objectives and Strategy	10
1.5	Literature Cited	13
Chapter 2	Preliminary Experiments	16
2.1	Introduction	16
2.2	Establishment of Analysis Method	17
2.2.1	Literature review	17
2.2.2	Experimental section	19
2.2.3	Results and discussion	23
2.3	Preliminary Experiments	32
2.3.1	Introduction	32
2.3.2	Experimental section	34
2.3.3	Results and discussion	36

2.4	Conclusions and Recommendations	43
2.5	Literature Cited	45
Chapter 3	Chemistry of Reactions between Hydrogen Sulfide and Sulfuric Acid	48
3.1	Introduction	48
3.2	Thermodynamic Analysis	49
3.3	Experimental Section	55
3.4	Results and Discussion	59
	3.4.1 Determination of possible reactions using experiments	59
	3.4.2 Mass balance	62
3.5	Conclusions	67
3.6	Cited Literature	68
Chapter 4	Kinetics and Mechanism of Oxidation of Hydrogen Sulfide and Concentrated Sulfuric Acid	70
4.1	Introduction	70
4.2	Theoretical Considerations	71
4.3	Experimental Section	72
4.4	Results and Discussion	77
	4.4.1 Blank experiments	77
	4.4.2 Effect of mass transfer	80

4.4.3	Effect of reaction area and volume	80
4.4.4	Order of reaction with respect to H ₂ S and sulfuric acid	81
4.4.5	Effect of temperature	91
4.4.6	Effect of acid concentration on k_{p1}	92
4.5	Conclusions	98
4.6	Nomenclature	99
4.7	Literature Cited	101
Chapter 5	Kinetics of Reaction between Hydrogen Sulfide and Sulfur Dioxide in Sulfuric Acid Solutions	103
5.1	Introduction	103
5.2	Experimental Section	109
5.3	Results and Discussion	111
5.3.1	Selection of acid concentration range	111
5.3.2	Reaction rate measurement and calculation	112
5.3.3	SO ₂ dissolution	113
5.3.4	Introduction of H ₂ S	116
5.3.5	Order of reaction with respect to H ₂ S and SO ₂	116
5.3.6	Effect of surface area	121
5.3.7	Effects of temperature and acid concentration	124
5.3.8	Extended experiments	124
5.3.9	Prediction of conditions to convert all sulfur	126
5.4	Conclusions	129

5.5	Nomenclature	131
5.6	Literature Cited	133
Chapter 6	Simulation of Operation in Batch Reactor	137
6.1	Introduction	137
6.2	Operation Description	138
6.3	Establishment of the Simulation Models	140
6.4	Results and Discussion	142
	6.4.1 Simulation of overall pressure-drop	142
	6.4.2 H ₂ S and SO ₂ partial pressure change vs. time	143
	6.4.3 Change of each reaction rate vs. time	145
6.5	Conclusions	149
6.6	Nomenclature	150
Chapter 7	Reactions of H₂S and H₂SO₄ in a Packed Column Reactor	151
7.1	Introduction	151
	7.1.1 Absorption with chemical reaction in packed columns	152
	7.1.2 Estimation of mass transfer coefficients	152
7.2	Two-Film Model Analysis on H ₂ S-Sulfuric Acid System	154
7.3	Physicochemical Properties	160
	7.3.1 Surface tension	160

7.3.2	Viscosity	161
7.3.3	Diffusivity	161
7.4	Experimental Section	162
7.5	Results and Discussion	166
7.5.1	Estimation of liquid-side mass transfer coefficient	166
7.5.2	H ₂ S absorption companied with reaction	169
7.5.3	Discussion on effective surface area	171
7.5.4	Analysis on reaction in 96 wt% acid	174
7.5.5	Reactor design	175
7.6	Conclusions	177
7.7	Nomenclature	179
7.8	Literature Cited	182
Chapter 8	Suggested Applications and Recommendations	184
8.1	Introduction	184
8.2	Application in Flare Gas Recovery	184
8.2.1	Flare gas problems	184
8.2.2	Application to sulfur removal from flare gas	185
8.2.3	Column reactor design	187
8.2.4	Discussion and recommendations	188
8.3	Sulfur Recovery: Substitution of Claus Process	190
8.3.1	Claus process and its suitability	190
8.3.2	Application to sulfur recovery	191

8.3.3 Case study	193
8.4 Conclusions and Recommendations	196
8.5 Literature Cited	198
Chapter 9 Summary and Conclusions	199
9.1 Literature Review on H ₂ S-Sulfuric Acid Reaction System	200
9.2 Reactions of Sulfuric Acid with Components other than H ₂ S	200
9.3 Reaction Scheme and Overall Stoichiometry	201
9.4 Kinetics of Two Reactions	202
9.5 Simulation for Batch Reactor Operation	203
9.6 Mass Transfer and Reaction Behaviors in Packed Column	203
9.7 Suggestions and Recommendations	204
Appendix A Calibrations of Apparatuses	206
A.1 Calibration of Mass Flow Controllers	206
A.2 Calculation of GC Detectors	207
A.3 Verification of Thermocouples	213
Appendix B Tables for Kinetics Data	214
Appendix C More Discussion on Reaction (4-1)	227
Appendix D Arrays of Stoichiometric Coefficients of Reactions and Its Reduction	229

List of Tables

Table 1-1	Oxidation reactions of hydrogen sulfide	8
Table 2-1	Parameters under which GC and detectors work	21
Table 2-2	Composition of gas samples	24
Table 2-3	Conversion and products of COS contacting sulfuric acid at 120°C	37
Table 2-4	Conversion and products of CS ₂ contacting sulfuric acid at 120°C	38
Table 2-5	Conversion and products of mercaptan contacting sulfuric acid at 120°C	39
Table 2-6	Conversion and products of thiophene contacting sulfuric acid at 120°C	40
Table 2-7	Conversion and products of ethylene contacting sulfuric acid at 120°C	41
Table 3-1	Possible reactions and their thermodynamic properties at 25°C	53
Table 3-2	Experimental results for determining possible reactions	60
Table 3-3	Results from mass balance experiments	63
Table 3-4	Values of z at various acid concentrations	65
Table 4-1	Reaction rate at various surface areas and solution volumes	82
Table 4-2	Values of k_{P1} at all temperatures and acid concentrations	86
Table 4-3	Values of I and j in Equation (4-9)	90
Table 4-4	Values of $\ln A_0$ and E_a for various acid concentrations	94

Table 4-5	Values of a , b , c , d and r^2 in Equations (4-17) and (4-18)	96
Table 5-1	Summary of products distribution of liquid phase Claus reaction	105
Table 5-2	Experimental results for order of reaction	119
Table 6-1	Parameters used in simulations	144
Table 7-1	Measured and estimated values of k_L for H ₂ S-water system	168
Table 8-1	Specifications of sour gas from a gas plant	194
Table 8-2	Outputs from simulations of a reactor column	195
Table A-1	Data for the rate of reaction 1	215
Table A-2	Data for the rate of reaction 2	223
Table A-3	Stoichiometric coefficient array of reactions in Table 3-1	229
Table A-4	Stoichiometric coefficient array of reactions on page 52	229
Table A-5	Reduced stoichiometric coefficient array	230

List of Figures

Figure 1-1	Molarity of species in sulfuric acid solutions	5
Figure 1-2	Activity of molecular H ₂ SO ₄ in sulfuric acid solutions at 25°C	6
Figure 1-3	Solubility of sulfur dioxide in sulfuric acid solutions at 1 atm	9
Figure 2-1	Schematic drawing of parallel sulfur chemiluminescence and thermal conductivity detectors within one gas chromatograph	22
Figure 2-2	SCD chromatogram of typical sulfur containing compounds separated using a CP-Sil PCB capillary column at a chosen temperature program	26
Figure 2-3	TCD chromatogram of typical sulfur and non-sulfur gas mixtures containing separated using a CP-Sil PCB capillary column at a chosen temperature program	27
Figure 2-4	Detector linearity and measuring range	29
Figure 2-5	SCD calibration curves for selected sulfur compounds	30
Figure 2-6	TCD calibration curves for selected compounds	33
Figure 2-7	Schematic drawing of semibatch reactor for preliminary experiments	35
Figure 3-1	Chemical equilibrium constant for possible reactions over temperature range from 0 to 120°C	55
Figure 3-2	Schematic diagram of the batch reactor experimental setup	56

Figure 3-3	Dependence of overall stoichiometric coefficient, z , on acid concentration	66
Figure 4-1	Schematic diagram of experimental apparatus	74
Figure 4-2	Plot of pressure drop against time for reaction between H_2S and H_2SO_4 solution	75
Figure 4-3	Blank experiment	78
Figure 4-4	Rate of reaction between H_2S and sulfuric acid solutions of various concentrations	79
Figure 4-5	Plots of initial H_2S consumption rate against initial H_2S pressure	84
Figure 4-6	Correlation between reaction rate and H_2SO_4 activity at $25^\circ C$	87
Figure 4-7	Correlation between $\log k_{p1}$ and the acidity function	88
Figure 4-8	Arrhenius plots for reactions at various acid concentrations	93
Figure 4-9	Correlations between $\ln A_0$ and acid concentration, C_a , and between E_a and C_a	95
Figure 5-1	Typical curves for pressure drop versus time	114
Figure 5-2	SO_2 dissolving rate in sulfuric acid solutions of 29.60 wt% and 96.04 wt%	116
Figure 5-3	Effect of stirring speed	118
Figure 5-4	Reaction orders with respect to P_{H_2S} and $[SO_2]$	120
Figure 5-5	Effect of surface area (a) on the reaction rate	122
Figure 5-6	Arrhenius plot of reaction in sulfuric acid from 30 wt% to 60 wt%	125

Figure 5-7	Comparison of second reaction rate predicted by Equation (5-28) with that obtained in experiment when two reactions occur simultaneously in 90 wt% and 96 wt% sulfuric acid	127
Figure 5-8	Rate ratio of reaction (1) to reaction (2) estimated at various temperatures and acid concentrations when $P_{H_2S}=1.013$ kPa and $P_{SO_2}=0.5065$ kPa	128
Figure 6-1	Comparison between simulated and experimental data on total P in batch reactor	139
Figure 6-2	Changes in total P and partial P 's for H_2S and SO_2 in 95.91 wt% acid	146
Figure 6-3	Changes in total P and partial P 's for H_2S and SO_2 in 79.01 wt% acid	147
Figure 6-4	Reaction rate vs. time at 120°C and 95.91 wt% of acid concentration	148
Figure 7-1	Concentration profile for two-film model	153
Figure 7-2	Concentration profile for H_2S and H_2SO_4 reaction in packed column	156
Figure 7-3	Concentration profile for H_2S and H_2SO_4 reaction in packed column when mass transfer is rate-controlling step	158
Figure 7-4	Concentration profile for H_2S and H_2SO_4 reaction in packed column when reaction is rate-controlling step	159
Figure 7-5	Photos of column reactor	163
Figure 7-6	Schematic diagram of experimental setup for column reactor	166

Figure 7-7	Rate coefficient, $K_G a$ vs. height of packing, z	170
Figure 7-8	Temperature-dependence of estimated k_G and k_{P1} and measured K_G for reaction of H_2S and 90 wt% acid	172
Figure 7-9	Analysis of rate controlling regime for reaction in 96 wt% acid	176
Figure 8-1	Flowsheet of suggested application to flare gas recovery	186
Figure 8-2	Equilibrium stages needed vs. SO_2 exit concentrations	189
Figure 8-3	Flowsheet of suggested application for sulfur recovery from sour gas	192
Figure A-1	Mass flowrate calibration for N_2	208
Figure A-2	Mass flowrate calibration for H_2S	209
Figure A-3	Mass flowrate calibration for SO_2	210
Figure A-4	SCD calibration for H_2S	212

Chapter 1

Introduction

1.1 Introduction to Sulfur Removal and Recovery Technologies

Hydrogen sulfide is present in natural gas, refinery streams and coal gas, naturally or as a byproduct of processing operations. It has to be removed from these sour gases before they can be utilized because hydrogen sulfide is toxic and corrosive. A number of processes for treating sour gases have been invented to remove hydrogen sulfide. An elaborate introduction to these processes can be found in many handbooks and encyclopedia (Capone, 1997; Sander, et al., 1984). Here, the disadvantages of the current processes are analyzed according to a classification of the primary mechanism, *e.g.*, absorption, adsorption, and conversion. Absorption, either physical or chemical, consists of a trapping unit and a regeneration unit. The lean liquid solvent absorbs H_2S from the sour gas stream in the trapping unit to produce a sweet gas stream and an H_2S -enriched solvent. The regeneration unit restores the H_2S -enriched solvent to lean solvent for reuse, producing an H_2S -enriched gas stream, which, depending on the scale of production, either goes to a sulfur recovery unit or is burned. Obviously, burning H_2S leads to SO_2 emission and air pollution. As environmental protection policies become tighter, the absorption and burning, suitable for sweetening the sour gas that contains small amounts of H_2S or is tapped from isolated sites, is being banned. Adsorption occurs when the H_2S -containing gas stream is passed through a fixed bed of metal oxides such as iron oxide or

zinc oxide, where H₂S reacts to form either the metal sulfides or sulfur. The slow reaction rate in this process restricts its use to treating gas streams of limited flowrate and low concentration of H₂S. The disposal of the used adsorbent causes secondary environmental pollution. Adsorption using molecular sieves may enable the adsorbent to be regenerated; however, the H₂S-enriched gas resulting from the regeneration needs to be treated. The conversion processes, among which the modified Claus process is the mostly widely-used, convert hydrogen sulfide into elemental sulfur, a saleable product. The burning unit of the Claus process, where 1/3 H₂S is converted to SO₂ for the Claus reaction, consumes a great amount of energy and emits SO₂ and other pollutants into the air. Such conversion processes are economically justifiable only when sulfur production is large.

1.2 Advantages of Technology to be Developed

The technology to be developed in this study is based on two reactions occurring between hydrogen sulfide, H₂S, and concentrated sulfuric acid. First, H₂S is oxidized by concentrated sulfuric acid, generating sulfur, sulfur dioxide and water, *i.e.*,



Second, H₂S also reacts with the produced SO₂ in the solution, forming sulfur and water, *i.e.*,



If all the SO₂ is consumed, the overall stoichiometric reaction is



The expectation from this study would be that this overall reaction will be carried out in one or more vessels such that hydrogen sulfide in the gas stream will be converted into sulfur; and, the latter remains trapped in the liquid. The sulfur will be separated from the

sulfuric acid solution after which the diluted acid will be upgraded to the initial concentration. Under these circumstances, sulfur or other pollutant will not be discharged into the atmosphere. Compared to the modified Claus process, this novel technology could be more economical since sulfuric acid is inexpensive and the operation of the units will be simpler. Because of acid consumption, this novel process is more suitable for treatment of sour gases containing small amounts of hydrogen sulfide. The flexibility of the process allows it to be applicable to isolated gas reservoirs and to the recovery of separated flare gases. Moreover, the unit where hydrogen sulfide is oxidized by concentrated sulfuric acid to produce sulfur dioxide might replace the burning unit in the Claus process. If the useful components in the gas stream are not reactive, this novel process will allow the Claus reaction to be utilized directly, eliminating the H₂S absorption-regeneration units and the tail-gas problem.

1.3 Properties of Sulfuric Acid, Hydrogen Sulfide and Sulfur Dioxide

The substances that are involved in this reaction system are sulfuric acid, hydrogen sulfide and sulfur dioxide. Their properties likely determine the behavior of the reactions; therefore, it is necessary to review the relevant physical and chemical properties of sulfuric acid, hydrogen sulfide and sulfur dioxide.

1.3.1 Sulfuric acid

Sulfuric acid is referred as to a mixture of sulfuric acid and water at a special concentration. For instance, in the *Kirk-Othmer Encyclopedia of Chemical Technology* (Muller, 1997), *sulfuric acid* is defined as a colorless, viscous liquid having a specific gravity of 1.8357 and a normal boiling point of approximately 274°C. However, the sulfuric acid - water mixture may vary over a wide concentration range. Then, the

mixture is also called sulfuric acid solution. Sulfuric acid is of commercial importance and has long been used by human beings. Its properties, both physical and chemical, are well studied and are described in many relevant data sources and handbooks. Hygroscopicity and oxidizing ability are the most characteristic chemical properties of concentrated sulfuric acid, due to which a number of reactions between sulfuric acid and other compounds, including hydrogen sulfide, occur. Also because of these, hydration and dissociation take place in the sulfuric acid solution and creates ionic species other than molecular sulfuric acid and water. The nominal concentration of sulfuric acid does not represent the concentration present in the molecular form. For example, Young, et al. (1970) studied the concentration of species in sulfuric acid solutions using Raman spectroscopy and showed that molecular sulfuric acid does not exist when the weight percent concentration is below 78 %. Their results are shown in Figure 1-1. Giaque, et al. (1960) found that when the weight percent concentration of sulfuric acid is as low as 60 wt%, the activity coefficient of sulfuric acid molecules becomes 10^{-5} , so low that it may be disregarded, as shown in Figure 1-2.

1.3.2. Hydrogen sulfide

Hydrogen sulfide is extremely toxic and therefore, hazardous to people who are exposed to it. Its adverse effects on health could be nervous system damage, cardiovascular, gastrointestinal and ocular disorders, unconsciousness, respiratory paralysis, and death, depending on the duration of exposure and the concentration of H_2S in the air. Because of corrosion and embrittlement, lines, fittings and other parts of the

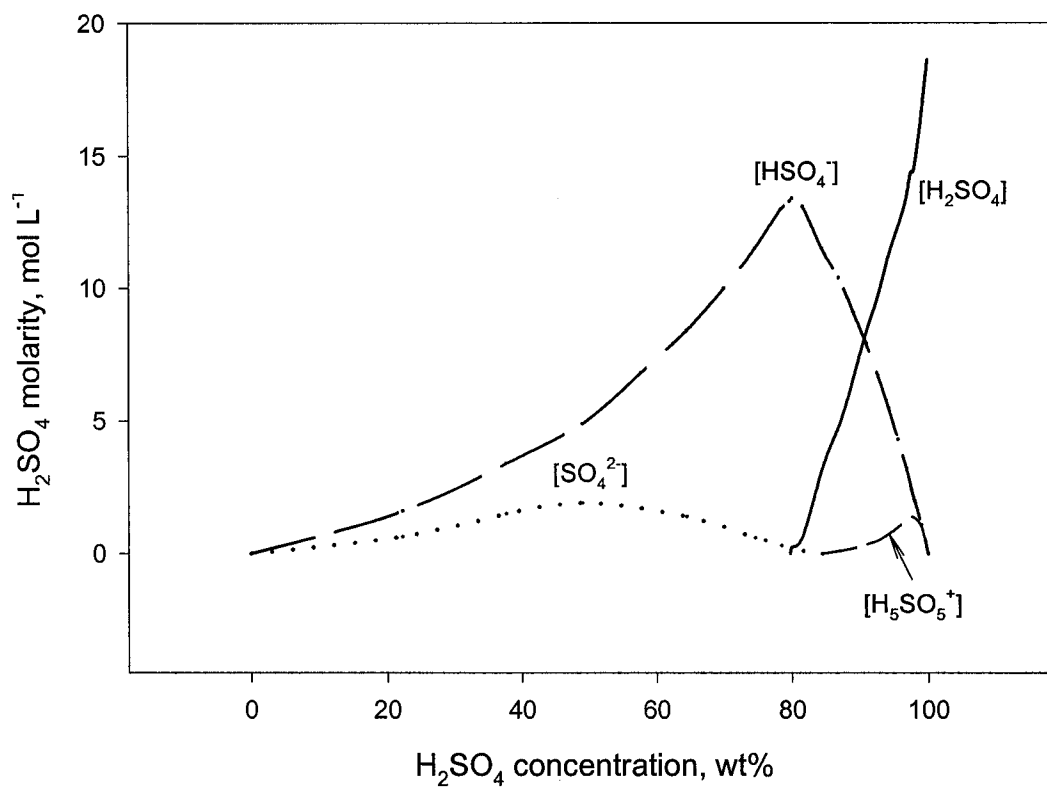


Figure 1-1. Molarity of species present in sulfuric acid solutions. (reproduced from Young and Walrefen 1961).

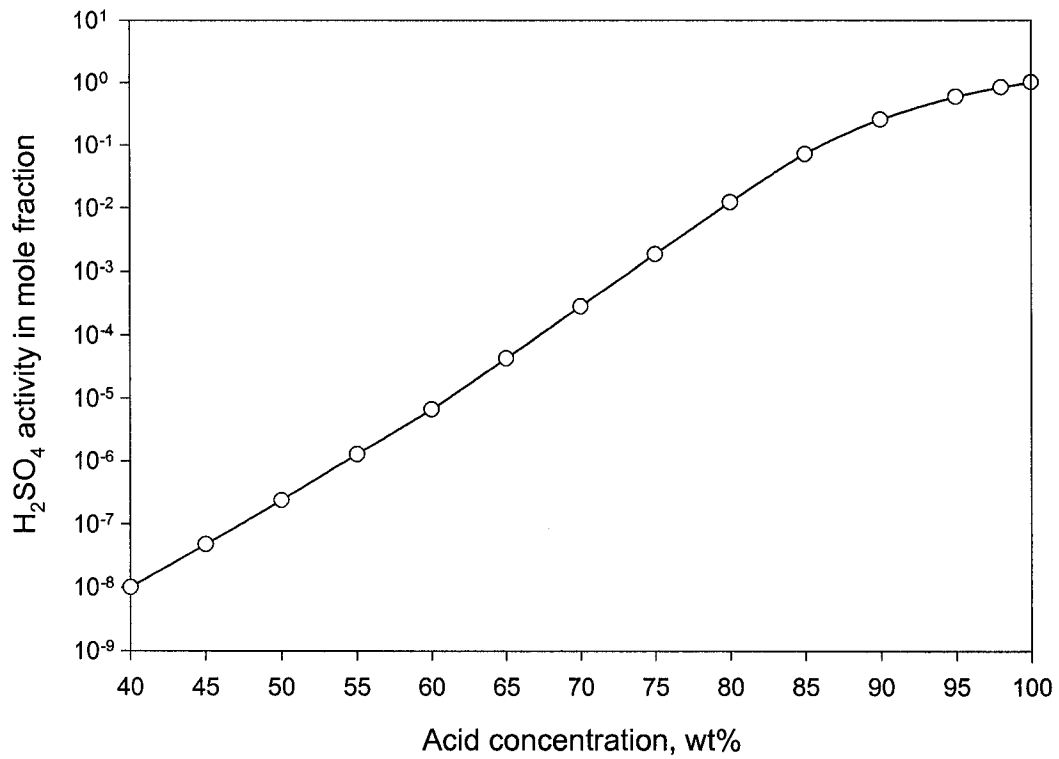


Figure 1-2. Activity coefficient of molecular H₂SO₄ in sulfuric acid solutions at 25°C. (plotted based on the data provided by Giaque, et al., 1960).

equipment that contact hydrogen sulfide are prone to develop leaks. Hydrogen sulfide existing in the processing gases can also poison the catalysts downstream. Weil and Sandler (2000) and the World Health Organization (1981) provided more detailed information on this aspect. Nonetheless, the most important property that relates to this study is that hydrogen sulfide can be oxidized by a number of oxidizing agents, as shown in Table 1-1. Some of these oxidations have formed the basis of industrial processes of sulfur removal and recovery, *e.g.*, Claus process and ferric oxide adsorption, and others are the basis of the H₂S analysis method.

1.3.3 Sulfur dioxide

The property of sulfur dioxide that would influence its reaction with H₂S will be its solubility in sulfuric acid solution since the reaction occurs in the liquid phase (Tiwari, 1976). Because of its industrial importance, the solubility of SO₂ in sulfuric acid solution has been studied by a number of authors (Miles and Fenton, 1920; Cupr, 1928; Johnstone and Leppel, 1934; Miles and Carson, 1946; Domka, et al., 1981; Chang, 1982; Hunger, 1990). In summary, Figure 1-3 (reproduced from Sander, et al., 1984) shows how the solubility of SO₂ changes with sulfuric acid concentration and the temperature. For every temperature, a "V" curve was observed when the solubility changes with acid concentration. The bottom of the "V" curves is located at about 85 wt% for all the temperatures. When the temperature increases, the curves become flatter. The forms of dissolved SO₂ change with acid concentration. Gold and Tyr (1950) found that the dissolved SO₂ mostly takes the molecular form when the acid concentration is high. Govindara and Gopalakrishna (1993) determined that the molecular form dominates when the sulfuric acid concentration is larger than 5 wt% because hydrolysis of SO₂ to H⁺ and HSO₃⁻ becomes negligible. Based on their own data and data from the literature,

Table 1-1. Oxidation reactions of hydrogen sulfide (Weil, 2000).

Oxidizing agent	Conditions	Sulfur containing products
O ₂	flame	SO ₂ , some SO ₃
	flame or furnace, catalyst (Claus process)	sulfur
	aqueous solution of H ₂ S, catalyst	sulfur
H ₂ O ₂	neutral; alkaline solution	sulfur; S ₂ O ₃ ²⁻ , SO ₄ ²⁻
Na ₂ O ₂	dry, elevated temperature	Na ₂ S, Na ₂ S _x
O ₃	aqueous	sulfur, H ₂ SO ₄
SO ₂	elevated temperature, catalyst	sulfur
	aqueous solution	sulfur, polythionic acids
H ₂ SO ₄	concentrated acid	sulfur, SO ₂
HNO ₃	aqueous	H ₂ SO ₄
NO	silica gel catalyst	sulfur
	aqueous at pH 5–7	sulfur, NO
	aqueous at pH 8–9	sulfur, NH ₃
Cl ₂	gaseous, excess Cl ₂	SCl ₂
	gaseous, excess H ₂ S	sulfur
	aqueous solution, excess Cl ₂	H ₂ SO ₄
I ₂	aqueous solution	sulfur (quantitative)
Fe ³⁺	aqueous solution	sulfur, FeS

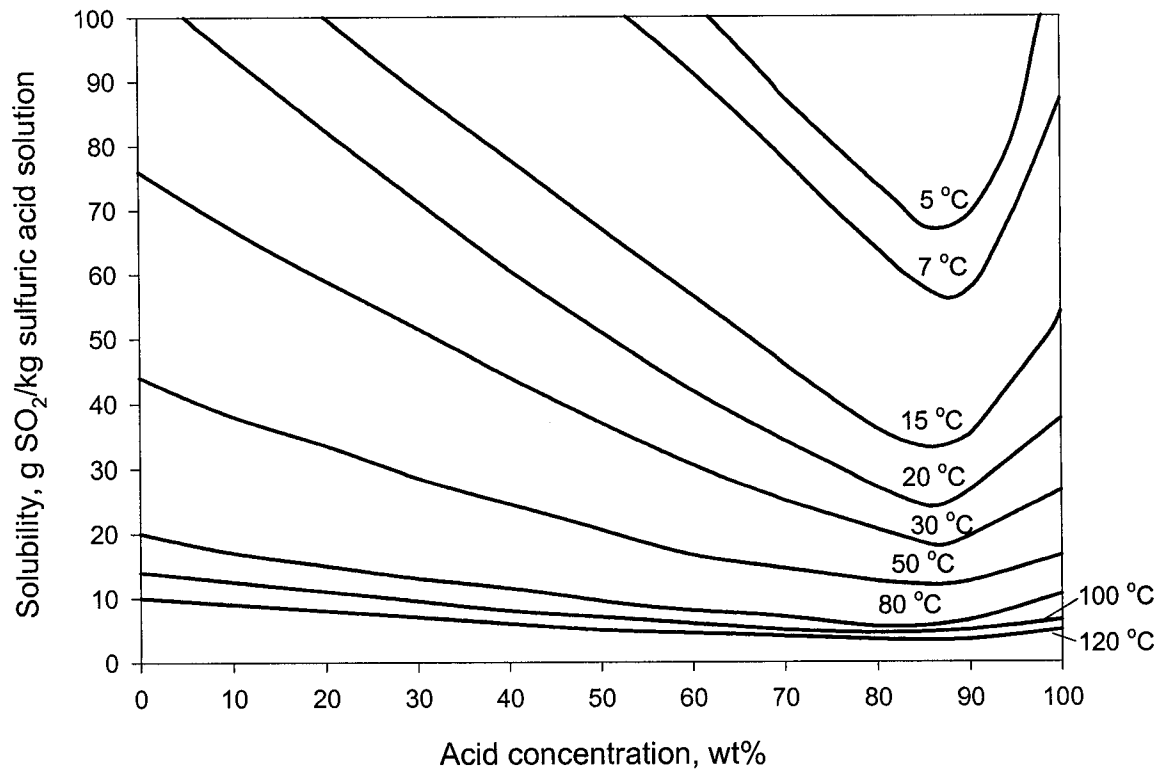


Figure 1-3. Solubility of sulfur dioxide in sulfuric acid solution at $P_{SO_2} = 1$ atm. (reproduced from Sander, et al., 1984).

Hayduk, et al. (1988) concluded that Henry's law is applicable for the relation between SO₂ solubility and partial pressure over an acid concentration range up to 78.40 wt%. They also discovered that the value of the Henry's law constant is independent of acid concentration over this concentration range; however, this is obviously not tenable according to Figure 1-3. Hayduk, et al. suggested a modified Henry law equation to correlate the solubility and equilibrium partial pressure of SO₂ in sulfuric acid. To provide a more suitable model for this study, we studied and correlated the solubility of SO₂ in sulfuric acid solutions over the concentration range from 65.71wt% to 95.91 wt% at 25°C, 100°C and 120°C (Zhang, et al., 1998).

1.4 Research Objectives and Strategy

The ultimate aim of this study is to develop a fundamental understanding of the reactions between hydrogen sulfide and sulfuric acid in a gas-liquid system, based on which a new technology for sulfur removal and recovery may be established. The new technology is anticipated to be inexpensive and simple so that it can be used for treating sour gases containing small amounts of hydrogen sulfide and can be easily operated even in isolated sites. In addition, the scale of operation for the process has to be flexible so that its use will not be limited by the flow rates of the gas to be treated.

To develop a sulfur removal and recovery technology based on a chemical process, one has to know if the process interacts with other components which may be present in the sour gas. For instance, methane and other light hydrocarbons in natural gas are useful components and should not be altered during the sulfur removal process. If they do react, then a separate separation unit is required to remove H₂S. If the valuable gas components are "inert", then the process can be used directly for treating gaseous

streams. The essential knowledge about the chemistry of the process, including the stoichiometry, reaction kinetics and mass transfer has to be obtained, if available, or studied, if unavailable. With more complete information the basic process units and their operating parameters may be suggested.

Based on this strategy, preliminary experiments were first carried out to see whether sulfuric acid reacts with components other than H_2S in the gas streams to be treated. These components included methane, ethylene, carbon monoxide, carbon dioxide and inert components like nitrogen. The interaction between sulfuric acid and other sulfides such as carbonyl sulfide, carbon disulfide, mercaptan and thiophene also needs to be investigated. To accomplish these reactivity tests accurately, we developed an analytical method to measure both the amounts of the sulfur-containing compounds over a wide range of concentration as well as the non-sulfur-containing compounds within a single gas chromatograph.

Because of the lack of prior knowledge of the reaction between hydrogen sulfide and sulfuric acid, this thesis starts with a systematic study of the chemical reactions and their stoichiometry. The possible reactions between H_2S and all species likely present in sulfuric acid solutions (0-100 wt%) and even between H_2S and the products from previous reactions must be considered.

The establishment of a rate equation for each of the independent reactions in the H_2S -sulfuric acid gas-liquid system is the final objective of this thesis. However, the results will be used to predict the reaction rate for the entire H_2S -sulfuric acid system. Diffusion and mass transfer may also be important in this gas-liquid reaction system.

A mathematical model based on the rate equations will be used to simulate the operation of the gas-liquid system carried out in a batch reactor. Second, the rate

equations should also be used to predict the rate of reactions carried out in a packed column reactor when the process is known to be rate-controlled by chemical reaction. To clarify the mass transfer behavior and rate-controlling regime of the $\text{H}_2\text{S}-\text{H}_2\text{SO}_4$ reaction system, the two-film analysis (Shah, 1979) and the empirical models on the effective interface area and mass transfer coefficients are used to interpret the experimental data obtained from the column reactor packed with ceramic Raschig rings.

Finally, the description of an integrated process based on this study is proposed and some case studies for its application are carried out. Although likely necessary to a more complete development of such a process, the influences of heat transfer and fluid mechanics must be considered; however, they are beyond the coverage of this thesis.

1.5 Cited literature

- Capone, M., "Sulfur Removal and Recovery", *Kirk-Othmer Encyclopedia of Chemical Technology*, John Wiley & Sons, Inc. (1997).
- Cupr, V., "About the Absorption of Hydrogen Chloride Gas and Sulfur Dioxide in Sulfuric and Acetic Acids", *Rec. Trav. Chim.*, **47**, 55 (1928).
- Chang, K. K., "Solubility of Sulfur Dioxide in Sulfuric Acid", *Hydrogen Energy Progress – IV Proc. 4th World Hydrogen Energy Conf.*, Pasadena, California, U.S.A. (June 13-17, 1982).
- Danckwerts, P. V., *Gas-Liquid Reactions*. McGraw-Hill Book Company, New York, pp180-201 (1970).
- Domka, F., J. Miciukiewicz, W. Zmierczak, and A. Juszcak, "Study of Solubility of SO₂ in H₂SO₄ as Function of Temperature and Pressure", *Phosphorus and Sulfur*, **10**, 61 (1981).
- Giauque, W. F., E. W. Hornung, J. E. Kunzler, and T. R. Rubin, "The Thermodynamic Properties of Aqueous Sulfuric Acid Solutions and Hydrates from 15 to 300 K", *J. Am. Chem. Soc.*, **82**, 62 (1960).
- Gold, V, and F. L. Tyr, "The State of Sulfur Dioxide Dissolved in Sulfuric Acid", *J. Am. Chem. Soc.*, **73**, 2932 (1950).
- Govindora, V. M. H., and K. V. Gopalakrishna, "Solubility of Sulfur Dioxide at Low Partial Pressure in Dilute Sulfuric Acid Solutions", *Ind. Eng. Chem. Res.*, **32**, 2111 (1993).
- Hunger, T., F. Lapique, and A. Stork, "Thermodynamic Equilibrium of Diluted SO₂ into Na₂SO₄ or H₂SO₄ Electrolyte Solutions", *J. Chem. Eng. Data*, **35**, 453 (1990).

- Johnstone, H. F., and P. W. Leppla, "The Solubility of Sulfur Dioxide at Low Pressure. The Ionization Constant and Heat of Ionization of Sulfurous Acid", *J. Am. Chem. Soc.*, **56**, 2233 (1934).
- Miles, F. D., and J. Fenton, "The Solubility of Sulfur Dioxide in Sulfuric Acid", *J. Chem. Soc.*, **117**, 59 (1920).
- Miles, F. D., and T. Carson, "The Solubility of Sulfur Dioxide in Fuming Sulfuric Acid", *J. Chem. Soc.*, **56**, 786 (1946).
- Muller, T. L., "Sulfuric Acid", *Kirk-Othmer Encyclopedia of Chem. Eng.* 4th Ed. John Wiley & Sons (Web version, 1997).
- Onda, K., E. Sada, and Y. Murase, "Liquid-side Mass Transfer Coefficients in Packed Towers", *AIChE J.*, **5**, 235 (1959).
- Onda, K., H. Takeuchi, and Y. Okumoto, "Mass Transfer Coefficients between Gas and Liquid Phases in Packed Columns", *J. Chem. Eng. Jpn.*, **1**, 56 (1968).
- Onda, K., E. Sada, and H. Takeuchi, "Gas Absorption with Chemical Reaction in Packed Columns", *J. Chem. Eng. Jpn.*, **1**, 62 (1968).
- Rinker, E. B., O. T. Hanna, and O. C. Sandall, "Asymptotic Models for H₂S Absorption into Single and Blended Aqueous Amines", *AIChE J.*, **43**, 58 (1997).
- Sander, U. H. F., H. Fischer, U. Rothe, and R. Kola, *Sulfur, Sulfur, Sulfur Dioxide and Sulfuric Acid*, edited by A. I. More, The British Sulfur Corporation Ltd. p153, (1984).
- Shah, Y. T., *Gas-Liquid-Solid Reactor Design*, McGraw-Hill International Book Company, New York, (1979).
- Tiwari, B. L., *The Kinetics of the Oxidation of Zinc Sulfide and Hydrogen Sulfide by Sulfur Dioxide in Aqueous Sulfuric Acid*, Ph. D. Thesis, Columbia University (1976).

- Weil, E. D., and S. R. Sandler, "Sulfur Compounds", *Kirk-Othmer Encyclopedia of Chemical Technology*, John Wiley & Sons, Inc. (Web version, 2000).
- World Health Organization, *Hydrogen Sulfide*, Geneva: World Health Organization, 1981.
- Young, T. F., and G. E. Walrafen, "Raman Spectra of Concentrated Aqueous Solubility of Sulfuric Acid", *Trans. Faraday Soc.*, **57**, 34 (1961).
- Zhang, Q., H. Wang, I. G. Dalla Lana, and K. T. Chuang, "Solubility of Sulfur Dioxide in Sulfuric Acid of High Concentration", *Ind. Eng. Chem. Res.*, **37**, 1167 (1998).

Chapter 2

Preliminary Experiments

2.1 Introduction

The gas streams from which hydrogen sulfide is to be removed usually consist of compounds that fall into three categories: 1) useful components, 2) inert gases, and 3) sulfur-containing species. Depending on the origin of the gas streams, the composition of the useful components may vary. For instance, the useful components in natural gas are mainly methane and a small amount of other light hydrocarbons; whereas those present in coal-delivered gas are hydrogen, carbon monoxide, and small amounts of methane and organic compounds. The inert gases are mostly nitrogen and carbon dioxide, the content of which also varies. Besides hydrogen sulfide, the other sulfur-containing compounds include sulfur dioxide, carbonyl sulfide, carbon disulfide, mercaptan and thiophene. The sulfur removal process is not expected to interfere with the useful components and to convert the inert gases into more polluting products, like N_2 to NO_x . However, it is desired to remove as much as possible of the sulfides. In this chapter, sample gases containing different compositions of the three categories of components were prepared and, in turn, treated with sulfuric acid of various concentrations. The interaction between sulfuric acid and each of the above-mentioned components was detected analytically using a GC coupled with both thermal conductivity (TCD) and sulfur chemiluminescence (SCD) detectors. To efficiently

accomplish the tasks, a GC analysis method enabling the simultaneous measurement of sulfur-containing compounds and non-sulfur-containing compounds over a wide range of concentrations was first established. With this capability, the reactivity of each component could be measured when the sample gas was passed through a semi-batch reactor containing concentrated sulfuric acid at a certain volume and concentration.

2.2 Establishment of Analysis Method*

2.2.1 Literature review

Sulfur chemiluminescence detectors (SCD) allow precise measurement of sulfur-containing molecules down to parts-per-billion (ppb) levels (Benner and Stedman, 1989; Shearer, 1992; Shearer, et al, 1990 and 1993). Coupled with GC separation using an appropriate column, SCD can detect all sulfur compounds present. As a selective detector, however, it does not sense the co-eluting species that do not contain sulfur atoms. Whereas, the thermal conductivity detector (TCD) is able to detect both sulfur-containing and non-sulfur-containing compounds as long as the thermal capacity of these compounds differs from that of the carrier gas. However, its sensitivity is limited such that it cannot detect the species that are present in very small concentration. A combination of these two detectors may enable one to measure not only the concentrations of both sulfur and non-sulfur-containing compounds but also at both high and low concentrations of sulfur-containing species, a situation often encountered in research and commercial practice.

* A version of this section has been published in *Journal of Chromatographic Science*, **36**, 605 (1998).

The principle under which the SCD works, suggested by Shearer (1992), is that the sulfur-containing compounds being eluted from a gas chromatograph separation column to a reducing hydrogen-air flame form sulfur monoxide and that this SO that is formed is subsequently detected because of its chemiluminescent reaction with ozone. Benner and Stedman (1989) carried out the systematic studies on the design of sulfur chemiluminescence detectors and possible influencing factors. Shearer, et al. (1990) coupled SCD to a GC and evaluated its performance and operating features, initiating a commercially available means of sulfur-selective detection. They modified the SCD using an externally heated ceramic combustion assembly that allowed it to operate at low pressure and fuel-rich conditions outside of the flammability limits of hydrogen in air. This flameless SCD, as it was termed (Shearer, 1992), improved the ease of use, reliability, and detectability of the commercially available equipment.

Following the above fundamental work, a number of researchers and users have worked to extend the use of SCD in the measurement of sulfur-containing compounds in various sample sources. Shearer, et al. (1993) extended the use of SCD to examination of sulfur compounds in liquefied petroleum products by adding an inert sample inlet assembly to the flameless SCD and GC system. Hines (1993) measured the specific sulfur compounds in liquefied petroleum gases and natural gas streams, and Harryman and Smith (1994) determined the sulfur species distribution of streams at Texaco's NGL Fractionation Plant. The results of the latter indicated that concentrations higher than those predicted by using the Soave-Redlich-Kwong (SRK) or the Peng-Robinson (PR) equations of state were present. Chawla and Sanzo (1992) also studied the optimization and operational characteristics such as linear response, sensitivity, and stability of SCD

coupled to a GC. Tang, et al. (1996) developed a multi-purpose sampling loop with a cryogenic trap that, when coupled to a GC-SCD, permitted analysis from nanogram-per-cubic meter to million-per-cubic-meter levels of sulfur compounds in the atmosphere, natural gas and gaseous fuels. To deal with the wide range of concentration, Lechner-Fish (1996) used two separate chromatographs with different detectors; one for measuring the components of higher concentrations and the other for measuring those of lower concentrations.

2.2.2 Experimental section

2.2.2.1 Design considerations

Two options are available for combining the SCD and the TCD within a single GC. The first option is to put them in series after a single GC column, as most apparatus do, and the other option is to arrange them in parallel, each of the detectors sensing an effluent from separate GC columns. The large difference in the intrinsic sensitivity between the TCD and the SCD renders the consecutive combination impractical. For example, if the TCD-SCD series monitors the effluent from a single *packed column*, when the TCD obtains a suitable response, the SCD may be overloaded. Or if the series combination comes after a *capillary column* with a split sample injection, the SCD may get an appropriate response, but the TCD may not. Both situations will result in unsatisfactory analysis. In addition, the connection between TCD and SCD can lead to GC peaks with tails that adversely influence the precision of the measurement. The parallel combination, however, acts as two separate GC's, except that the two columns share the same oven, each detector coming after its own sampling loop and GC column, and having its own carrier gas stream. The best separation is the function of carrier gas

flow rate, the column length and the kinds of packing, the sampling loop size, the oven temperature and its program, and even the concentration of the gas stream to be measured. So are the response, the resolution and the sensitivity. A set of parameters under which the GC and its detectors worked in this study are shown in Table 2-1. Some of them, marked with a "*" after their names, were determined by optimization. Figure 2-1 shows a schematic drawing of the GC with parallel SCD and TCD. The original carrier gas line of the HP 5890 II GC (Hewlett-Packard, Palo Alto, CA) was retained for the capillary column-SCD line, and another carrier gas line was added for the packed column-TCD line, the gas flow rate of the latter being controlled by a separate mass flow controller. A 10-way valve was used to connect the sampling lines, the two sampling loops, and the two carrier gas lines. This valve, driven by an automatic timer, is the key part for simultaneous sampling.

2.2.2.2 Instrumentation

A Hewlett-Packard model 5890 II GC fitted with a TCD and a Sievers model 350B SCD (Sievers Instruments, Boulder, CO) were used in this study. Hewlett-Packard ChemStation software was used for data acquisition and chromatogram analysis. This software enables data processing for two simultaneous detector signals. For the SCD, a CP-Sil 5CB capillary column (50 m × 0.32 mm × 0.5 μm, fused-silica WCOT) was purchased from Chrompak (Middelburg, the Netherlands). For the TCD, the packed column was made from a stainless steel tube (4 m × 3.2 mm o.d.), and packing was Porapak Q (Waters Associates, Milfors, MA). Prepurified helium (Praxair Products, Edmonton, Alberta, Canada) was used as a carrier gas. The thermal conductivity detector was maintained at 200°C. Meanwhile, the burner of the SCD was operated at

Table 2-1. Parameters under which GC and detectors work

<i>Description</i>	<i>value</i>
Oven temperature program*	75 °C for 3 minutes; to 120 °C at 20 °C/min; and held for 5~10 minutes
Capillary column head pressure	65 kPa gauge
Splitting flow rate	200 mL/min
Volume of sampling loop for SCD*	38.5 µL (measured by water and capillary syringe)
SCD burner temperature	800-810 °C
SCD burner pressure	34.6 kPa absolute
Flow rate of H ₂ to the burner	100 mL/min
Flow rate of air to the burner	40 mL/min
Pressure of air in the ozone generator	41.4 kPa gauge
Packed column size*	3 m × 3.2 mm o.d.
Packing in packed column	Porapak Q
Carrier gas flow rate for packed column*	30 mL/min
Volume of loop for TCD*	146 µL (measured by water and capillary syringe)
TCD temperature*	200 °C

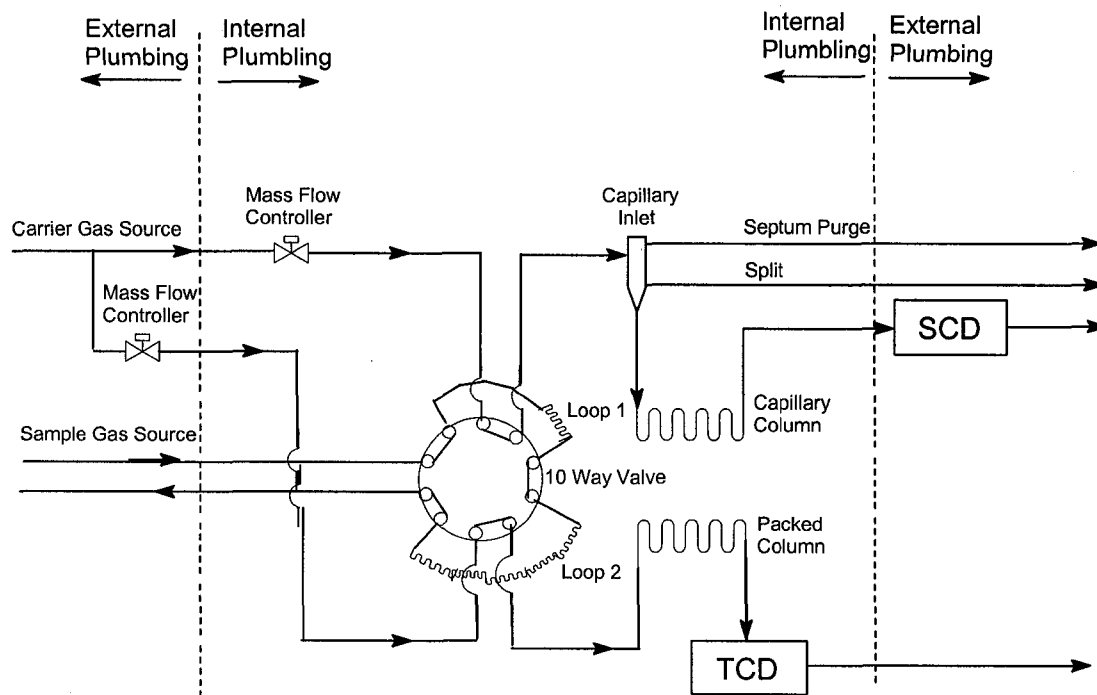


Figure 2-1. Schematic drawing of parallel sulfur chemiluminescence and thermal conductivity detector within one gas chromatograph.

the conditions that the manufacturer suggested: 40 mL/min air (Praxair Products), 100 mL/min hydrogen (Praxair Products), 34.6 kPa and 800°C.

2.2.2.3 Gas sample preparation

The following mixtures were used: 1.49% H₂S (balance: methane; Praxair Products), 3% SO₂ (balance: nitrogen; Union Carbide, Quebec, Canada), and 5% COS (balance: nitrogen; Matheson Gas Products, Toronto, Ontario, Canada). Liquid reagents (R grade) such as carbon disulfide (Fisher Scientific, NJ), 1-propyl mercaptan (Eastman Kodak Company, Rochester, NY), thiophene (Aldrich Chemical Company, WI) and 1-propanol (Fisher Scientific) were used to prepare additional sulfur-containing gas samples. Non-sulfur-containing gases included nitrogen (Praxair Products), carbon dioxide (Union Carbide Canada), and ethylene (Union Carbide Canada). Mass flow controllers (Sierra Instruments, Monterey, CA) were used to control the gas flow rates. Each liquid component (CS₂, thiophene, or C₃H₇SH) was introduced into the gas sample by bubbling nitrogen through a propanol solution of the sulfur-containing compounds. Their amount was determined from the gas-liquid equilibrium data and an assumption that the composition of the solution does not change because a large volume of solution was used. The compositions of the sample gases used in this study are listed in Table 2-2. The error in the data was mainly contributed by the reading of the mass flow controller, estimated as large as ± 1 %.

2.2.3 Results and discussion

2.2.3.1 Separation test

A CP-Sil 5CB capillary column was designed to separate the sulfur species. However, the separation of H₂S and SO₂ was very sensitive to the oven temperature.

Table 2-2. Composition of gas samples

<i>Components</i>	<i>Sample 1</i>	<i>Sample 2</i>	<i>Sample 4</i>	<i>Sample 4</i>	<i>Sample 5</i>
CH ₄ (%)	8.70	13.8	9.11	7.45	5.89
CO ₂ (%)	8.07	13.0	8.59	7.05	5.55
C ₂ H ₄ (%)	5.98	0	0	0	0
H ₂ S (ppm)	1300	2090	1370	1130	890
SO ₂ (ppm)	991	1540	1020	835	658
COS (ppm)	1440	2320	1530	1260	991
CS ₂ (ppm)	139	224	148	121	95.4
Thiophene (ppm)	69.4	112	73.8	60.6	47.7
C ₃ H ₇ SH (ppm)	69.4	112	73.8	60.6	47.7
Balance gas	N ₂				

Therefore, using sample gas number 1, oven temperatures around the suggested value were chosen to test the separation until an optimum temperature or temperature program at which H₂S and SO₂ can both be separated satisfactorily was finally found. Figure 2-2 shows the SCD responses to typical sulfur compounds at the optimum temperature program, indicating a satisfactory separation allowing a good quantitative analysis of H₂S and SO₂.

Once the oven temperature or temperature program was determined, a packed column was to be available to separate properly the common non-sulfur compounds such as N₂, CO₂, CH₄, ethylene as well as sulfur-containing compounds in large concentrations (H₂S, SO₂, and COS). A commercial packed column (HayseSep DB SS column, 100/120 mesh, 3 m × 3.2 mm o.d.), designed to separate sulfide and hydrocarbons, was found not to perform well at the selected temperature. A column was fabricated by changing the parameters such as the length of the column, the packing type (R, Q and QS of the Porapak packing), and the carrier gas flow rate. Finally, the following specifications were chosen for the packed column: the packing type: Porapak Q; the column length: 3 m; the column diameter: 3.2 mm o.d.; the carrier gas flow rate: 30 mL/min. And this packed column performed well at the chosen temperature. Figure 2-3 shows the TCD chromatogram of certain sulfur species of higher concentrations and non-sulfur containing species.

Thus, all the conditions under which the capillary column and the self-made packed column reached a satisfactory separation with sample gas number 1 have been determined.

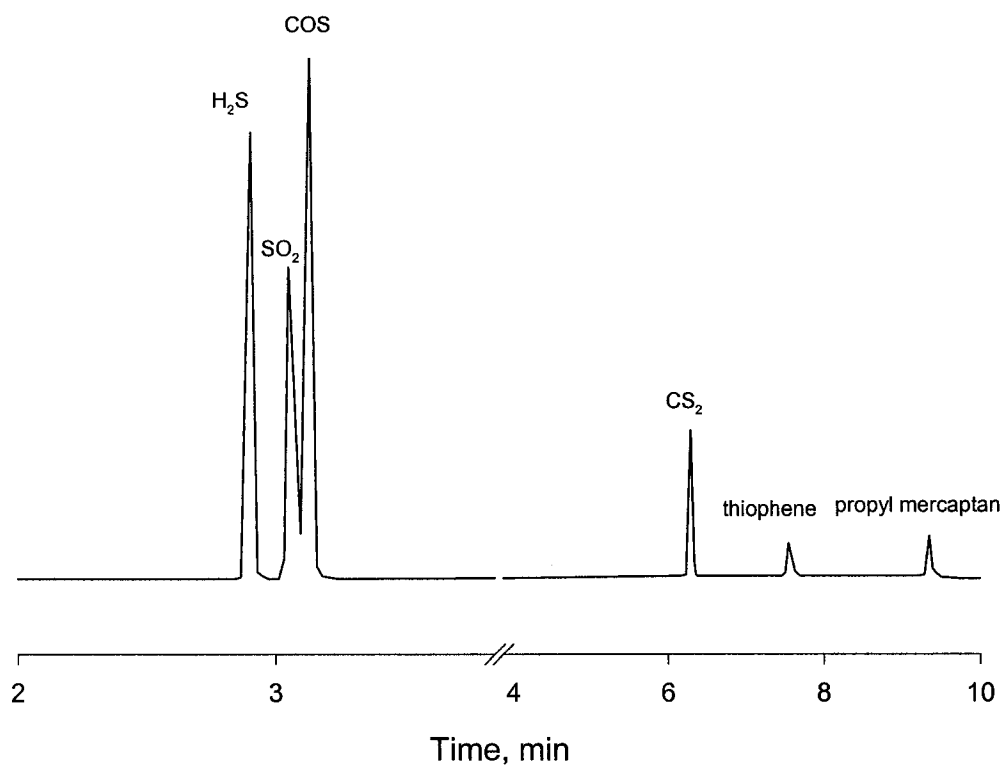


Figure 2-2. SCD chromatogram of typical sulfur-containing compounds separated using a CP-Sil PCB capillary column at a chosen temperature program. Oven temperature: 75°C for 3 min, to 120°C at 20°C/min and held for 10 min.

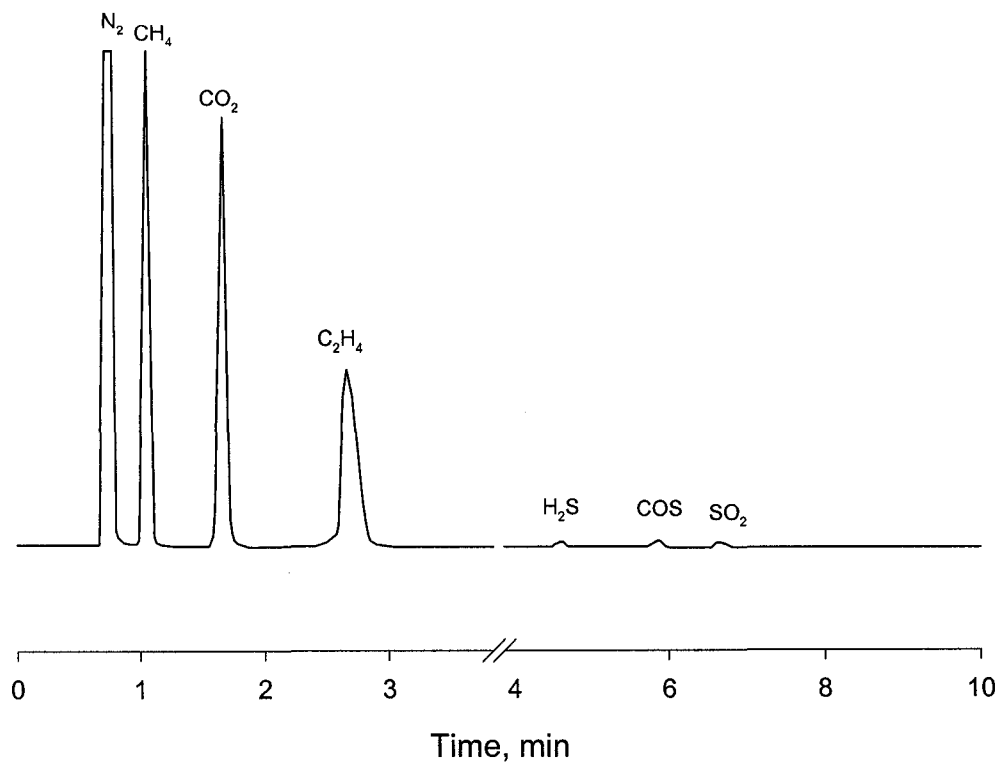


Figure 2-3. TCD chromatogram of sulfur and non-sulfur containing gas mixture separated using a packed column with Parapak Q packing at a chosen temperature program. Oven temperature: 75°C for 3 min, to 120°C at 20°C/min and held for 10 min.

2.2.3.2 Linearity and measuring range

A variety of concentrations of H₂S (from 20 ppm to 20 %) were used to determine the linearity of the signals and the measuring range. The response intensity plotted against the H₂S concentration is shown in Figure 2-4. The SCD signals show good linearity from 20 ppm to 10,000 ppm (1 %) and a large response factor (4000). Although a concentration lower than 20 ppm was not measured, such a large response factor indicates that the SCD should easily detect the sulfur species at ppb levels. The linear TCD response covers the H₂S concentration range from 500 ppm to 20 %, also shown in Figure 2-4. Therefore, coupling SCD and TCD in parallel to a single GC greatly extended the measuring range of sulfur compounds, compared to the GC with only a single detector.

It should be mentioned that even though the linearity of the SCD could cover the sulfur concentration up to 10,000 ppm, the SCD was designed for the measurement of the sulfur-containing compounds at lower concentrations. The frequent exposure of the detector to high content sulfur samples may cause adverse influence on its precision, resolution, linearity and even the life span of the equipment.

2.2.3.3 Calibration curves

Gas samples #2-5 were used for calibrations. The results shown in Figure 2-5 clearly illustrate that the linear calibration curves for different sulfur species do not coincide but have different response factors. Although this observation agrees with that obtained by other researchers (Hines, 1993; Harryman and Smith, 1994; Tang, et al., 1996, 1997; ASTM D5504-94, 1995), it is contrary with what Shearer (1993) reported

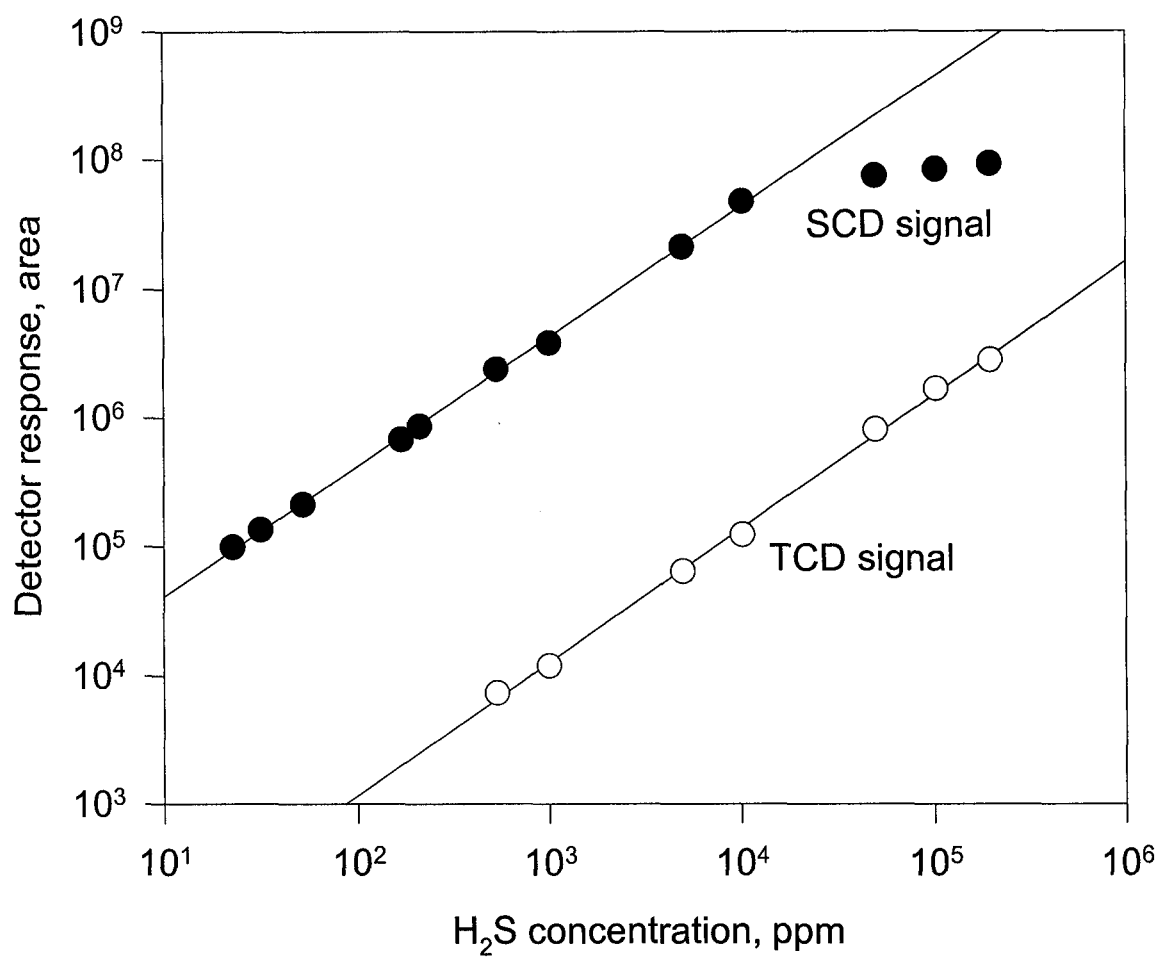


Figure 2-4. Detector linearity and measuring range. Oven temperature: 75°C for 3 min, to 120°C at 20°C/min and held for 10 min.

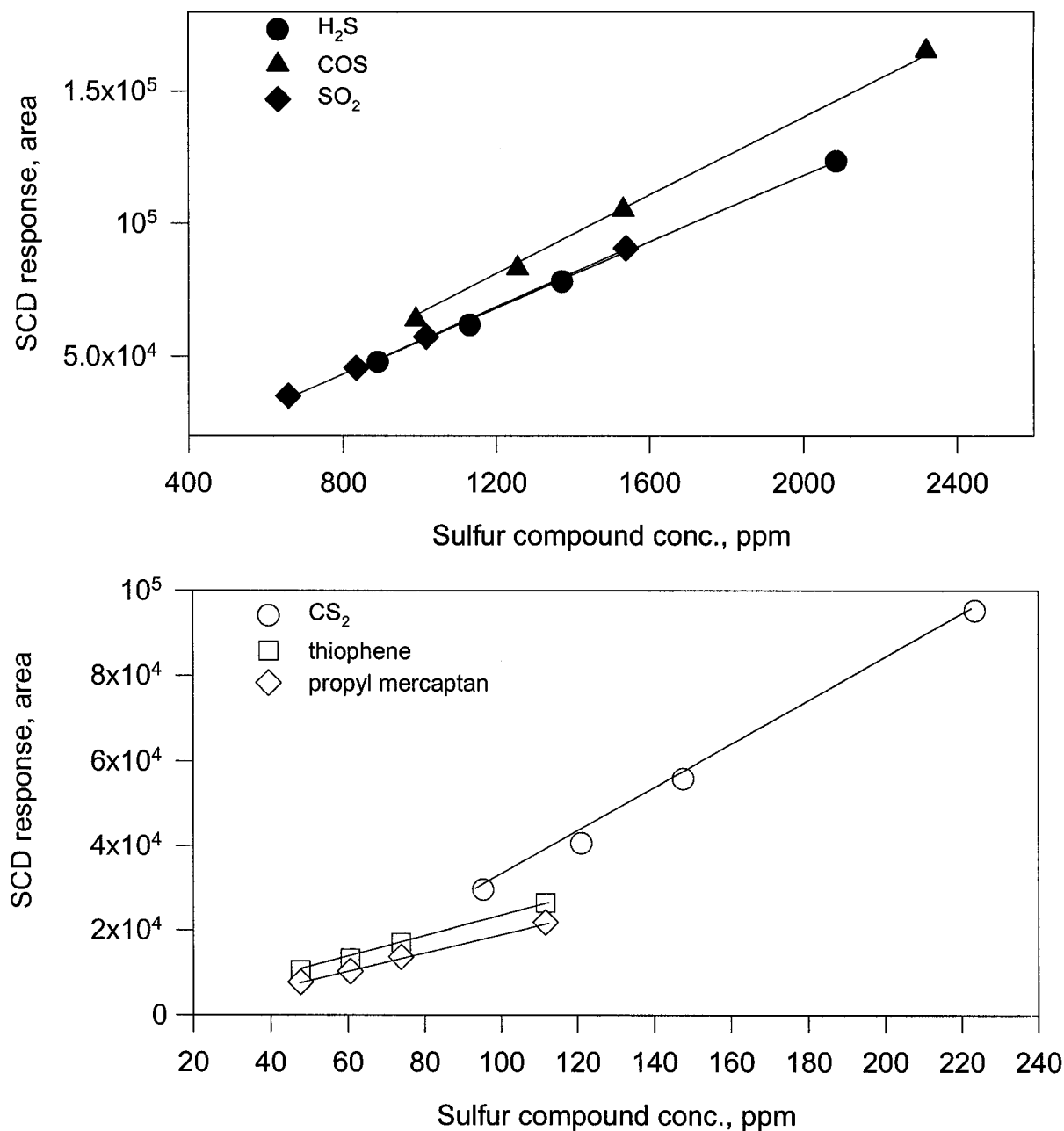


Figure 2-5. SCD calibration curves for selected sulfur compounds. Oven temperature: 75°C for 3 min, to 120°C at 20°C/min and held for 10 min.

from a theoretical point of view. Shearer believed that the SCD produced a linear response to sulfur and that all sulfur species should be equivalent on a molar basis. In other words, the SCD signals of all sulfur species should fall on the same straight line in the plot of response versus concentration.

Different authors offer different explanations as to why various sulfur species show different response factors. Tang, et al. (1997) studied the response factors of sulfur compounds using the SCD coupled with GC and pointed out that many factors may contribute to the differences in response. These factors included those relating to the SCD, such as the ceramic probe position, the H₂/air ratio for the flame ionization detector (FID); and, those relating to the GC, such as the initial and final oven temperatures, sample states and concentration, etc. Based on our results, it is believed that the differences in conversion for the sulfur species in the SCD burner are the main cause of the different responses. The capacity of the burner converting the effluent sulfur species into SO is certainly limited by conditions such as the H₂/air ratio to the FID, the burner temperature, the ceramic probe position, and even the amount of sulfur that is fed. The lower response at higher H₂S concentration (Figure 2-4) probably suggests that when the sulfur content in the effluent is high, the burner is unable to convert the sulfur species completely to SO. Generally speaking, as chemical reactions occur in the burner, the resulting conversion depends on the properties of the reactants and the reaction conditions determined by the burner. Therefore, differences in species and concentration could result in different conversion and accordingly, in different responses. Relative to the reactions converting sulfur species to SO, the reaction $\text{SO} + \frac{1}{2} \text{O}_2 = \text{SO}_2$ that takes place in the chemiluminescence reaction cell does not seem to be the major factor in

accounting for the differences in response factors. Finally, the calibration results of the TCD in the combination, shown in Figure 2-6, does not appear to have any difference from that obtained in a GC with TCD only.

2.3 Preliminary Experiments

2.3.1 Introduction

As mentioned previously, the aim of the preliminary experiments was to study the interaction between sulfuric acid and the possible components that are present in the gas streams from which H₂S is to be removed. Although the literature may tell us whether or not these compounds would interact with sulfuric acid, it was necessary to measure these reactions and their conversion at our laboratory conditions.

The chemical properties, especially those relating to the interaction with sulfuric acid, of the compounds involved in the preliminary experiments are reviewed as follows. Methane and other light alkanes are not reactive to sulfuric acid of any concentration. However, Ethylene and other short olefins are reactive. They react with electrophilic reagents like strong acids (Sundaram, 2001). The hydration of ethylene can be catalyzed by sulfuric acid of 90 - 98 wt %, forming ethyl sulfate as an intermediate, which, in turn, forms ethyl alcohol as the final product. The dilute sulfuric acid can also help the other addition reaction of ethylene (Orchin, et al., 1980). The chemistry of molecular nitrogen is marked by its relative inertness (Henrici-Oliver, 1976). It does not react with sulfuric acid. Hydrogen is also stable to sulfuric acid. Carbon monoxide and carbon dioxide are inert to sulfuric acid of any concentration. Sulfur dioxide dissolves in sulfuric acid of any concentration (Sander, et al., 1984). Carbonyl sulfide does not

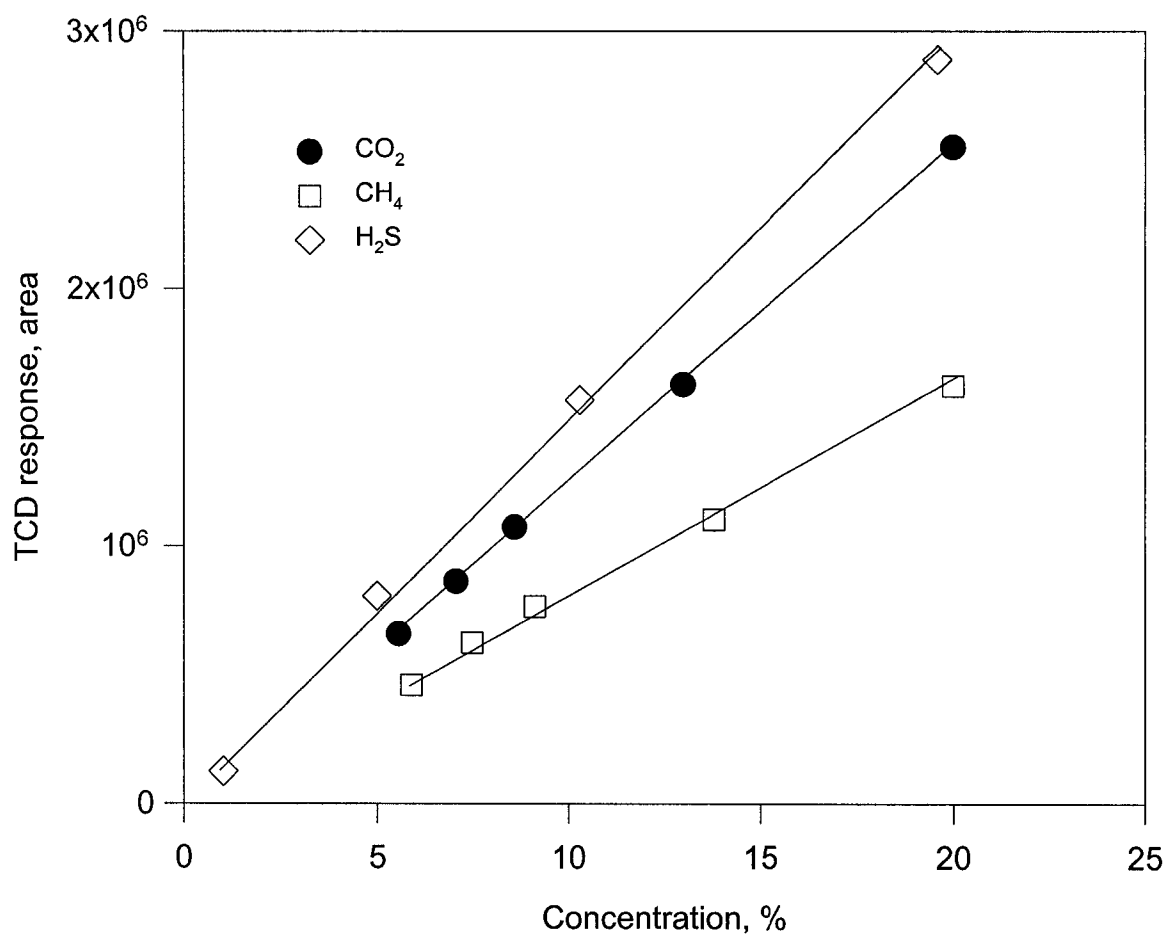


Figure 2-6. TCD calibration curves for selected compounds. Oven temperature: 75°C for 3 min, to 120°C at 20°C/min and held for 10 min.

interact with sulfuric acid (Weil, 1997). Contrarily, carbon disulfide undergoes oxidation and hydrolysis (Smith, 1993), which would take place with or in sulfuric acid solution. Mercaptan is able to undergo oxidation with chlorine, oxygen, elemental sulfur and hydrogen peroxide (Roberts, 1997). It is believed that it can be oxidized by concentrated sulfuric acid, though this information was not found. Strong oxidizing agents can rupture the thiophene ring structure, leading to maleic acid as the product (Fuller, L. S., 1997). This oxidation could occur with concentrated sulfuric acid.

2.3.2 Experimental section

A semi-batch operation, as shown in Figure 2-7, where the liquid is kept in the reactor and the gas continuously flows through the liquid, was applied. The reactor was a cylindrical pyrex vessel of 79 mm i.d. and 700 mL in capacity. Two baffles were attached to the inner wall to maintain the liquid surface flat. Two impellers (one for each of the two phases) were placed at the center, driven by the same shaft, which, in turn, was driven by a variable-speed motor (Baldor Electric CO., Pt. Smith, AR). The flow rates of gas components were controlled by mass flow controllers (Sierra Instruments, Inc., Monterey, CA), which were calibrated using the BIOS primary air flow meter, Model DryCal DC-2M (BIOS International Corporation, Pompton Plains, NJ). The gas mixture was directed to the bottom of the reactor, bubbling through the liquid phase and exiting from the top of reactor. The concentration of every component in the gas, both feeding in and exiting from the reactor, was measured using the method established in section 2.2.

Concentrated sulfuric acid of about 96 wt% was purchased from Fisher Scientific. The solutions with lower acid concentration were prepared by dilution with

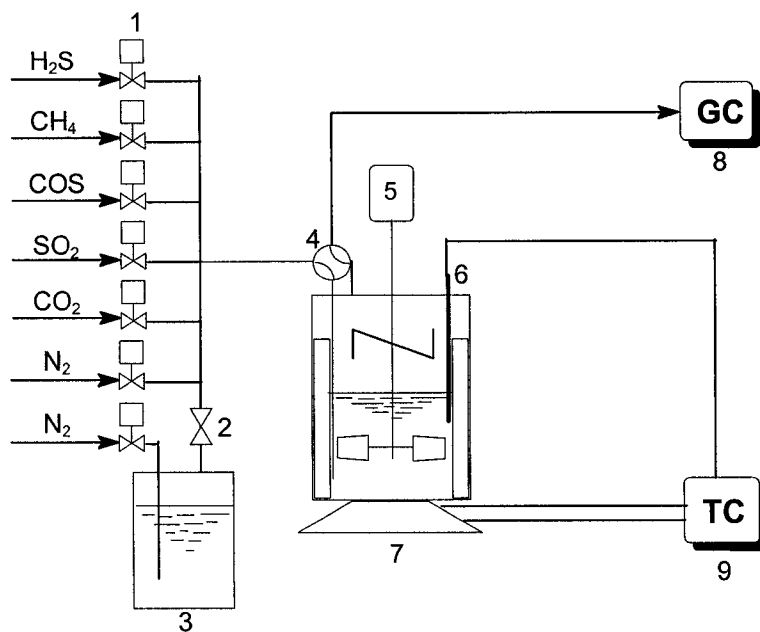


Figure 2-7. Schematic drawing of semibatch reactor for preliminary experiments. 1. mass flow controllers; 2. stop valve; 3. propanol solution of CS_2 , $\text{C}_3\text{H}_7\text{SH}$ and thiophene; 4. 4-way valve; 5. motor; 6. thermocouple; 7. hot plate; 8. gas chromatograph; 9. temperature controller.

water. The acid concentration was determined by titration using 0.1 N sodium hydroxide solution (Fisher Scientific) and 0.1 % methyl orange solution (Fisher Scientific) as the indicator. For every run of the experiment, 400 mL of the sulfuric acid solution was charged into the reactor, which, in turn, was connected to the feed system. Then, the solution was heated to the preset temperature. The gas mixture was bubbled into the liquid in the reactor at the flow rate of 200 mL/min and the stirring speed was kept at 100 rpm. The composition of the tail gas was analyzed three times by sampling every 10 or 15 minutes. The concentration of acid in the remaining solution was measured by titration as described previously.

2.3.3 Results and discussion

A N₂-balanced mixture of CH₄, CO₂, C₂H₄, H₂S, COS, CS₂, thiophene, and propyl mercaptan was passed through sulfuric acid solutions of 80 wt % and 96 wt%, respectively, at 120°C. The qualitative results obtained from these runs indicate: 1) CH₄ and nitrogen did not interact with acid solution because no product was detected to indicate the occurrence of the interaction. 2) CO₂, COS and CS₂ also did not seem to have reactivity with sulfuric acid solution of either concentration, even though a trace amount of CS₂ was observed being hydrolyzed. 3) Significant conversions of H₂S, ethylene, thiophene and mercaptan by sulfuric acid from 80 to 96 wt% were observed. Because this chapter focused on the interaction between acid and components other than H₂S, the conversions of ethylene, COS, CS₂, mercaptan and thiophene, which showed reactivity when contacting the sulfuric acid solutions, were measured in addition to the products from the corresponding reactions. The two acid concentrations used in these measurements were 80 and 96 wt%. Tables from 2-3 to 2-7 list the results, each for one

Table 2-3. Conversion and products of COS contacting sulfuric acid at 120°C.

	<i>Feed</i>	<i>Effluents from</i>	
		96 wt % acid	80 wt % acid
COS	20 %	20 %	20 %
H ₂ S	714 ppm	0	570 ppm
CO ₂	172 ppm	170 ppm	168 ppm
CS ₂	143 ppm	142 ppm	125 ppm
SO ₂	0	450 ppm	0

Table 2-4. Conversion and products of CS₂ contacting sulfuric acid at 120°C.

	<i>Feed</i>	<i>Effluents from</i>	
		96 wt % acid	80 wt % acid
CS ₂	20 %	20 %	20 %
H ₂ S	0	0	0
CO ₂	0	0	0
COS	0	6 ppm	38 ppm
SO ₂	0	7 ppm	0

Table 2-5. Conversion and products of mercaptan contacting sulfuric acid at 120°C.

	<i>Feed</i>	<i>Effluents from</i>	
		96 wt % acid	80 wt % acid
C ₃ H ₇ SH	10 %	0	220 ppm
H ₂ S	0	0	0
CO ₂	0	0	0
COS	0	0	0
CS ₂	0	0	0
SO ₂	0	5.61 %	3.80 %

Table 2-6. Conversion and products of thiophene contacting sulfuric acid at 120°C.

	<i>Feed</i>	<i>Effluents from</i>	
		96 wt % acid	80 wt % acid
Thiophene	10 %	0	250 ppm
H ₂ S	0	0	0
CO ₂	0	0	0
COS	0	0	0
CS ₂	0	0	0
SO ₂	0	260 ppm	1470 ppm

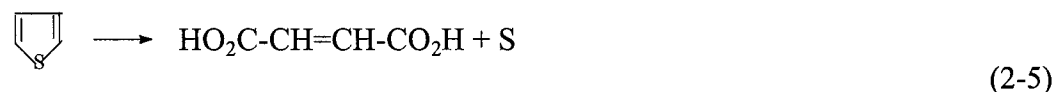
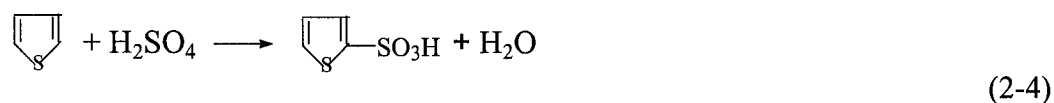
Table 2-7. Conversion and products of ethylene contacting sulfuric acid at 120°C.

	<i>Feed</i>	<i>Effluents from</i>	
		96 wt % acid	80 wt % acid
Ethylene	5 %	0.14 %	2.62 %
H ₂ S	0	0	0
CO ₂	0	0	0
COS	0	0	0
CS ₂	0	0	0
SO ₂	0	3000~3500 ppm	0

substance mentioned. COS does not seem to be converted in sulfuric acid of either concentration. Even after increasing the temperature to 180°C, no reaction was observed. However, the COS supply cylinder contains 3575 ppm of H₂S, 859 ppm of CO₂ and 714 ppm of CS₂. When COS was diluted to 20% by mixing with nitrogen, they were diluted accordingly. The conversions of H₂S and CS₂ by sulfuric acid of 96 wt% and 80 wt%, respectively, are in agreement with the results when they individually react with these solutions (Table 2-3). The SO₂ present in the exit gas was from the H₂S oxidation. When CS₂ was passed through the solutions, traces of COS were observed in the exit gas, indicating that a very small amount of hydrolysis had taken place, i.e.,



The produced H₂S was oxidized in sulfuric acid of 96 wt %, forming SO₂. It seemed that more COS was formed in the solution of 80 wt% than of 96 wt%. Nearly complete conversions were observed when propyl mercaptan and thiophene were passed through separately the sulfuric acid solutions of 96 wt% and 80 wt%. However, gas products such as CO₂ and SO₂ were not detected by GC, probably indicating an incomplete oxidation which produced products which remained in the liquid. From knowledge of organic chemistry (Jones, 1997), the likely reactions are:



The interaction between ethylene and sulfuric acid was also studied individually because it is present in refinery flare gas. Table 2-7 shows the ethylene conversion and product distribution. For 96 wt% acid, 5% ethylene in the feed gas was converted by 97.2%, leaving 0.14% in the effluent. About 3,000 - 3,500 ppm of SO₂ were also observed in the effluent. The colorless acid solution turned black during the reaction. This evidently indicated that deep oxidation of ethylene



may happen to some extent. However, the products from the bulk of the ethylene reaction(s) remained unknown. In 80 wt% sulfuric acid solution, the ethylene conversion was 47.7%. No SO₂ was detected in the effluent. An alcohol smell came from the reactor when it was disconnected. Combining this observation and the knowledge of organic chemistry (Jones, 1997) suggests that the hydration of ethylene had occurred.

2.4 Conclusions and Recommendations

The single GC coupled with parallel SCD and TCD is able to analyze sulfur and non-sulfur containing compounds simultaneously. Such a combination of the SCD and the TCD extends the sulfur detection range by a single GC, which now covers from ppb levels to percentage levels. In addition to allowing the measurement of both low and high concentrations of sulfur species, the simultaneous sampling and analysis of sulfur- and non-sulfur-containing gases eliminates errors arising from the multiple sample injection. The establishment and completion of this GC separation and detection method provided much ease and convenience and reliable analysis results not only in this

experimental work but also to any GC user who is involved in the analysis of sulfur-containing gases.

The preliminary experiments, including the literature review in this section, show that methane, CO and nitrogen are inert to sulfuric acid. CO₂, COS and CS₂ are not converted by sulfuric acid, although trace amounts of CS₂ were hydrolyzed. The sulfuric acid converts propyl mercaptan and thiophene to nearly 100 %, meaning these sulfur-containing components can be removed from the gas using process. However, the conversion of ethylene by sulfuric acid renders this process unsuitable when treating the gas in which ethylene and other olefins are valuable constituents.

2.5 Cited literature

- ASTM, America Society for Testing and Materials, "D5504-94 Standard Test Method for Determination of Sulfur Compounds in Natural Gas and Gaseous fuel by Gas Chromatography and Chemiluminescence". Philadelphia, PA: *Annual Book of ASTM Standards* (1995) Vol 05.
- Benner, R. L., and D. H. Stedman, "Universal Sulfur Detection by Chemiluminescence", *Anal. Chem.*, **61**, 1268-1271 (1989).
- Chawla, B., and F.D. Sanzo, "Determination of Sulfur Components in Light Petroleum Stream by High-resolution Gas Chromatography with Sulfur Chemiluminescence Detection", *J. Chromatogr.*, **32**, 271-279 (1992).
- Fuller, L. S., "Thiophene and Thiophene Derivatives", *Kirk-Othmer Encyclopedia of Chemical Technology*, John Wiley & Sons, Inc. (1997).
- Harryman, J. M., and B. Smith, "Sulfur Compound Distribution in NGL: Plant Data GPA Section A Committee, Plant Design", *Proc. of 73th GPA Annual Convention*, 118-122 (1994), March 10-12, San Antonia, Texas, USA.
- Hines, W. J., "Sulfur Speciation by Capillary Gas Chromatography and Sulfur Chemiluminescence Detection - GPA Sulfur Research Project", *Proc. of 72th GPA Annual Convention*, 50-54 (1993), March 11-13, New Orleans, Louisiana, USA.
- Henrici-Oliver, G., *Coord. Catal.*, **9**, 289 (1976).
- Jones, M., *Organic Chemistry*, W. W. Morton & Company, New York (1997).
- Lechner-Fish, T. J., "Analysis of Natural Gas-mixture Using Multidimensional Gas Chromatography", *American Laboratory*, **28**(21), 37-41 (1996).

- Roberts, J. S., "Thiols", *Kirk-Othmer Encyclopedia of Chemical Technology*, John Wiley & Sons, Inc. (1997).
- Sander, U. H. F., H. Fischer, U. Rothe, and R. Kola, *Sulfur, Sulfur, Sulfur Dioxide and Sulfuric Acid*, edited by A. I. More, The British Sulfur Corporation Ltd. p159, (1984).
- Shearer, R. L., D. L. O'Neal, R. Rios, and M. D. Baker, "Analysis of Sulfur Compounds by Capillary Column Gas Chromatography with Sulfur Chemiluminescence Detection", *J. Chromatogr. Sci.*, **28**, 24-28 (1990).
- Shearer, R. L., "Development of Flameless Sulfur Chemiluminescence Detection: Application to Gas Chromatography", *Anal Chem.*, **64**, 2192-96 (1992).
- Shearer R. L, E. B Poole and J. B. Nowalk, "Application of Gas Chromatography and Flameless Sulfur Chemiluminescence Detection to the Analysis of Petroleum Products", *J. Chromatogr. Sci.*, **31**, 82-87 (1993).
- Sievers Instruments, Inc., *SCDTM 355 Operation and Service Manual*, Reversion C, 1996.
- Smith, D. E., and R. W. Timmerman, "Carbon Dioxide", *Kirk-Othmer Encyclopedia of Chemical Technology*, John Wiley & Sons, Inc. (1993).
- Sundaram, K. M., M. M. Shreehan, and E. F. Olszewski, "Sulfur Removal and Recovery", *Kirk-Othmer Encyclopedia of Chemical Technology*, John Wiley & Sons, Inc. (Web version, 2001).
- Tang, H., P. Heaton and M. Hadley, "A Multipurpose Sampling Loop for Analysis of Nanogram to Milligram per Cubic Meter Levels of Sulfur Compounds in the

Atmosphere, Natural gas and Gaseous Fuels”, *J. Environ. Anal. Chem.*, **64**, 59-69 (1996).

Tang, H., P. Heaton, B. Brassard and J. Dunbar, “A Study of Response Factors of Sulfur Compounds in a Sulfur Chemiluminescence Detector with GC”, *American Laboratory*, **29**(25), 26-27 (1997).

Weil, E. D., and S. R. Sandler, “Sulfur Compounds”, *Kirk-Othmer Encyclopedia of Chemical Technology*, John Wiley & Sons, Inc. (Web version, 1997).

Wilhite, W. F., and O.L. Hollis, “The Use of Porous-Polymer beads for Analysis of the Martian Atmosphere”, *J. Chromatogr.*, **6**, 84-88, (1966).

Chapter 3

Chemistry of Reactions between Hydrogen Sulfide and Sulfuric Acid*

3.1 Introduction

Little information has been available dealing with the chemistry of reactions between hydrogen sulfide and sulfuric acid, since the interaction between them was first reported in 1858 (Geuther, 1858). Although Snurnikov (1967) observed that solid sulfur, sulfur dioxide and water were produced when hydrogen sulfide and concentrated sulfuric acid reacted, the stoichiometry of any single reaction did not agree with the results from mass balance measurements for this reaction system. In addition, no data are available regarding the influence of temperature and acid concentration on the product distribution from the reaction.

The aim of this chapter is to determine the individual reactions that occur in the H₂S-sulfuric acid gas-liquid reaction system. The strategy used in this study is, (1) to list all the possible reactions between H₂S and species likely present in sulfuric acid solutions of the entire concentration range, (2) to exclude the reactions that are either summative of others or insignificant under the chosen conditions, (3) to examine the remaining reactions experimentally and exclude those that do not occur actually, and (4) to

* A version of this chapter has been published in *Ind. Eng. Chem. Res.*, **39**, 2505 (2000). Another version has been accepted for publishing by *Canadian Journal of Chemical Engineering* (February 2003 issue).

determine the reaction network of the system and its stoichiometry using mass balance measurements.

3.2 Thermodynamic Analysis

Sulfuric acid solutions at different concentrations are used in this study. The solution, as one of the reactants, may contain more than one species which complicates the analysis. It is necessary to determine which of the species present in sulfuric acid solutions may react with H₂S. Pure sulfuric acid (100 wt%) contains not only molecules of H₂SO₄ but also cations and anions resulting from,



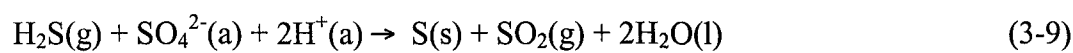
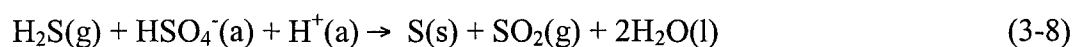
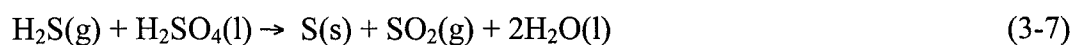
The mole fraction of H₂SO₄ molecules is as large as 99.58 % (Durrant 1970). Diluting the pure sulfuric acid with water may lead to more ions such as H₃O⁺, H⁺, H₅SO₅⁺, HSO₄⁻ and SO₄²⁻ (Durrant, 1970; Sander, et al., 1984) by virtue of the following reactions



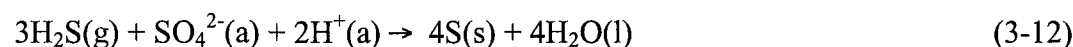
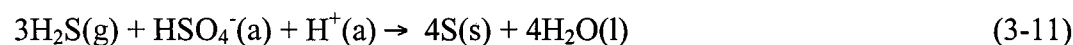
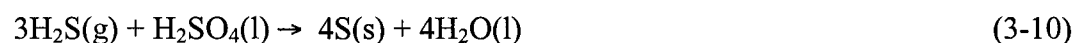
In summary, the species likely present in sulfuric acid solutions of concentrations from 0 to 100 wt% are H₂O, H₂SO₄, HSO₄⁻, SO₄²⁻, HS₂O₇⁻, H⁺, H₃O⁺, H₃SO₄⁺, H₅SO₅⁺. Young and Walrafen (1961) observed the sulfur-containing species which are present in relatively large concentrations in the solution and determined their molarity against the wt% concentration using photoelectric Raman spectroscopic measurements (Figure 1-2).

From this figure, it can be seen that the presence of H_5SO_5^+ may be neglected because its amount is relatively much smaller than those of H_2SO_4 and HSO_4^- in concentrated sulfuric acid. Thus, above 80 wt%, H_2SO_4 and HSO_4^- are the two possible reactive species; below 80 wt%, HSO_4^- and SO_4^{2-} are the possible reactive species. The possible reactions between H_2S and these species are listed in the following three groups.

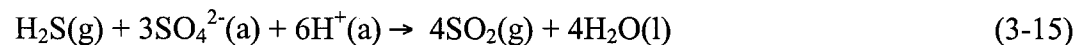
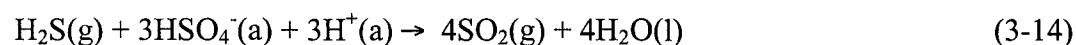
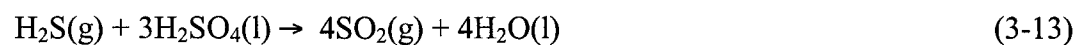
Group (a)



Group (b)



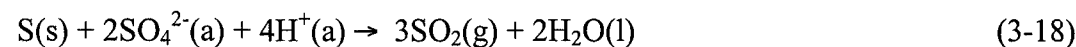
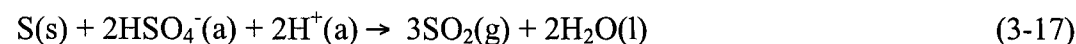
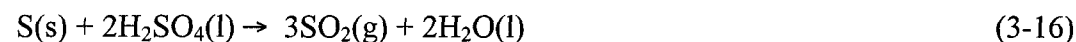
Group (c)



The possible reactions between the produced sulfur and the species are listed in Group

(d):

Group (d)



Theoretically, there would be more reactions in the system, for instance, the reactions between produced sulfur and either H₂S or SO₂. But these reactions will never take place in terms of the knowledge of chemistry. Besides, the reaction between H₂S and SO₂ must be taken into account. Klein (1911) has shown that the reaction between hydrogen sulfide and sulfur dioxide in gas phase does not occur at all without the presence of a third liquid or solvent or a catalyst. Thus, in this system, the produced SO₂ dissolves or stays in sulfuric acid solution



and reacts with H₂S



In the above chemical reaction equations, the letter in the parenthesis after the chemical symbols represents the state of that substance. “g”, “l” and “s” denote *gas*, *liquid*, and *solid*, respectively; and “a” denotes *aqueous*. Using the HSC Chemistry Windows, a commercially available software package (Roine, 1993)*, the thermodynamic properties such as the heat of reaction, ΔH_{rxn} , the Gibbs free energy change, ΔG_{rxn}^0 , and the chemical equilibrium constant, K , for the reactions are calculated. The results at 25°C and 1 atm are

* HSC uses the following definitions to calculate the enthalpy, entropy, and Gibbs free energy for each of the chemical formula and the equilibrium constant for every reaction equation at a particular T , e.g., $H(T)$, $S(T)$, $G(T)$ and K :

$$H(T) = Hf(298) + \int_{298}^T Cp(T)dT + Htr \quad (a)$$

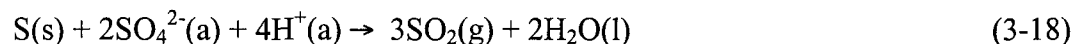
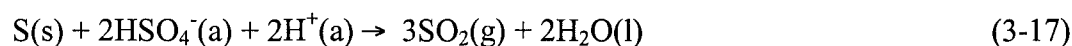
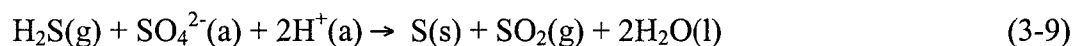
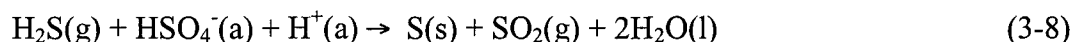
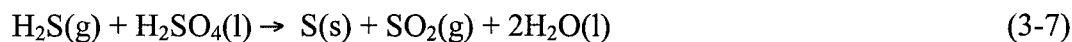
$$S(T) = S^0(298) + \int_{298}^T \frac{Cp(T)}{T} dT + \frac{Htr}{Ttr} \quad (b)$$

$$G(T) = H(T) + T * S(T) \quad (c)$$

$$K = \exp\left(-\frac{\Delta G(T)}{RT}\right) \quad (d)$$

where, $Cp(T)$ is the specific heat, $Hf(298)$ the standard enthalpy of formation, Htr the enthalpy of phase transitions, $S^0(298)$ the standard entropy, and Ttr the transformation temperature. K takes the unit according to the individual reaction equation.

shown in Table 3-1. Obviously, either the reaction equations or the thermodynamics properties indicate that these reactions are not independent. For instance, reaction (3-10) is the summation of reactions (3-7), (3-19) and (3-20). Disregarding those being summative of others, eight reactions remain as follows,

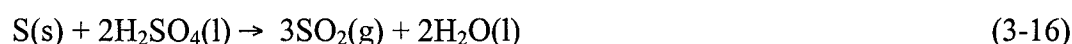
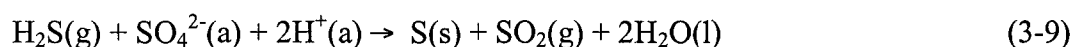
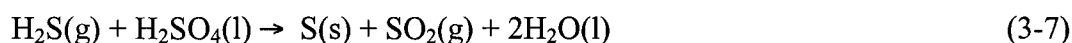


The algebra analysis on the array constituting of the stoichiometric coefficients of the reactions (Reklaitis, 1983) illustrates that this eight reactions represent as the same reaction system as all the reactions in Table 3-1 do, as shown in Appendix D. It also shows that five independent reactions are among those reactions. In other words, those eight reactions are still not independent. Further analysis indicates that the first six reactions relate with each other by the dissociation of H_2SO_4 , *i.e.*, reactions (3-5) and (3-6). In spite of the dependence, the purpose of this study is to determine which reaction does occur in this gas-liquid reaction system of H_2S and sulfuric acid, including the reactions between ions. Following up, therefore, the significance of the seven reactions - reaction (3-19) is a phase change process and has been studied elsewhere (Zhang et al., 1998) - will determined from their thermodynamic properties. Chemical thermodynamics

Table 3-1. Possible reactions and their thermodynamic properties at 25°C

Reactions	Equation No.	ΔH_{rxn} , kJ mol ⁻¹	ΔG_{rxn}° , kJ mol ⁻¹	K
$\text{H}_2\text{S}(\text{g}) + \text{H}_2\text{SO}_4(\text{l}) = \text{S} + \text{SO}_2(\text{g}) + 2\text{H}_2\text{O}(\text{l})$	(3-7)	-34.012	-51.127	$9.08 \times 10^{+08}$
$\text{H}_2\text{S}(\text{g}) + \text{HSO}_4^-(\text{a}) + \text{H}^+(\text{a}) = \text{S} + \text{SO}_2(\text{g}) + 2\text{H}_2\text{O}(\text{l})$	(3-8)	39.426	14.825	2.53×10^{-03}
$\text{H}_2\text{S}(\text{g}) + \text{SO}_4^{2-}(\text{a}) + 2\text{H}^+(\text{a}) = \text{S} + \text{SO}_2(\text{g}) + 2\text{H}_2\text{O}(\text{l})$	(3-9)	61.392	3.484	2.45×10^{-01}
$3\text{H}_2\text{S}(\text{g}) + \text{H}_2\text{SO}_4(\text{l}) = 4\text{S} + 4\text{H}_2\text{O}(\text{l})$	(3-10)	-267.826	-158.515	$5.94 \times 10^{+27}$
$3\text{H}_2\text{S}(\text{g}) + \text{HSO}_4^-(\text{-a}) + \text{H}^+(\text{+a}) = 4\text{S} + 4\text{H}_2\text{O}(\text{l})$	(3-11)	-194.389	-92.563	$1.65 \times 10^{+16}$
$3\text{H}_2\text{S}(\text{g}) + \text{SO}_4^{2-}(\text{-2a}) + 2\text{H}^+(\text{+a}) = 4\text{S} + 4\text{H}_2\text{O}(\text{l})$	(3-12)	-172.423	-103.904	$1.60 \times 10^{+18}$
$\text{H}_2\text{S}(\text{g}) + 3\text{H}_2\text{SO}_4(\text{l}) = 4\text{SO}_2(\text{g}) + 4\text{H}_2\text{O}(\text{l})$	(3-13)	131.78	-45.992	$1.14 \times 10^{+08}$
$\text{H}_2\text{S}(\text{g}) + 3\text{HSO}_4^-(\text{-a}) + 3\text{H}^+(\text{+a}) = 4\text{SO}_2(\text{g}) + 4\text{H}_2\text{O}(\text{l})$	(3-14)	352.093	151.863	2.47×10^{-27}
$\text{H}_2\text{S}(\text{g}) + 3\text{SO}_4^{2-}(\text{-2a}) + 6\text{H}^+(\text{+a}) = 4\text{SO}_2(\text{g}) + 4\text{H}_2\text{O}(\text{l})$	(3-15)	417.991	117.84	2.26×10^{-21}
$\text{S} + 2\text{H}_2\text{SO}_4(\text{l}) = 3\text{SO}_2(\text{g}) + 2\text{H}_2\text{O}(\text{l})$	(3-16)	165.792	5.135	1.26×10^{-01}
$\text{S} + 2\text{HSO}_4^-(\text{-a}) + 2\text{H}^+(\text{+a}) = 3\text{SO}_2(\text{g}) + 2\text{H}_2\text{O}(\text{l})$	(3-17)	312.667	137.038	9.76×10^{-25}
$\text{S} + 2\text{SO}_4^{2-}(\text{-2a}) + 4\text{H}^+(\text{+a}) = 3\text{SO}_2(\text{g}) + 2\text{H}_2\text{O}(\text{l})$	(3-18)	356.599	114.356	9.20×10^{-21}
$\text{SO}_2(\text{g}) = \text{SO}_2(\text{a})$	(3-19)	-26.192	-0.462	1.205
$2\text{H}_2\text{S}(\text{g}) + \text{SO}_2(\text{a}) = 3\text{S} + 2\text{H}_2\text{O}(\text{l})$	(3-20)	-207.652	-106.953	$5.49 \times 10^{+18}$

(Sandler, 1989) believes that reactions having positive ΔG_{rxn}^0 do not occur for practice purpose. In other words, reactions having equilibrium constant less than 1 would be regarded as insignificant reactions. Based on Figure 3-1, the chemical equilibrium constants of the seven reactions at the atmospheric pressure and temperatures from 0 to 120°C, the significant reactions in the system of H₂S and sulfuric acid are,



3.3 Experimental Section

Figure 3-2 shows the schematic diagram of the experimental apparatus. The reactor, 122 cm³ in volume and made of Pyrex glass, contained a magnetic stirring bar. The sulfuric acid solution in the reactor was heated using a hot plate coupled with a magnetic stirrer (Model 542A, Barnstead/Themolynn, Bubuque, IO, U.S.A.). The temperature was monitored using a microcomputer thermometer (Model DP701, Omega Engineering, Inc., Connecticut, U.S.A.) with a resolution of 0.1°C. A sensitive Heiss compound pressure gauge, which has a resolution of 0.25 psi, was used to measure the gas pressures within the reactor or the gas reservoir.

First, experiments were performed to determine which of the four reactions that would occur significantly under the experimental conditions. The reactor, charged with a known volume of sulfuric acid solution of known concentration, was connected to the feed system in the experimental setup. The solution was first heated by the hot plate to a

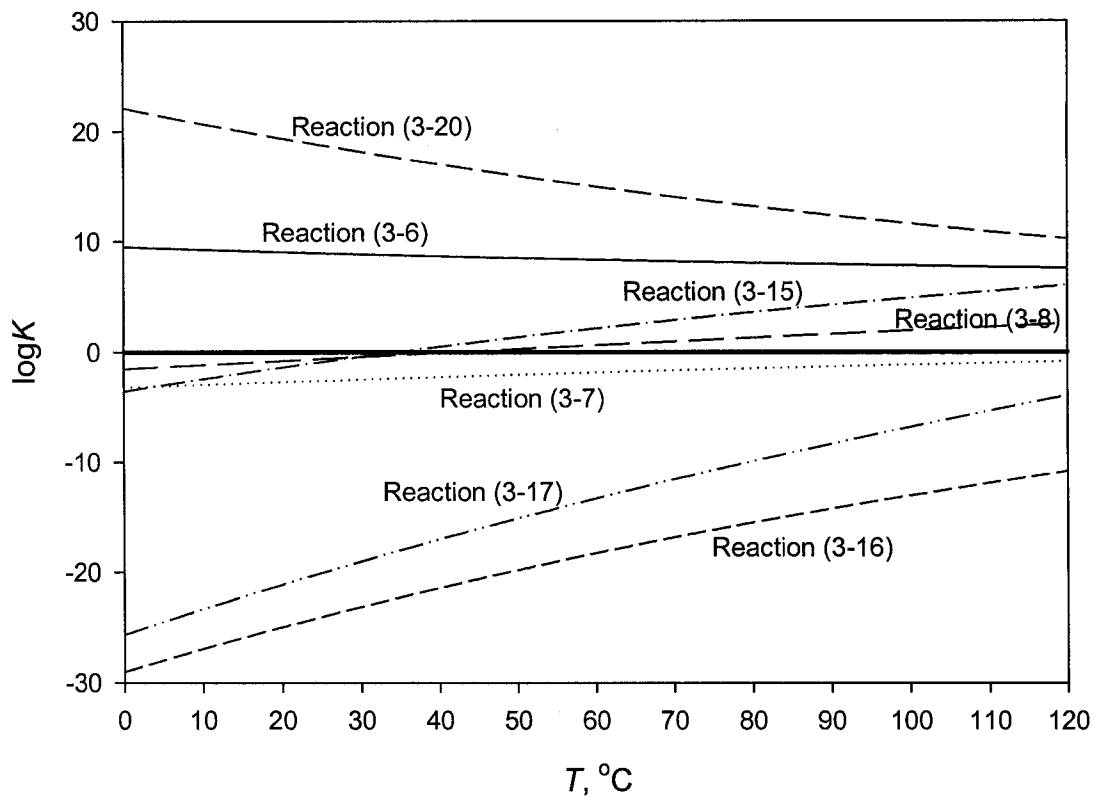


Figure 3-1. Chemical equilibrium constant for possible reactions over temperature range from 0 to 120°C.

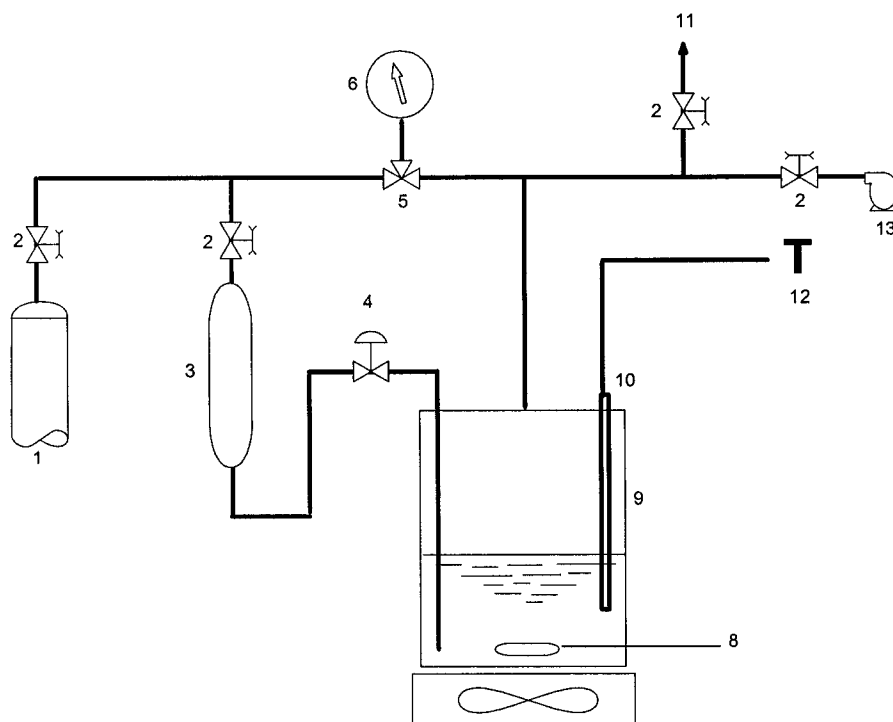


Figure 3-2. Schematic diagram of the batch reactor experimental setup.
 (1) H₂S cylinder; (2) stop valve; (3) gas reservoir; (4) needle valve;
 (5) three way valve; (6) Heiss compound pressure gauge;
 (7) hot plate and magnetic stirrer; (8) magnetic spin bar;
 (9) reactor of Pyrex glass; (10) thermocouple; (11) vent;
 (12) thermometer; (13) vacuum pump.

certain temperature while the air in the reactor was evacuated using an Edwards-5 2-stage vacuum pump (Edwards High Vacuum, Oakville, Ontario, Canada). Then, pure H₂S was introduced into the reactor from the reservoir and the reaction was monitored through the pressure change, the formation of sulfur, and the gas composition change before and after reaction.

Second, mass balance calculations were used to decide the stoichiometry of the reaction network. The experiment started with accurately (± 0.001 g) weighing the amount of acid solution (around 70g) to be charged to the reactor. Then, the solution was transferred into the reactor; the latter was installed in the feed system. The solution was purged using nitrogen and then evacuated under vacuum for 20 min to remove the dissolved oxygen. Afterwards, it was heated to the experimental temperature, 120°C. Hydrogen sulfide (>99.9%) was introduced from the cylinder into the reservoir to a known pressure. After the initial pressure of the reactor and temperature of the acid solution were recorded, H₂S was then introduced from the reservoir into the reactor. The final pressure in the reservoir was recorded. From the difference between the initial and final pressures of H₂S in the reservoir, and the volume of the reservoir, and the value of room temperature, the amount of H₂S fed into the reactor was calculated using the equation of state for an ideal gas. Immediately following the introduction of H₂S into the reactor, the stirrer was turned on and a strong mixing was established. The run was terminated when the pressure of the reactor was observed to remain unchanged by ± 0.25 psi over 30 min. Depending upon the acid concentration, runs lasted from 4 to 6 h. Then, the system was cooled down to room temperature and the pressure was recorded. Based on these measurements, the amount of gas (H₂S and/or SO₂) remaining in the

reactor was calculated. The gas in the reactor was sampled and its composition was analyzed using a gas chromatograph with chemiluminescence sulfur and thermal conductivity detectors. The details of the GC analysis were described in Chapter 2 and have been published by Wang, et al. (1998). The amount of SO₂ dissolved in the acid was estimated using SO₂ solubility data (Sander, et al., 1984) or a more recent correlation from our research group (Zhang, et al., 1998). These measurements showed the moles of H₂S consumed and the moles of SO₂ produced. The mixture of sulfur and acid was purged with nitrogen for 3 hours to remove any dissolved SO₂ gas before being weighed. The mixture was then heated at 140°C for 5 h and then cooled, enabling the sulfur to form large solid flakes which were easily separated by filtration. The separated sulfur was washed, dried and weighed. The concentration of the solutions was measured by titration using standard 0.1 N sodium hydroxide solution (Fisher Scientific, Nepean, Ontario, Canada), using 0.1% methyl orange solution (Fisher Scientific, Fair Lawn, New Jersey, U.S.A.) as an indicator. Using these results, the amount of sulfuric acid consumed and the amounts of sulfur and water produced were determined.

The sulfuric acid solutions of various concentrations were prepared by diluting ~96 wt% sulfuric acid (Fisher Scientific, Nepean, Ontario, Canada) with distilled water. The concentration of the solutions was also determined by titration. The cylinders of hydrogen sulfide (CP grade) and prepurified nitrogen were obtained from Praxair Products Inc. (Mississauga, Ontario, Canada).

3.4 Results and Discussion

3.4.1 Determination of possible reactions using experiments

The thermodynamic analysis suggests four independent reactions which may occur in the H₂S-sulfuric acid gas-liquid reaction system. Experiments were carried out to determine whether these reactions would occur under the conditions chosen for this study. The results are shown in Table 3-2. The Raman spectroscopy measurement by Young and Walrafen (1961) showed that the species in 96 wt% sulfuric acid are mainly H₂SO₄ and HSO₄⁻. The thermodynamic calculation has excluded the reaction between H₂S and HSO₄⁻ ions, *i.e.*, reaction (3-8). When H₂S was introduced into the reactor containing fresh acid solution of 96.04 wt% at 21°C and 120°C, respectively, not only a pressure drop but also the formation of sulfur was observed, indicating that the reaction between H₂S and molecular H₂SO₄, *i.e.*, reaction (3-7), occurred. Then, for the run at 120°C, the gas phase in the reactor, including SO₂ dissolved in the solution, was evacuated and an inert gas, nitrogen, was introduced. The sulfur and sulfuric acid slurry were heated and maintained at 140°C overnight. Neither production of SO₂ nor change in acid concentration was detected by GC and titration, respectively. As a result, the reaction between sulfur and molecular H₂SO₄, *i.e.*, reaction (3-16), does not occur during the experiments. Young and Walrafen (1961) also showed that the main species present in the solution of 30 wt% acid are HSO₄⁻ and SO₄²⁻. No reaction was observed for the solution of 29.60 wt% acid at 21°C and 50°C, indicating that both HSO₄⁻ and SO₄²⁻ do not react with H₂S or reactions (3-8) and (3-9) do not occur. When 30 wt% acid solution was previously saturated with SO₂ ($P_{SO_2} = 101.3$ kPa), the introduction of H₂S into the reactor caused both pressure drop in the gas phase and formation of sulfur in the liquid phase,

Table 3-2. Experimental results for determining possible reactions

Run#	Acid Concentration wt%	Temperature °C	Pre-saturated with SO ₂	Contact time	Pressure drop	Formation of sulfur	Components in product gas
BT1	96.04	21	No	120 s	Yes	Yes	H ₂ S, SO ₂
BT2	96.04	120	No	120 s	Yes	Yes	SO ₂
BT4	29.60	21	No	10 min	No	No	H ₂ S
BT5	29.60	50	No	10 min	No	No	H ₂ S, H ₂ O
BT6	29.60	21	Yes	5 min	Yes	Yes	H ₂ S, SO ₂
BT3	96.04 ^{a)}	140	No	15 h	No	No	N ₂

a) After the run, BT2, the SO₂ in the reactor, either in the gas phase or dissolved in the solution, was evacuated by a vacuum pump and the reactor was filled with N₂. Then, the solution, with formed sulfur in it, was heated to 140°C and maintained over night. The composition of the gas phase was analyzed using GC to check whether SO₂ was produced.

showing that reaction (3-20) takes place in the presence of dilute sulfuric acid solution.

Thus, two of the four reactions, *i.e.*,



could be excluded experimentally. The other two occurred in the experiments,



In this study, (3-7) was denoted as reaction 1 (or the first reaction), and (3-20) as reaction 2 (or the second reaction).

The experiments excluded the possibility for the following two reactions under the experimental conditions, even though the thermodynamics showed them to be feasible,



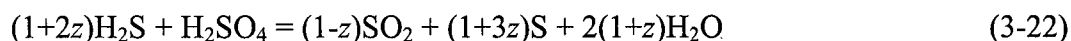
Probably, the reaction conditions do not favor them. The calculations show that both reactions are endothermic and that they may need considerable energy to initiate them. As a result, they likely take place at higher temperatures. In practice, there are many reactions that are thermodynamically feasible but do not occur unless specific conditions are met. From the sulfur recovery point-of-view, however, it is fortunate that reaction (3-16) does not occur; otherwise, the final product in the process would be sulfur dioxide instead of sulfur.

3.4.2 Mass balance

The experimental results from mass balance measurements are shown in Table 3-3. For each run, the moles of sulfur consumed are almost equal to the moles of sulfur produced, indicating that nothing was lost during the experiment and that the data are reliable. However, the consumption of H₂S and sulfuric acid and the production of sulfur, SO₂ and water could not be reconciled with the amounts predicted by the stoichiometry of a single reaction equation, (3-7). More H₂S seems to be converted and less SO₂ to be produced. This suggests that SO₂ must be an intermediate product that would be consumed to some extent in a consecutive reaction. Both S and H₂O must be produced and H₂S be consumed by a reaction in addition to that of (3-7). Combining the conclusion from thermodynamic analysis, we may suggest that reaction (3-7) occur first. Once SO₂ is produced, the consecutive reaction, (3-20), may commence. The existence of SO₂ in the final products indicates that the second reaction has not completely consumed the SO₂ generated from the first step. The more concentrated the sulfuric acid is, the more the SO₂ remains in the final gas; and vice versa. For each of the reaction (3-7), it seems that an entire reaction (3-20) does not follow. Instead, what is following is a reaction with varying coefficients,



where, z is varying from 0 to 1 according to experimental conditions. This leads to an overall reaction



When $z = 0$, Equation (3-22) becomes reaction (3-7), which was not encountered in experiments. When $z = 1$, Equation (3-22) becomes the sum of reactions (3-7) and (3-20),

Table 3-3. The results from mass balance experiments

Run#	Acid Conc.	Consumption		Production			Total S	Total S
		H ₂ S	H ₂ SO ₄	S	SO ₂	H ₂ O	consumed	produced
	Wt%	mmol	mmol	mmol	mmol	mmol	mmol	mmol
B38	95.91	24.2	14.5	29.1	9.63	38.5	39.9	36.9
B40	91.56	17.1	9.01	21.1	4.96	26.1	26.1	26.1
B44	87.72	16.2	8.39	18.5	4.11	24.6	24.6	22.6
B34	84.37	17.7	6.58	23.3	1.00	24.3	24.3	24.3
B42	79.01	13.6	4.94	18.0	0.59	18.6	18.5	18.6
B39	75.19	16.4	5.48	21.9	0.01	21.9	21.9	21.9
B43	65.72	14.9	5.12	19.6	0.00	20.7	21.0	20.7

resulting in a complete conversion of SO_2 as observed with acid concentration at 75 and 65 wt%. When $0 < z < 1$, the SO_2 generated from (3-7) is partly consumed by (3-20), which is the case for acid concentration ranging from 75 to 96 wt%. In terms of Equation (3-22), the value of z can be determined from the data in Table 3-3. As shown in Table 3-4, at an acid concentration, the values of z obtained from the measurements of different substances are close to each other. The largest deviation, for 87.72 wt%, is below 10%.

From the definition, z should vary from 0 to 1. The magnitude of z is actually measurement of the ratio of SO_2 consumed by the second reaction to that generated from the first reaction. For instance, $z = 0.336$ for 96 wt% acid, meaning 33.6% of the SO_2 generated in the first reaction was converted by the second reaction. When the acid concentration was changing from 96 wt% to 75 wt%, two reactions coexist and the decreasing z illustrates that more and more first-step-generated SO_2 has been consumed by the second reaction. When the concentration was at 75 wt% and below, complete conversion of SO_2 was indicated. The effect of acid concentration on the value of z is roughly illustrated in Figure 3-3.

It should be mentioned that the values of z shown in Table 3-4 and Figure 3-3 are operation-dependent. The magnitude of z somehow represents the ratio of the first reaction rate to the second reaction rate in the period of operation under a certain conditions such as acid concentration, temperature, stirring strength, etc. For the mass balance experiments in 96 wt% acid, the first reaction is relatively faster so that when the reaction is terminated by complete consumption of H_2S , the slower second reaction is not able to convert the SO_2 generated from the first reaction. As the acid becomes more dilute, the first reaction becomes slower, or the second reaction becomes faster, or both

Table 3-4. Values of *z* at various acid concentrations

Run#	Acid Conc. Wt%	Reactants		Products			Average “z” values
		H ₂ S	H ₂ SO ₄	S	SO ₂	H ₂ O	
		<i>z</i>	<i>z</i>	<i>z</i>	<i>z</i>	<i>z</i>	
B38	95.91	0.334	n/a	0.336	0.336	0.337	0.336±0.001*
B40	91.56	0.449	n/a	0.447	0.450	0.448	0.449±0.001
B44	87.72	0.465	n/a	0.402	0.510	0.466	0.461±0.044
B34	84.37	0.845	n/a	0.847	0.840	0.847	0.845±0.003
B42	79.01	0.877	n/a	0.881	0.880	0.883	0.880±0.002
B39	75.19	0.996	n/a	0.998	0.998	0.998	0.998±0.001
B43	65.72	0.955	n/a	0.935	1.00	1.02	0.978±0.036

*the mean ± the standard deviation

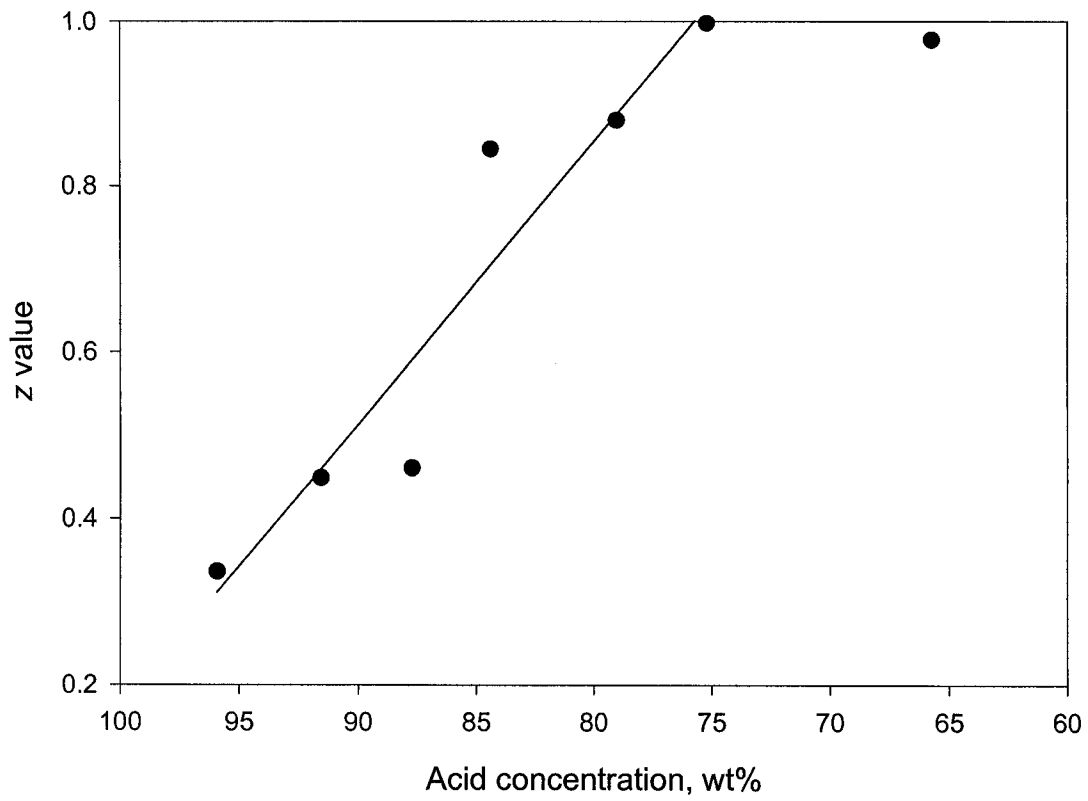


Figure 3-3. Dependence of overall stoichiometric coefficient, z , on acid concentration. Reaction temperature: 120°C; Initial gas feed: pure H₂S.

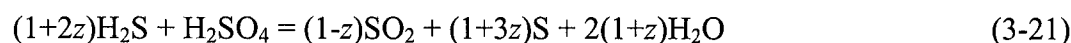
apply. The net effect is that more SO₂ is converted. The data of z in Table 3-4 and Figure 3-3 also indicate that zero sulfur emission can be realized using sulfuric acid as dilute as below 75 wt%. However, to find an acid concentration where the process is able to proceed more efficiently, knowledge of the kinetics of the reactions seem to be necessary.

3.5 Conclusions

Thermodynamics calculations and experiments show that only two reactions occur independently when H₂S and concentrated sulfuric acid are contacted. They are:



The first reaction occurs between H₂S and molecular H₂SO₄, those between H₂S and other ionic species being unlikely. The two-reaction scheme agrees well with the mass balance measurements, leading to an overall reaction with a variable stoichiometry coefficient



with the value of z strongly depending on the acid concentration. Further oxidation of sulfur into sulfur dioxide by the concentrated sulfuric acid is not likely near 120°C, enabling the liquid sulfur to be separated, being immiscible with the sulfuric acid solutions.

3.6 Literature Cited

- Dobereiner, I.W. Schweigger's J. 13, 481 (1814).
- Durrant, P. J. and B. Durrant, *Introduction to Advanced Inorganic Chemistry*, 2nd Ed. John Wiley & Sons, New York, pp853-854 (1970).
- Geuther, A. Ueber Wasserfreie Schwefelsaure. *Lieb. Ann.*, **109**, 71 (1858).
- Klein, D., "The Influence of Organic Liquids upon Interaction of Hydrogen Sulfide and Sulfur Dioxide" *J. Phys. Chem*, **15**, 1-19 (1911).
- Reklaitis, G. V., *Introduction to Material and Energy Balances*. John Wiley and Sons, New York, p159, 1983.
- Roine, A. "Qutokumpo HSC Chemistry for Windows", Version 1.20, Chemical Reaction and Equilibrium Software with Extensive Thermodynamic Database (1993).
- Sander, U. H. F., H. Fischer, U. Rothe and R. Kola, Sulfur, Sulfur Dioxide and Sulfuric Acid – An Introduction to their *Industrial Chemistry and Technology*, English Ed. More, A. I. The British Sulfur Corporation Ltd, p271, p159, pp265-269 (1984).
- Sandler, S.I., *Chemical and Engineering Thermodynamics*. John Wiley and Sons, New York, p499, (1989).
- Snurnikov, A. P., V. F. Larin and T. G. Temofeeva, "Study of the Reaction of Hydrogen Sulfide with Sulfuric Acid", *J. appl. Chem. (USSR)*. **40**, 13-15 (1967).
- Tiwari, B. L., *The Kinetics of Oxidation of Zinc Sulfide and Hydrogen Sulfide by Sulfur Dioxide in Aqueous Sulfuric Acid*. Ph. D. Thesis, Columbia University, Columbia, S.C. (1976).
- Vogel, A. *J. prakt. Ch.* **4**, 231 (1824).

- Wang, H., Q. Zhang, I. G. Dalla Lana and K. T. Chuang, "Analysis of Both Sulfur and Non-sulfur Compounds Using a Single Gas Chromatograph with Parallel Sulfur Chemiluminescence and Thermal Conductivity Detectors", *J. Chromatographic Sci.*, **36**, 605-611 (1998).
- Young, T. F. and G. E. Walrafen, "Raman Spectra of Concentrated Aqueous Solutions of Sulfuric Acid", *Trans. Faraday Soc.* **57**, 34-39 (1961).
- Zhang, Q., H. Wang, I. G. Dalla Lana and K. T. Chuang, "Solubility of Sulfur Dioxide in Sulfuric Acid of High Concentration", *Ind. Eng. Chem. Res.*, **37**, 1167-1172 (1998).

Chapter 4

Kinetics of Oxidation of Hydrogen Sulfide by Concentrated Sulfuric Acid*

4.1 Introduction

The chemistry studied in the last chapter showed that two independent reactions are involved in the H₂S-sulfuric acid gas-liquid reaction system. First, H₂S is oxidized by sulfuric acid molecules present in concentrated sulfuric acid solutions



and the produced SO₂ then reacts with H₂S in the acid solution



For H₂S, the two reactions are parallel and for SO₂, they are consecutive. If these two reactions occur to stoichiometric completion, the overall reaction results



Reaction (4-3) implies the possibility of a new sulfur removal and recovery technology with zero sulfur emission. It has been mentioned that the kinetics of the reactions is necessary to establish the operating parameters under which reaction (4-3) may be realized. Also, knowledge of the chemical reaction kinetics is essential to reactor design.

* A version of this chapter has been published in *Industrial and Engineering Chemistry Research*, **41**, 6656 (2002).

In this chapter, the kinetics of reaction (4-1) will be studied. And that of reaction (4-2) will be studied in the following chapter.

4.2 Theoretical Considerations

Contacting H₂S with sulfuric acid solution is a gas-liquid reaction system. The diffusing gas, H₂S, reacts with the liquid, H₂SO₄, or with a form of SO₂ generated or previously dissolved in the liquid. In the quiescent liquid, the mass balance across a differential element along the direction perpendicular to the liquid surface gives rise to (Danckwerts, 1970)

$$D_A \frac{\partial^2 C_A}{\partial x^2} - r_A(x,t) = \frac{\partial C_A}{\partial t} \quad (4-4)$$

Specific design of experiments can render the diffusion term zero so that the accumulation term equals the reaction rate. The elimination of diffusion and mass transfer effects will be discussed later.

As long as a change in the number of moles in the gas phase occurs with the reaction, it is possible to determine the reaction rate by measuring the rate of pressure-change in a constant-volume batch reactor (Fogler, 1986). For a reaction carried out isothermally,

$$\frac{V}{\delta RT} \frac{dP_T}{dt} = \frac{V}{\delta RT} R_p = -r_A \quad (4-5)$$

where, δ is the change in the total number of moles per mole of A reacted. For reaction (4-1), the change in moles of gas phase is zero because it consumes one mole of gas, H₂S, and generates one mole of gas, SO₂. However, at the initiation of reaction, we are

measuring the total pressure change, the sum of the partial pressures of H₂S and SO₂. Analysis of the direction of electron transfer indicates that SO₂ is formed from the sulfuric acid molecule. In other words, it is generated in the liquid phase. Our research on the solubility of SO₂ in concentrated sulfuric acid (Zhang, et al., 1998) shows that the volume of sulfuric acid solution in the reactor is more than capable of dissolving all of the SO₂ which may be produced during the experiment. It is likely that the net pressure drop observed would account for the rate of H₂S consumption rate, $-r_{H_2S1}$, the rate of reaction (4-1), at reaction initiation. Thus, δ becomes 1 and $-r_A$ equals $-r_{H_2S1}$.

Other complications may arise after the reaction starts. For example, reaction (4-2) would initiate once SO₂ has been produced from reaction (4-1); the produced sulfur in the solid state could block the reaction surface; and the water produced would dilute the acid concentration. To eliminate these uncertainties and to enable measurement of the reaction rate under known conditions, the initial rate analysis method is applied. The reaction rate can be calculated by recording the rate of change of pressure drop with time in a constant-volume batch reactor. By extrapolating the pressure-drop/time function to the initial moment, an initial rate is obtained for the conditions such as the pressure of hydrogen sulfide, the concentration of the sulfuric acid solution, the known area of the clear solution surface and only reaction 1 occurring.

4.3 Experimental Section

Based on the above discussion, an experimental apparatus was constructed. Figure 4-1 shows its schematic diagram. The procedure of a run is described as follows:

- (1) Charge 100 or 200 mL of sulfuric acid solution into the reactor.

- (2) Connect the reactor to the feed part of the experiment setup and check for leaks.
- (3) Evacuate the air from the system using an Edwards-5 two-stage vacuum pump (Edwards High Vacuum, Oakville, Ontario, Canada).
- (4) Heat the solution to the desired temperature.
- (5) Record the pressure of the solution, denoted as P_1 .
- (6) Introduce pure H_2S from its reservoir into the reactor to a pre-set initial pressure. Take this moment as time zero. Record this pressure, denoted as P_2 .
- (7) Once H_2S has been introduced into the reactor, record the pressure of the gas phase, P , every second using an Alphaline pressure transmitter (Model 1151, Rosemount Inc., Chanhassen, Minnesota, USA) which transmits to an Opto22 data acquisition module. The accuracy of the pressure transmitter is 0.1 psi.
- (8) Obtain the initial pressure drop rate, R_p , in terms of the slope at $t=0$ of the curve of ΔP , or $P-P_2$, against time, t , as shown in Figure 4-2. Usually under the initial condition where the interface between gas and liquid is clear and stable, the pressure dropped linearly with time within the first 5-10 seconds. R_p was obtained from the regression of $P-t$ curve of the linear section. In the determination of the value of R_p , it was important to eliminate the effect of other factors such as surface area change by solid sulfur produced during the reaction. It was believed that these effects were negligibly small during the period in which the pressure dropped linearly. The reaction rate, $-r_{H_2S1} = -\frac{dN_{H_2S}}{dt}$, was calculated based on R_p in terms of Equation (4-5). The data for R_p and $-\frac{dN_{H_2S}}{dt}$ are reported in Table A-1 in the Appendix.

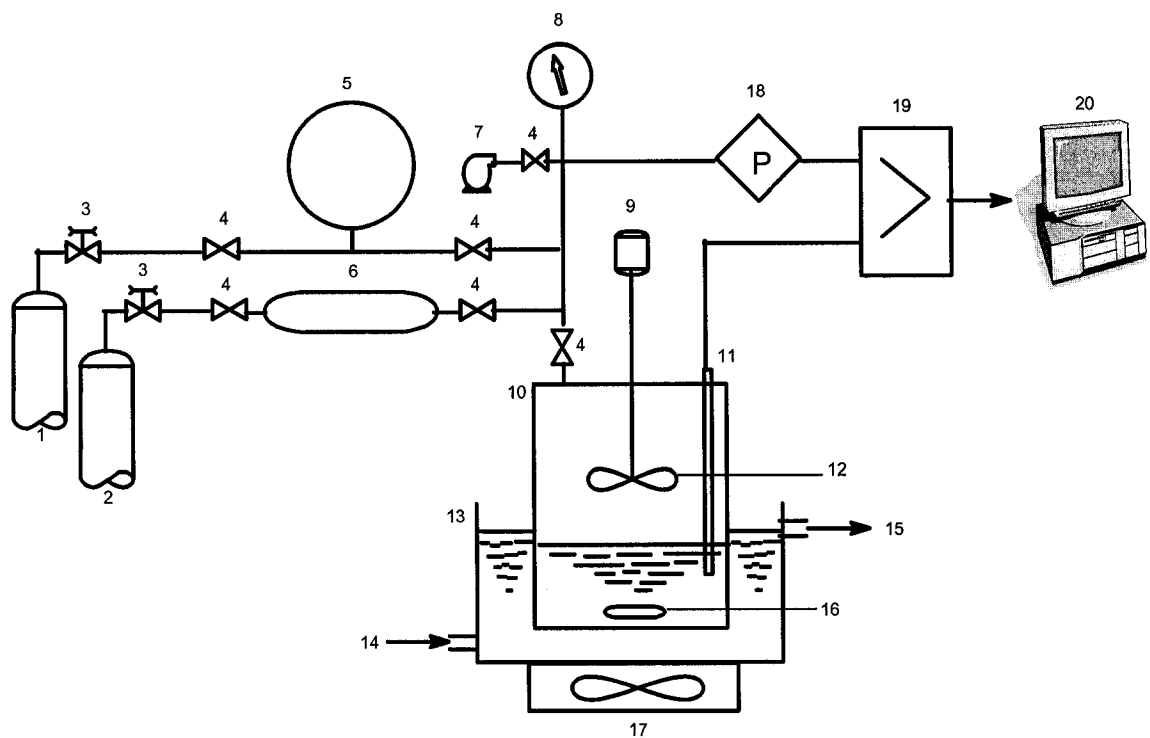


Figure 4-1. Schematic diagram of experimental apparatus. 1. SO₂ cylinder; 2. H₂S cylinder; 3. regulator; 4. stop valve; 5. SO₂ reservoir; 6. H₂S reservoir; 7. vacuum pump; 8. pressure gauge; 9. speed-varying motor; 10. reactor; 11. thermocouple; 12. impeller; 13. thermobath; 14. warm water inlet; 15. warm water outlet; 16. magnetic spin bar; 17. magnetic stirrer; 18. pressure transducer; 19. Opto-22; 20. computer.

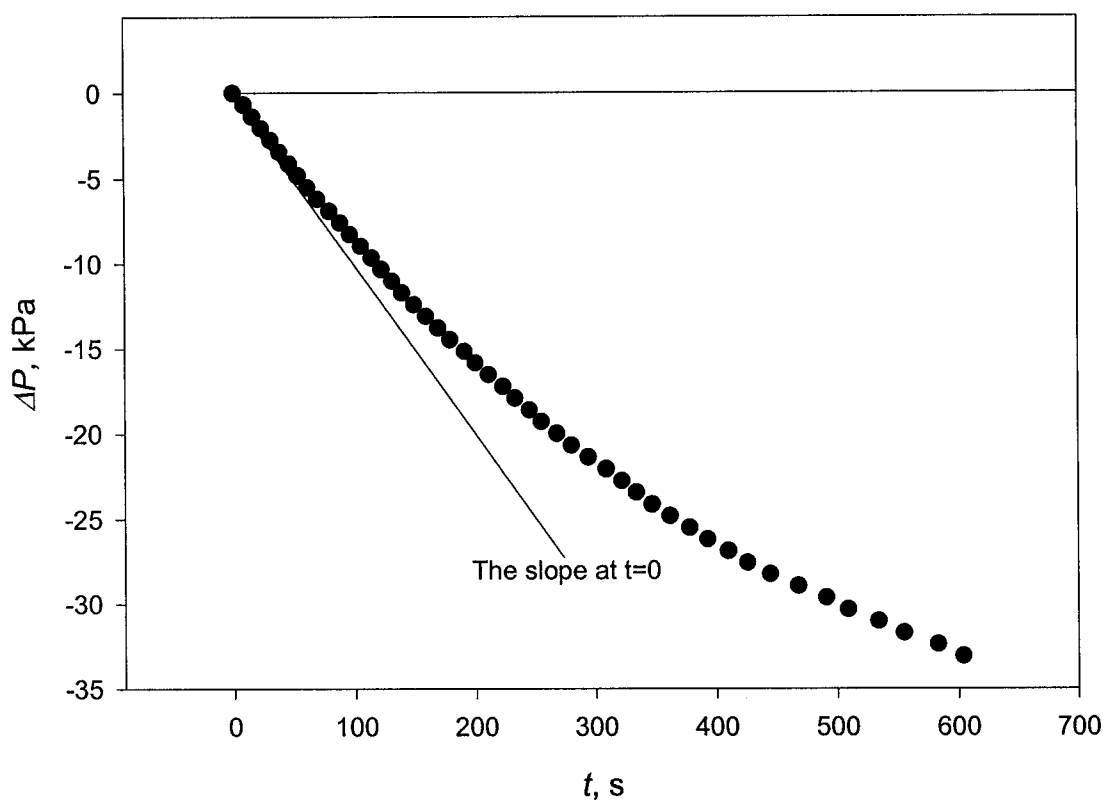


Figure 4-2. Plot of pressure drop against time for reaction between H_2S and H_2SO_4 solution: the slope at time zero gives the initial rate of the reaction. Acid concentration: 96.04 wt %; Temperature: 37 °C; Run#: pd_96_t3.

The temperatures of the gas and the liquid in the closed reactor should be the same and constant even though this may be difficult to realize. In this study, the temperature of the liquid was controlled by a warm water bath, using a thermomix (Model 1460, B. Braun Inc., Toronto, Ontario, Canada). The liquid phase temperature, read to 0.1°C, was taken as the reaction temperature. The gas phase was not heated directly and therefore, was assumed to be at room temperature when the moles of gas were calculated using the equation of state for an ideal gas. In fact, as the temperatures of gas and liquid differed, the warmer liquid would heat the gas close to the liquid, leading to a temperature gradient in the gas phase. However, the error thus introduced to the calculation of total moles would not be significant because (1) H₂S at room temperature was introduced into the reactor just before the reaction started, (2) the gas phase was at room temperature initially and only the gas adjacent to the liquid would be heated, and (3) the temperature difference between the gas (21-23°C) and the liquid (60°C at the most) phases was not large (maximum 40°C).

The sulfuric acid solutions of various concentrations were prepared by diluting ~96 wt % sulfuric acid (Fisher Scientific, Nepean, Ontario, Canada) with distilled water. The 100 wt % acid was prepared by mixing 20 % free SO₃ fuming sulfuric acid (Acros Organics, Fairlawn, New Jersey, U.S.A.) and 96 wt % sulfuric acid solution. The concentration of the solutions was determined by titration with a standard 0.1 N sodium hydroxide solution (Fisher Scientific, Nepean, Ontario, Canada) using 0.5 % methyl orange solution (Fisher Scientific, Nepean, Ontario, Canada) as the indicator. The cylinder of hydrogen sulfide (CP grade) and the cylinder of nitrogen were provided by Praxair Products Inc. (Mississauga, Ontario, Canada).

4.4 Results and discussion

4.4.1 Blank experiments

The blank experiments were designed to evaluate the performance of the apparatus. For kinetics studies, what we are mostly concerned with is whether the signals collected and displayed instantly and linearly reflect the pressure in the reactor, because any time delay or signal deformation will introduce errors. Also, what we want to know from the blank experiments is whether there are factors other than reaction and dissolving process that contribute to the pressure change. Following the same experimental procedure but using nitrogen instead of hydrogen sulfide, blank experiments were carried out. Figure 4-3 indicates that the apparatus is able to record the pressure change instantly. No time delay, signal deformation, or oscillation was observed. The mass balance for nitrogen in both reactor and reservoir, before and after the introduction, showed no mass loss during the gas introduction. Because N_2 is inert to sulfuric acid and does not dissolve in the solution, we may say that the system will not cause any pressure change by factors other than reaction or dissolution of gas components.

Following the blank experiments, acid concentration range was selected. Significant interaction between hydrogen sulfide and sulfuric acid only occurs when the concentration of the acid solution is larger than 88 wt%. As shown in Figure 4-4, the reaction rate in both 87.86 and 30.0 wt% sulfuric acid solutions at room temperature was too slow for this setup to detect but that in 96 wt% acid it was large enough to measure. Therefore, the range of sulfuric acid concentration chosen in this study was from 88 wt% to 100 wt%. For 88 wt% acid, higher temperatures were applied to observe significant reaction.

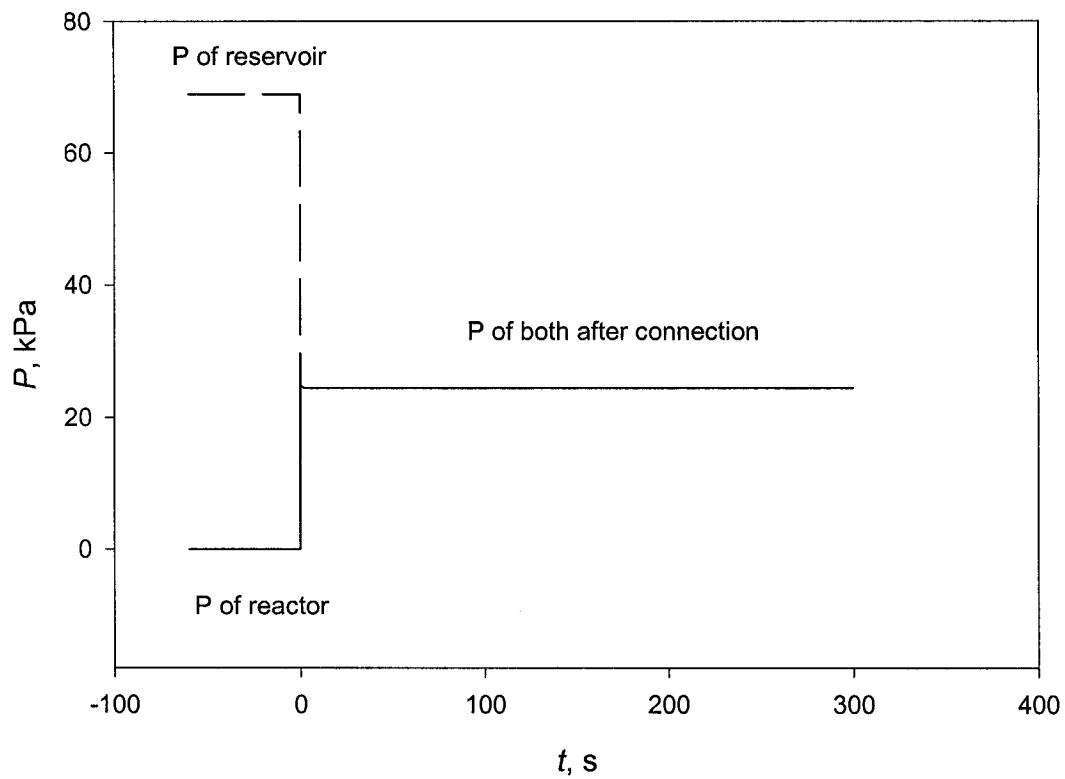


Figure 4-3. Blank experiment: pressure response when introducing nitrogen into reactor filled with 200 mL sulfuric acid solution of 96.04 wt %. Temperature: 21 °C; Run#: pd_96_test.

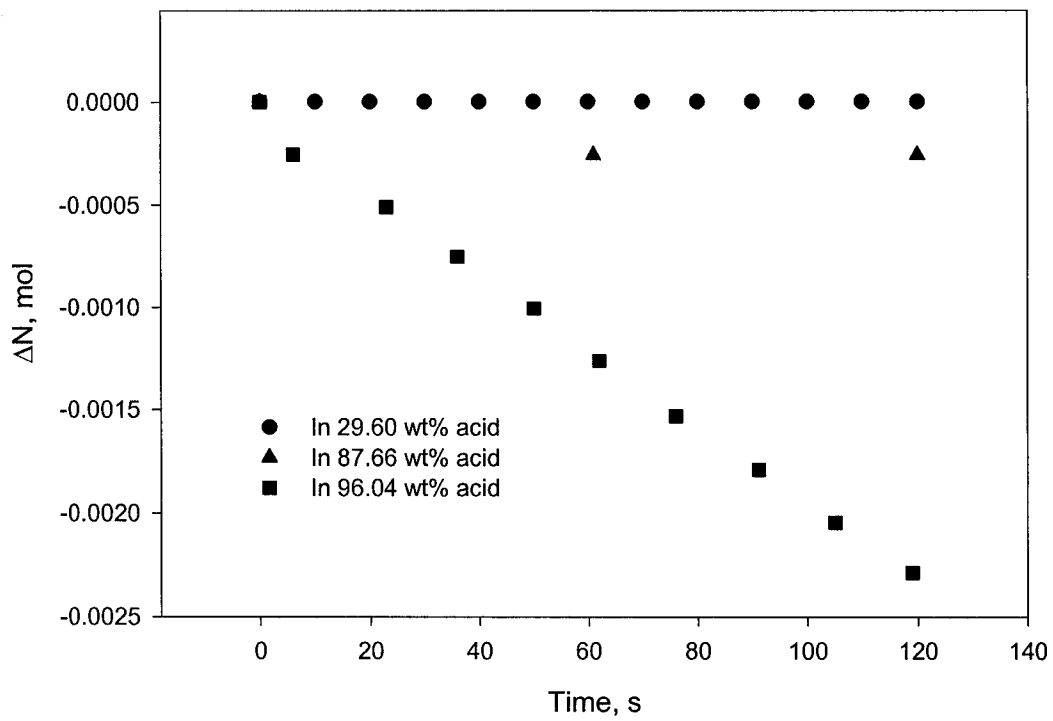


Figure 4-4. Rate of interaction between H₂S and sulfuric acid solutions of various concentrations. Temperature: 21 °C; Initial pressure of H₂S: 61-65 kPa; Run#: pd_96_s4, pd_88_t1, pd_30_s1.

4.4.2 Effect of mass transfer

As was mentioned in the section of theoretical considerations, to measure the reaction rate for a gas-liquid reaction, the influence of mass transfer and diffusion had to be eliminated so as to render the accumulation rate in the reactor to be equal to the reaction rate. Because only the initial reaction rate was taken into account, it was important to analyze the mass transfer and diffusion features at time zero of the measurement. At this moment, the gas phase consisted of pure H₂S, ignoring the small amount of vapor from the acid solution, the highest of which in this study was 0.050 kPa, compared to 20 kPa of H₂S, the lowest H₂S pressure in the runs. Thus, there would be no concentration gradient in the gas phase and the mass transfer by diffusion could be neglected. The liquid phase was pure solution with a certain acid concentration, uniform everywhere in the liquid. Furthermore, Figure 4-4 has indicated that when the acid concentration decreased as low as 30 wt% and the reaction between H₂S and sulfuric acid solution no longer occurred, no significant pressure drop was observed over a reasonably long period of time, implying that no process other than reaction would contribute to the pressure drop. Even though the solubility of H₂S in the diluted sulfuric acid was studied by a number of researchers (Alexandrova and Yaroshchuk, 1978; Douabul and Riley, 1979) the dissolution rate in this study can be ignored. Based on this analysis, at time zero, mass transfer and diffusion in the liquid phase was also insignificant. Therefore, the pressure-drop that was measured was only contributed by reaction (4-1).

4.4.3 Effect of reaction area and volume

For a gas-liquid reaction, the gaseous reactant must contact the liquid phase to facilitate chemical reaction. Because the interface is where the reactant molecules in the

different phases meet and react, its area would influence the reaction rate. To determine whether and how the interfacial area and the volume of liquid phase affect the reaction rate measurement, two reactors of different shapes were used: a cylindrical reactor which changes the acid solution volumes but keeps the interface area constant, and a conical reactor in which different surface areas of the acid solution result from changing different acid volumes. First of all, the results obtained using the cylindrical reactor, as shown in the upper three rows in Table 4-1, indicate that the reaction rate at unit H₂S pressure (Pa) was nearly constant no matter the volume of the sulfuric acid solution. Secondly, in the conical reactor, the reaction rate was proportional to the interfacial area, shown in the lower four rows of Table 4-1. Identical rate constants per unit area were obtained from all the runs. The reaction rate is proportional to the interfacial area but independent of the acid volume, indicating that reaction (4-1) might take place only at the surface of the liquid phase. On the other hand, comparing the diffusion rate and reaction rate (Figure 4-4), the latter is so large that no H₂S remains to diffuse and react in the bulk of the acid.

4.4.4 Order of reaction with respect to H₂S and sulfuric acid

For a reaction mainly occurring at the interface and involving two reactants, each from gas phase and liquid phase, respectively, it is expected that a rate equation such as

$$r_{H_2S1} = k_1 a C_a^m P_{H_2S}^n \quad (4-6)$$

can be determined from the experimental data. First, at a given acid concentration and temperature, the initial reaction rates at various initial H₂S pressures, $-\frac{dN_{H_2S}}{dt}$, were found from Table A-1 in the appendix (The procedure of the reaction rate calculation has been shown in the experimental section in step 8) . The order of reaction with respect to

Table 4-1. Reaction rate at various surface areas and solution volumes.

Acid Concentration: 96.04 wt%; Reaction temperature: 21.5 °C

Run #	Surf. Area	Acid vol.	rate $\times 10^{10}$	$k_{p1}\times 10^8$
	m ²	mL	mol s ⁻¹ Pa ⁻¹	mol s ⁻¹ Pa ⁻¹ m ⁻²
Pd_96_a1	0.00442	200	2.83	6.40
Pd_96_a2	0.00442	300	2.86	6.48
Pd_96_a3	0.00442	400	2.81	6.35
Pd_96_a4	0.00501	800	3.22	6.42
Pd_96_a5	0.00864	500	5.33	6.30
Pd_96_a6	0.0119	300	7.63	6.41

the pressure of H₂S was obtained by correlating the initial rates with the initial pressures. As an example, the result for 96.04 wt% sulfuric acid solution is shown in Figure 4-5. Because the reaction rate is nearly linearly proportional to the H₂S pressure, this figure clearly illustrates a first order behavior with respect to H₂S at various temperatures, that is

$$\frac{r_{H_2S1}}{a} = k_1 C_a^m P_{H_2S} \quad (4-7)$$

The slope corresponds to the value of $k_1 C_a^m$ at a given acid concentration. As the temperature increases to 54°C, a slight curvature appears in the plots indicating that the order of reaction with respect to H₂S is decreasing slightly from first order behavior. The increased extent of reaction (4-2) as temperature increases may be introducing a small error in the extrapolation such shown in Figure 4-2. The same analysis was carried out to the data for other acid concentrations in Table A-1 in the Appendix, indicating that, for all acid concentrations from 88 to 100 wt% and temperatures from 20 to 60°C, the reaction is first order with respect to H₂S pressure, as indicated in Equation (4-7).

Then, attempts were made to correlate the reaction rate at a given pressure of H₂S with the measures of acid concentration in order to determine the values of the reaction order, m , with respect to sulfuric acid concentration and the rate constant, k_1 , in Equation (4-6). As discussed in Chapter 1, sulfuric acid-water mixture is a very complex aqueous solution, in which the species present are more than water and sulfuric acid molecules. Due to association and dissociation, ions such as H⁺, H₃O⁺, HSO₄⁻, and SO₄²⁻ may be present, depending on the acid concentration. Even for the molecules, various hydrates would form, rendering their properties different from when they exist separately, as shown

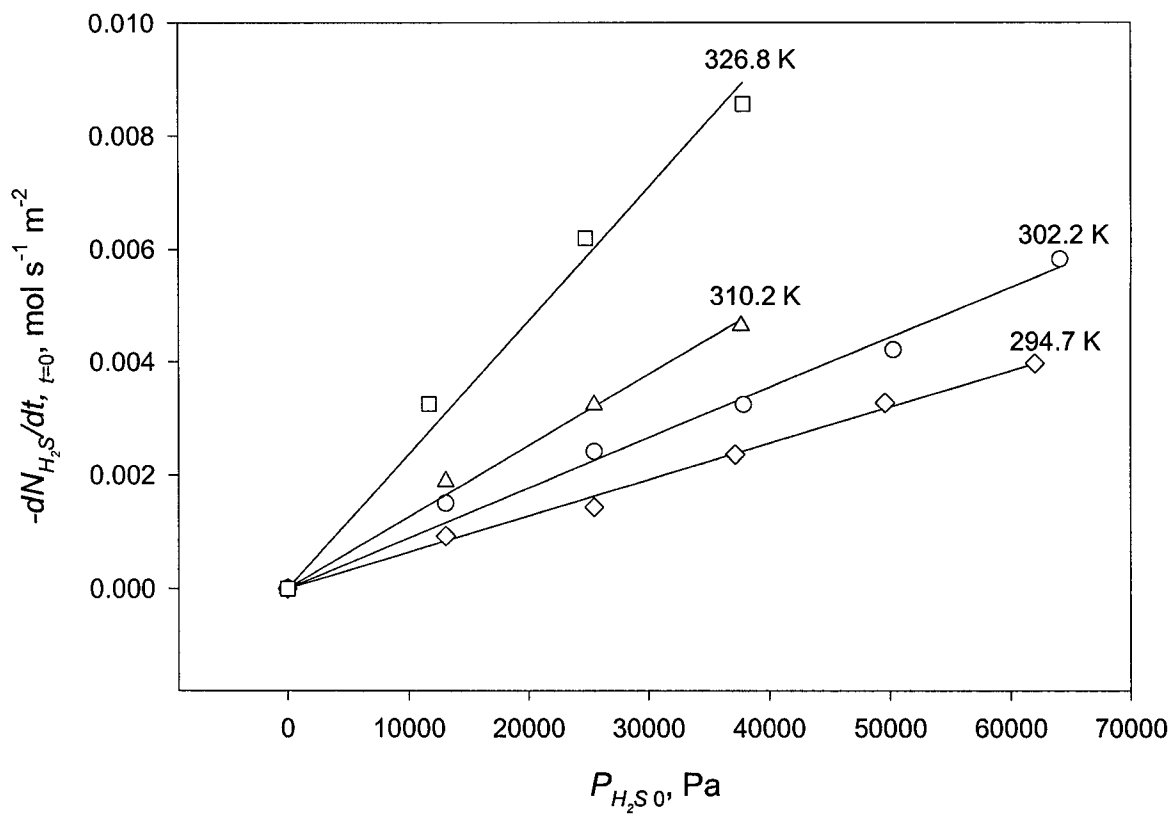


Figure 4-5. Plots of initial H₂S consumption rate against initial H₂S pressure. Acid concentration: 96.04 wt %; Run#: pd_96_t1, pd_96_t2, pd_96_t3, pd_96_t4.

in Figures 1-1 and 1-2. As a result, no correlations indicated a simple order of reaction with respect to sulfuric acid in overall molarity. However, Chapter 3 has shown that the oxidation of H₂S possibly occur between H₂S and molecular sulfuric acid. There must be some relationships between the reaction rate and the activity properties or oxidizing power of sulfuric acid. To find these relations, a new parameter, k_{p1} , is defined as the reaction rate per unit of the surface area and per unit of H₂S pressure from Equation (4-6), *i.e.*,

$$k_{p1} = k_1 C_a^m = \frac{r_{H_2S1}}{aP_{H_2S}} \quad (4-8)$$

As mentioned previously, k_{p1} can be evaluated from the slope of lines in figures such as Figure 4-5 by the linear regression of the rate data. The values of k_{p1} at all temperatures and acid concentrations used in this study are listed in Table 4-2. It is known that sulfuric acid plays a role of oxidizing agent in its reaction with H₂S. But oxidizing power of sulfuric acid is rarely discussed quantitatively either in textbooks (Durant, 1970) or in the literature (Sander, et al., 1984; Muller, 1997). No data for oxidizing power was found elsewhere. The correlation between the reaction rate and this property was unfortunately not allowed, as a result. However, Figure 4-6 seems to show a good linear relationship between k_{p1} and sulfuric acid activity (Giauque, et al., 1960) in a semi-logarithm diagram. In addition, the value of $\log k_{p1}$ and $-H_0$, the Hammett acidity function (Liler, 1971) can be linearly correlated over the acid concentration range from 88 to 98 wt%, as shown in Figure 4-7. The correlation is expressed as the following,

$$\log k_{p1} = i + j(-H_0) \quad (4-9)$$

The definition of the Hammett acidity function (Rochester, 1970) is

Table 4-2. Values of k_{p1} at all temperatures and acid concentrations

T, K	$k_{p1} \times 10^9$	T, K	$k_{p1} \times 10^9$	T, K	$k_{p1} \times 10^9$
<u>87.68 wt%</u>		<u>90.13 wt%</u>		<u>91.53 wt%</u>	
311.35	12.6±0.22	302.75	12.4±1.01	297.65	23.1±0.61
324.05	15.8±0.31	313.35	16.7±0.40	305.15	24.8±0.44
330.45	18.4±0.55	321.65	20.3±0.41	313.15	34.4±1.88
335.15	20.3±0.28	333.21	27.5±1.39	322.75	44.2±1.12
				331.05	59.8±1.34
<u>92.97 wt%</u>		<u>96.04 wt%</u>		<u>99.97 wt%</u>	
294.65	22.8±0.87	294.65	64.0±2.29	294.45	184±7.56
301.95	32.1±1.57	302.15	89.4±4.35	298.55	235±11.8
312.95	51.2±2.45	310.15	125±5.65	303.35	313±11.8
321.25	64.5±0.95	326.75	240±15.0	308.65	429±14.6
331.15	88.9±1.25				

*The unit of k_{p1} is $\text{mol s}^{-1}\text{m}^{-2}\text{Pa}^{-1}$

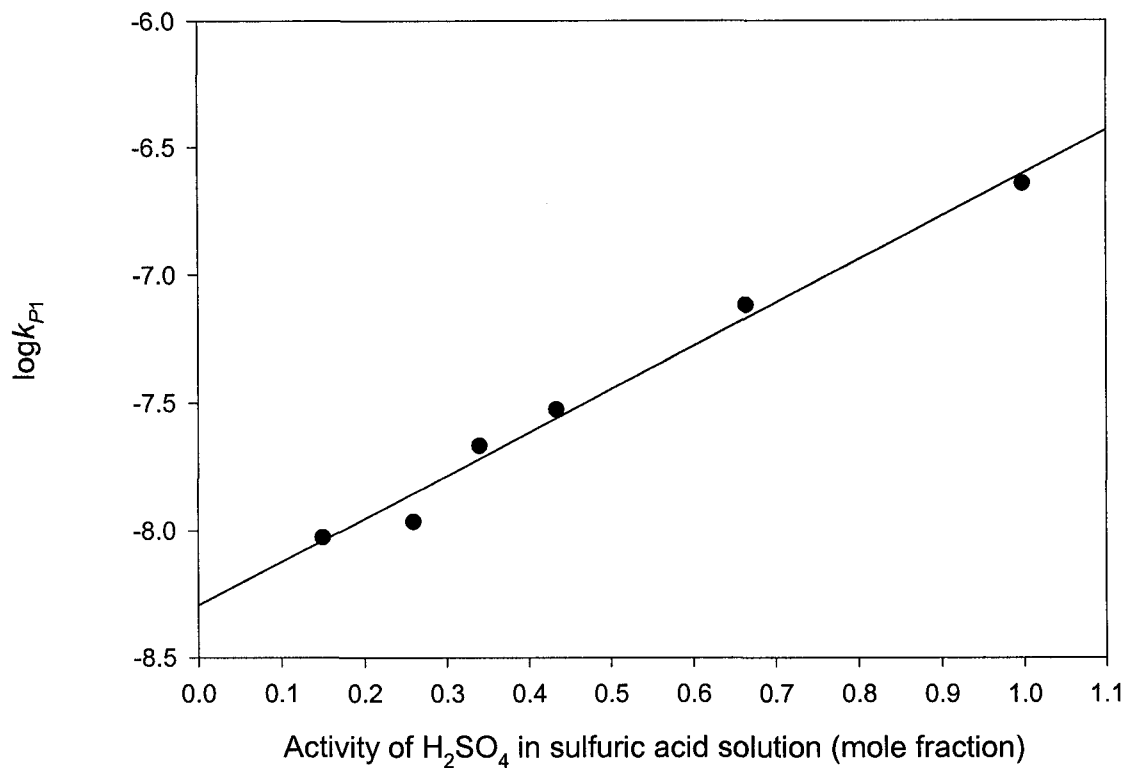


Figure 4-6. Correlation between reaction rate and H₂SO₄ activity at 25°C.

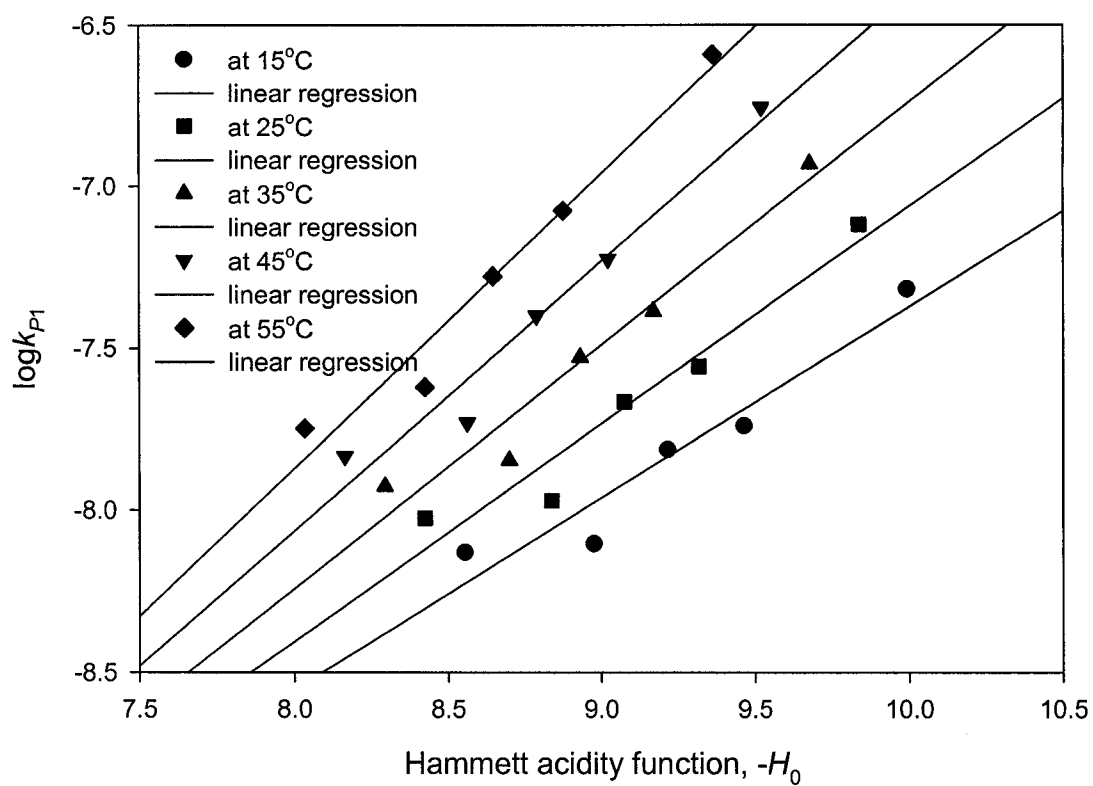


Figure 4-7. Correlation between $\log k_{P1}$ and the acidity function.

$$-H_0 = \log\left(a_{H^+} \frac{f_B}{f_{BH^+}}\right) \quad (4-10)$$

where, a_{H^+} is the activity of proton in sulfuric acid and f_B and f_{BH^+} are the activity coefficient of the reference base, B, used for determining the value of $-H_0$, and its conjugate acid, BH^+ , respectively. Because the properties of B and BH^+ are independent of sulfuric acid and can be assumed to be constants, Equation (4-10) becomes,

$$-H_0 = \log(Ca_{H^+}) \quad (4-11)$$

Combining Equations (4-9) and (4-11) leads to,

$$\log k_{P1} = i + j \log(Ca_{H^+}) \quad (4-12)$$

or

$$k_{P1} = 10^i C^j a_{H^+}^j = k_1 a_{H^+}^j \quad (4-13)$$

where C is a constant and $k_1 = 10^i C^j$. Substituting this k_{P1} into Equation (4-8) and rearranging, one has

$$r_{H_2S1} = k_1 a(a_{H^+})^j P_{H_2S} \quad (4-14)$$

The values of i and j from the regression using Equation (4-9) are shown in Table 4-3. Equation (4-14) indicates that j physically means the order of reaction with respect to the activity of proton present in sulfuric acid solutions. And the values in Table 4-3 show that j changes with temperature. Searching for a mechanism to explain the correlation of the rate data is generally a part of kinetics study. The phenomenon that the order of reaction changes with the reactant concentrations has been well studied from the mechanism point of view (Fogler, 1992). The temperature-dependent order of reaction was also found in

Table 4-3. Values of i and j in Equation (4-9).

$T, ^\circ\text{C}$	i	j	r^2
15	-13.27±0.88	0.5897±0.0954	0.9272
25	-13.77±0.86	0.6705±0.0947	0.9435
35	-14.25±0.85	0.7150±0.0951	0.9541
45	-14.71±0.85	0.8304±0.0961	0.9614
55	-15.15±0.85	0.9091±0.0979	0.9664

some catalytic reaction systems. For example, Chou and Vannice (1986) discovered that the order of reaction with respect to hydrogen in benzene hydrogenation over Pd catalysts increased from 0.5 to nearly 4 as temperature increased from 353 K to 573 K and that the order of benzene increased from 0 to 0.8 over the same temperature range. The true reaction order of the decompositions of ethylene, acetylene and benzene was 1 above 1400°C but decreased at lower temperatures (Wehrer, et al., 1983). This behavior seems to be easily interpreted as inhibition due to changes in adsorbed intermediate species when catalysts were involved. However, it is still difficult to explain the temperature-dependence of the values of i and j in a gas-liquid reaction system without any study on mechanism. It turns out that the power-law model is insufficient to explain the kinetics, and that the elementary reactions must be more complex. Moreover, although the value of j can be determined through the regression using Equation (4-9), k_1 cannot be evaluated from Equation (4-14) owing to the lack of data for the activity of protons in sulfuric acid.

As a result from the above discussion, an empirical rate equation for the oxidation of hydrogen sulfide by concentrated sulfuric acid is proposed. In this equation, the effects of acid concentration as well as temperature are included in the overall rate constant, k_{p1} .

$$r_{H_2S1} = k_{p1} a_{P_{H_2S}} \quad (4-15)$$

4.4.5 Effect of temperature on k_{p1}

The reaction kinetics believes that the exponential effect of temperature on reaction rate, as Arrhenius equation describes, often accurately represents experimental rate data for an overall reaction, even though the activation energy is not clearly defined and may be a combination of E_a values for several elementary steps (Smith, 1970). The

Arrhenius plots of the global rate constants, k_{p1} , for different acid concentrations are shown in Figure 4-8. Correlating the natural logarithm of k_{p1} and the reciprocal of absolute temperature, T , the values of the preexponential factor, A_0 , and the activation energy, E_a , of the reaction in acid solutions of different concentrations were obtained. The values of $\ln A_0$ and E_a for each acid concentration are listed in Table 4-4. The relationship between k_{p1} and temperature T may be described by

$$k_{p1} = A_0 \exp\left(-\frac{E_a}{RT}\right) \quad (4-16)$$

4.4.6 Effect of acid concentration on k_{p1}

As shown in Equation (4-8), the effect of acid concentration, denoted as C_a , is involved in the global rate constant, k_{p1} , which, in turn, can be decomposed to the preexponential factor, A_0 , and activation energy, E_a . The regression analysis between $\ln A_0$ and C_a , and between E_a and C_a , respectively, gave rise to the following linear relationships:

$$\ln A_0 = a + bC_a \quad (4-17)$$

$$E_a = c + dC_a \quad (4-18)$$

Figure 4-9 shows the regression results and Table 4-5 lists the values of the parameters a , b , c , and d , and the value of the regression coefficients as well, indicating a good correlation. This correlation between the rate constant and the acid concentration in weight percentage (wt%) is empirical, because the overall concentration does not represent the real amount of species existing in the solution. Equations (4-17) and (4-18)

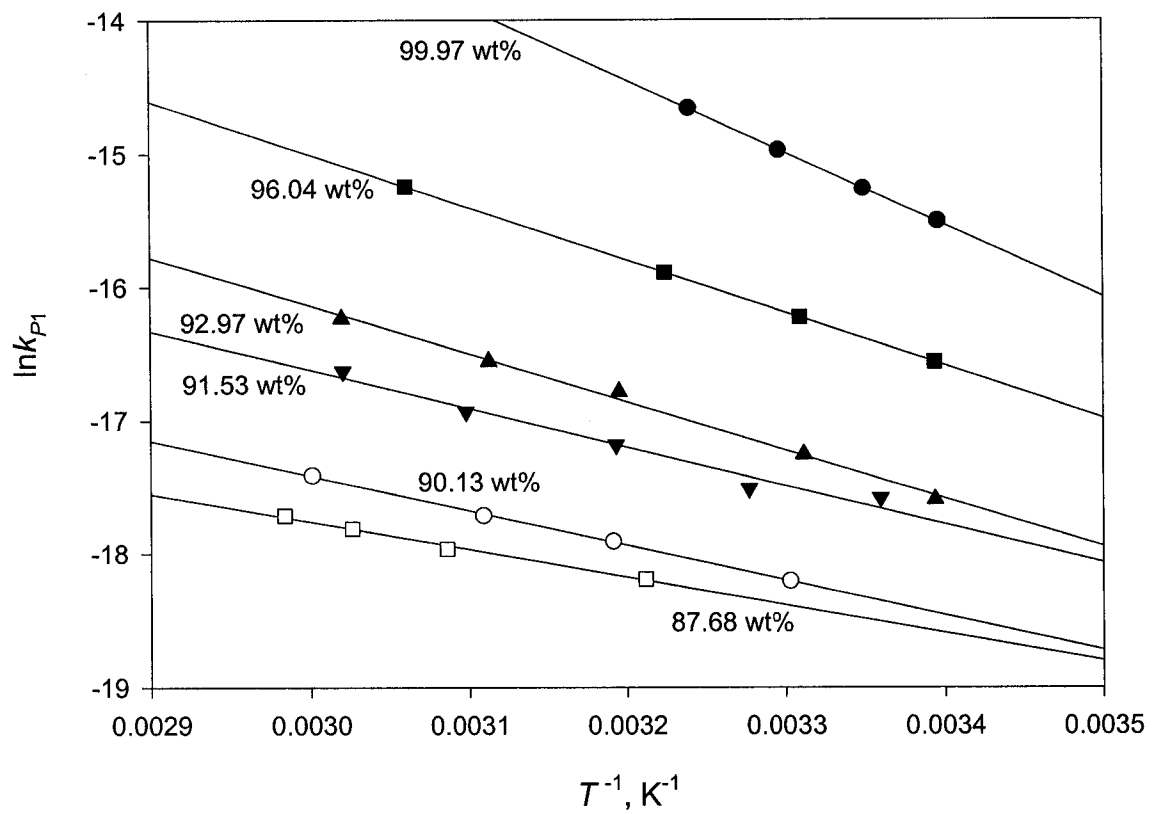


Figure 4-8. Arrhenius plots for reactions at different acid concentrations.

Table 4-4. Values of $\ln A_0$ and E_a for various acid concentrations

Acid concentration, wt %	Preexponential factor, $\ln A_0$	Activation energy kJ/mol	Regression coefficient, r^2
99.97	2.89±0.17*	45.1±0.42	0.9999
96.04	-3.12±0.002	32.9±0.004	0.9999
92.97	-5.30±0.45	30.0±1.16	0.9956
91.53	-7.93±0.89	24.1±2.34	0.9725
90.13	-9.56±0.17	21.8±0.45	0.9906
87.68	-11.5±0.38	17.3±1.03	0.9929

*the regression coefficient ± the standard deviation

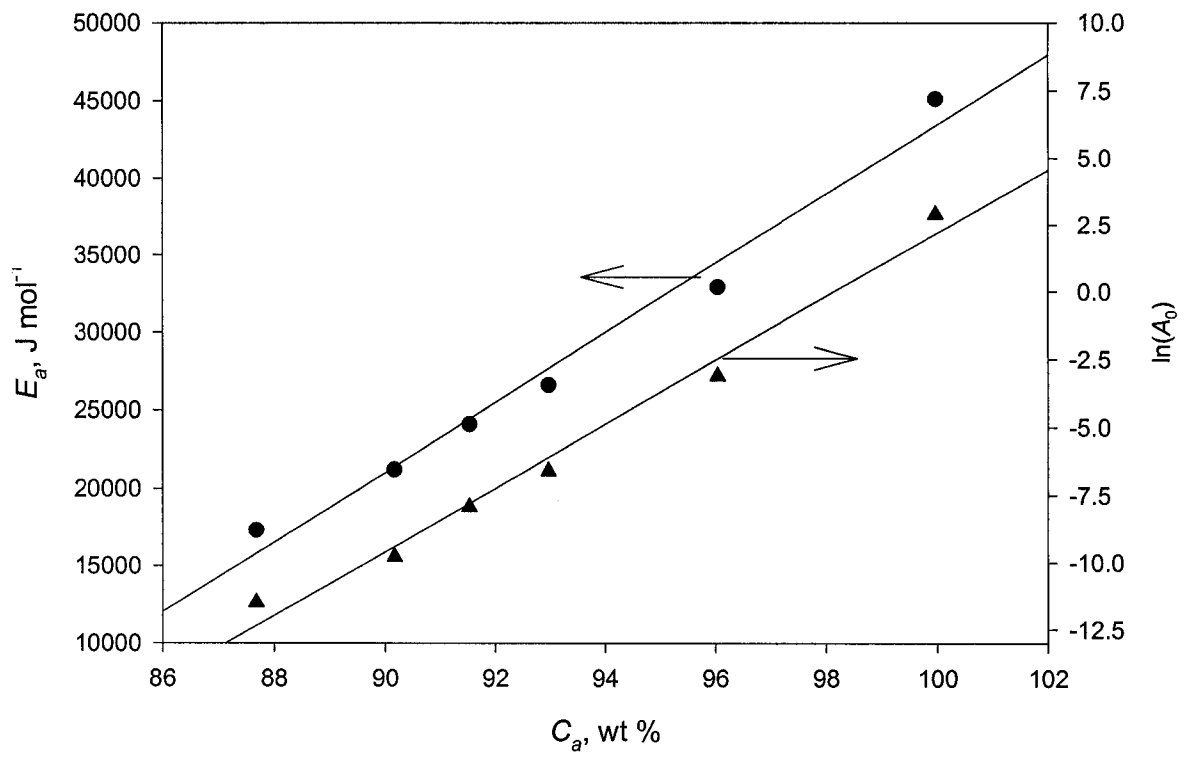


Figure 4-9. Correlation between $\ln A_0$ and acid concentration, C_a , and between E_a and C_a .

Table 4-5. Values of a , b , c , d and r^2 in Equations (4-17) and (4-18)

	intercept	slope	r^2
Equation (4-17) for $\ln A_0$	$a = -116 \pm 6.8^*$	$b = 1.18 \pm 0.07$	$r^2 = 0.9847$
Equation (4-18) for E_a	$c = -178 \pm 17$	$d = 2.23 \pm 0.18$	$r^2 = 0.9751$

* the regression coefficient \pm the standard deviation

indicate that both $\ln A_0$ and E_a decrease as the acid solution becomes more dilute. k_{p1} also decreases. The quantitative expression can be derived by combining Equations (4-16), (4-17), and (4-18),

$$k_{p1} = \exp\left(a + BC_a - \frac{c + dC_a}{RT}\right) \quad (4-19)$$

Rearrangement of Equation (4-19) leads to

$$k_{p1} = \exp\left[\left(a - \frac{c}{RT}\right) + \left(b - \frac{d}{RT}\right)C_a\right] = \exp(\alpha + \beta C_a) \quad (4-20)$$

where, α and β are constants at a constant T . It turns out that the concentration of sulfuric acid affects the oxidation of H_2S exponentially, similar to the effect of temperature. Sulfuric acid solutions of different concentrations seem to behave like different reactants. Due to the strong interaction between sulfuric acid and water, the presence of species in the solution and their concentrations depend on the ratio of sulfuric acid to water, resulting in qualitative as well as quantitative changes in properties of the solution, including the oxidizing ability. It is obvious that the rate equation, Equation (4-15), does not refer to an elementary process, and therefore, it does not provide details relating to the reaction mechanism. However, it is not necessary to know the mechanism of a reaction in order to design a reactor. An empirical rate equation which relates the necessary parameters would work satisfactorily from engineering point of view.

The other advantage from this correlation is that the rate of reaction at a given H_2S pressure can be easily compared between temperatures and between acid concentrations as well. Derived from Equation (4-20), the ratio of the reaction rates at

two different acid concentrations, C_{a1} and C_{a2} , can be described quantitatively as follows

$$\frac{k_{P1,C_{a1}}}{k_{P1,C_{a2}}} = \exp(\beta(C_{a1} - C_{a2})) \quad (4-21)$$

and the comparison of the reaction rates can be made between two temperatures using Equation (4-22), resulting from Equation (4-19)

$$\frac{k_{P1,T_1}}{k_{P1,T_2}} = \exp\left(\frac{c + dC_a}{R} \left(\frac{1}{T_2} + \frac{1}{T_1}\right)\right) \quad (4-22)$$

4.5 Conclusions

The oxidation of hydrogen sulfide by concentrated sulfuric acid is first order with respect to H_2S . Sulfuric acid plays the role of an oxidizing agent. Because of the complexity of sulfuric acid-water mixture, this role is not quantitatively regulated in a simple power-law rate equation. An empirical equation is suggested in which the effects of temperature and acid concentration are involved in a global rate constant. The temperature-dependence of the global rate constants fits the Arrhenius equation. And the acid effect is described in two linear relationships between $\ln A_0$ and the acid concentration of wt% and between E_a and the acid concentration of wt%. This empirical rate equation will be useful for the design of a reactor.

4.6 Nomenclature

A_0	Preexponential factor	$\text{mol s}^{-1}\text{m}^{-2}\text{Pa}^{-1}$
a	Surface area in rate equation	m^2
a	Regression constant arisen from Equation (4-17)	
b	Regression constant arisen from Equation (4-17)	
C	Constant in Equations (4-11), (4-12) and (4-13)	
C_A	Concentration of reactant A	mol L^{-1}
C_a	Apparent sulfuric acid concentration	wt% or mol L^{-1}
c	Regression constant arisen from Equation (4-18)	
d	Regression constant arisen from Equation (4-18)	
D	Diffusivity	m^2s^{-1}
E_a	Activation energy	kJ/mol
i	Regression constant arisen from Equation (4-9)	
j	Regression constant arisen from Equation (4-9)	
k	Specific reaction rate	
k_P	Specific reaction rate in terms of pressure of reactants	$\text{mol s}^{-1}\text{m}^{-2}\text{Pa}^{-1}$
m	Order of reaction	
N	Number of moles	
n	Order of reaction	
P	Pressure	Pa, kPa
R	Gas constant	$\text{J mol}^{-1}\text{K}^{-1}$
r	Reaction rate per volume in Equation (4-4)	$\text{mol s}^{-1}\text{m}^{-3}$
r	Reaction rate in other than Equation (4-4)	mol s^{-1}

T	Temperature	K
V	Volume of gas phase	m^3
t	Time	s
x	Direction perpendicular to the gas-liquid interface	m

Subscripts

a	Acid
T	Total
0	Refer to time zero
1	Refer to reaction 1
2	Refer to reaction 2

Greek

α	Constant arisen from Equation (4-12)
β	Constant arisen from Equation (4-12)
δ	The change in number of moles of gas reactants per mole of H_2S in reaction

4.7 Literature Cited

- Alexandrova, M. V., and E. G. Yaroshchuk, "Solubility and Gas-Liquid Equilibrium in the Systems of Nitrogen - Carbon Disulfide and Hydrogen Sulfide - Acidic Salt Solutions at 50°C", *J. Appl. Chem.*, **51**, 1221 (1978).
- Chou, P., and M. A. Vannice, "Benzene Hydrogenation over Supported Palladium", *Proc. AIChE 1986 Meeting*, Miami Beach, FL, AIChE, New York (1986).
- Danckwerts, P. V., *Gas-Liquid Reactions*, McGraw-Hill Book Company: New York, pp33-34 (1970).
- Douabul, A. A., and J. P. Riley, "The Solubility of Gases in Distilled Water and Seawater - Hydrogen Sulfide", *Deep-Sea Research*, **26A**, 259 (1979).
- Durrant, P. J., and B. Durrant, *Introduction to Advanced Inorganic Chemistry*, 2nd Ed. John Wiley & Sons, New York, pp842-843, pp853-854 (1970).
- Fogler, H. S., *Elements of Chemical Reaction Engineering*, Prentice-Hall, Engelwood Cliffs, pp338-366 (1986).
- Giauque, W. F., E. W. Hornung, J. E. Kunzler, and T. R. Rubin, "The Thermodynamic Properties of Aqueous Sulfuric Acid Solutions and Hydrates from 15 to 300 K", *J. Am. Chem. Soc.*, **82**, 62 (1960).
- Liler, M., *Reaction Mechanism in Sulfuric Acid and other Strong Acid Solutions*, Academic Press, London and New York, pp26-56, pp183-297 (1971).
- Muller, T. L., "Sulfuric Acid", *Kirk-Othmer Encyclopedia of Chem. Eng.* 4th Ed. John Wiley & Sons (Web version, 1997).
- Rochester, C. H., *Acidity Function*, Academic Press, London and New York, pp1-68 (1970).

- Sander, U. H. F., H. Fischer, U. Rothe, and R. Kola, *Sulfur, Sulfur Dioxide and Sulfuric Acid – An Introduction to their Industrial Chemistry and technology*. English Ed. More, A. I. The British Sulfur Corporation Ltd., London, pp271-273 (1984).
- Smith, J. M., *Chemical Engineering Kinetics*. 2nd Edition, McGraw-Hall Book Company, New York, pp37-38 (1970).
- Wehrer, A., P. Wehrer, and X. Duval, “Decomposition of Acetylene, Ethylene and Benzene on Carbon at Very High Temperatures and Low Pressures”, *Carbon*, 21(3), 247 (1983).
- Weil, E. D., and S. R. Randler, “Sulfur Compounds”, *Kirk-Othmer Encyclopedia of Chem. Eng.* 4th Ed. John Wiley & Sons (Web version, 1997).
- Zhang, Q., H. Wang, I. G. Dalla Lana and K. T. Chuang, “Solubility of Sulfur Dioxide in Sulfuric Acid of High Concentration”, *Ind. Eng. Chem. Res.*, **37**, 1167-1172 (1998).

Chapter 5

Kinetics of Reaction between Hydrogen Sulfide and Sulfur Dioxide in Sulfuric Acid Solutions^{*}

5.1 Introduction

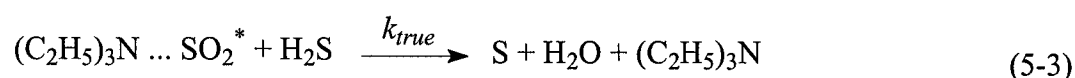
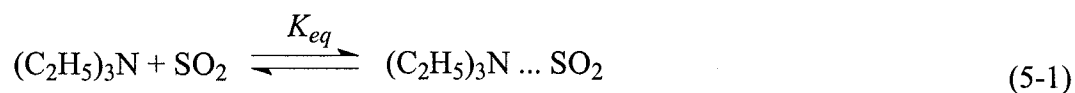
In the development of a new and efficient sulfur removal and recovery technology based on the reactions between hydrogen sulfide and sulfuric acid, it is expected that SO₂ generated from the first reaction will be completely consumed by the second reaction. To ensure this complete conversion of SO₂, knowledge of the kinetics behavior of the two reactions is essential. This chapter studies the kinetics of the second reaction.

The reaction between hydrogen sulfide and sulfur dioxide in liquid media has been extensively investigated during the last century. It has been found that hydrogen sulfide and sulfur dioxide do not react with each other unless moisture is present (Klein, 1911). Hydrogen sulfide and sulfur dioxide also react in solvents such as hydrocarbons (Bary, 1931), methanol (Kozak, 1980; Kozak et al., 1981), polyglycol ethers (Crean, 1987), amines (Bikbaeva et al., 1989), and in the presence of a solid surface (Taylor and Wesley, 1927) and catalysts (Dalla Lana et al., 1986; Murthy and Rao, 1951). The reaction occurring in the aqueous media is known as the *Wackenroder reaction*, in commemoration of his discovery of this reaction in 1846 (Volynskii, 1971). *Liquid phase*

^{*} A version of this chapter has been published in *Industrial and Engineering Chemistry Research*, **41**, 4707 (2002).

Claus reaction is also used to refer to the reaction that takes place in the liquid media (Donahue and Hayford, 1985).

Different liquid media lead to differences not only in reaction mechanisms but also in product distributions. Table 5-1 summarizes the product distributions from the liquid phase Claus reaction in a number of liquid media, indicating that the reaction in most of the organic solvents produces sulfur but that in water and alkali aqueous solutions produces either sulfur or polythionic acids depending on the H₂S/SO₂ ratio and temperature. Tracer studies (van der Heihde and Aten, 1953; Barbieri and Faraglia, 1962) show that either in product sulfur or in product polythionic acids, 2/3 of the sulfur atoms originate from H₂S and the other 1/3 from SO₂. The protonophilic interaction between organic solvents and SO₂ seems to be a prerequisite of the reaction leading to the production of sulfur. An intermediate of solvent-SO₂ is formed between the solvent and SO₂ which then reacts with H₂S to produce sulfur and water. For example, the reaction of H₂S and SO₂ in the solvent of triethyl amine was proposed to follow the mechanism, not especially revealing, suggested by Bikbaeva and Baranovskaya (1989)



SO₂ becomes reactive after a definite orientation in the complex with the solvent molecule. For this mechanism, the effective rate constant has been proposed to be

Table 5-1 Summary of products distribution of liquid phase Claus reaction

Liquid media	Temperature range	Products or reaction routes	References
Water	N/A	(a) $H_2S+3SO_2=H_2S_4O_6$ (b) $2H_2S+SO_2=3S+2H_2O$ When H_2S/SO_2 is small, (a) predominates; when H_2S/SO_2 is large, (b) does.	Riesenfeld and Feld (1921)
Tolune	Rm Temp.	Colloidal sulfur	Bary (1931)
Water Alkali soln.	N/A	Pentathionic acid Thiosulfate (passing $2H_2S+SO_2$ mixture into solutions)	Deines and Grassmann (1934)
Alkali metal sulfite	Below the decomposition temp. of the solution	$2H_2S+SO_2=3S+2H_2O$	Udy (1948)
Water-acid solution	N/A	Sulfur containing 80% insoluble in CS_2	Ross and Welde (1950); Welde (1951)
Colloidal aq. Soln. Of tragacanth gum	$-5^\circ C$	Water-soluble sulfur	Pagrien (1951)

Table 5-1 Continued

Liquid media	Temperature range	Products or reaction routes	References
Butane	Varying	Mixing H ₂ S-butane and SO ₂ -butane solutions produces (a) S and (b) H ₂ S ₅ O ₆ . When H ₂ S/SO ₂ =2, (a) predominates; when H ₂ S/SO ₂ =1, (b) predominates. Increasing temp. favors (b)	Dupasquier (1951)
Aqueous medium	N/A	(S ₂ O) _n H ₂ O	Schenk and Kretschmer (1962)
Diethylene glycol	20-30°C	Sulfur	Andreev et al. (1970)
K benzoate-polyethyleneglycol	130°C	Solid sulfur	Franckowiak et al. (1974)
Dilute sulfuric acid	14.7-36.3°C	Sulfur	Tiwari (1976)
Methanol	N/A	Filterable sulfur	Kozak (1980)
Citrate-based soln.	120-130°F	Elemental sulfur	Madenburg and Seesee (1980)
Water vapor	N/A	Sulfur	Vilesov (1980)

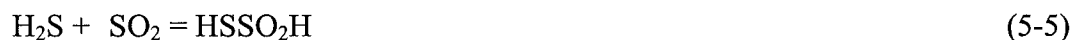
Table 5-1 Continued

Liquid media	Temperature range	Products or reaction routes	References
Methanol + sulfuric acid	Rm temp. ~50°C	Allotropic sulfur	Kozak (1981)
Phosphate	120-160°C	Sulfur	Donahue and Hayford (1985)
Triethylene glycol dimethyl ether; diethylene glycol methyl ether, plus 3-pyridyl carbinol as catalyst	22°C	Sulfur	Crean (1987)
R _x XO(X=N,P,S)	21-60°C	Sulfur	Bikbaeva, et al. (1988)
Heterocyclic amines	N/A	Sulfur	Bikbaeva, et al. (1989)
Ammoniacal buffer solution	N/A	Sulfur	Paj, et al. (1995)

$$k_{\text{eff}} = \frac{k_{\text{true}} K_{\text{eq}} K_{\text{eq}}^* [(C_2H_5)_3N][SO_2]}{1 + K_{\text{eq}}[SO_2]} \quad (5-4)$$

Bikbaeva et al. (1988 and 1989) also proposed similar mechanisms for the reaction in other solvents such as aromatic amine, pyridine and sulfoxides with various aliphatic and aromatic groups as the liquid media. It is apparent that Equation (5-4) was not based upon the stoichiometric reaction.

Volynskii (1971) proposed a mechanism for the reaction of H₂S and SO₂ in aqueous solutions. As shown in this mechanism, the formation of sulfur follows the steps below.



The overall equation for the three steps is



And the formation of polythionic acids results from the interaction of ionized SO₂ and monoatomic or polyatomic sulfur, *i.e.*,



where, x can range from 1 to 7. Tiwari (1976) believed that the reaction of H₂S and SO₂ in dilute sulfuric acid (below 10 wt%) follows the scheme from (5-5) to (5-7). His kinetic data showed that the reaction is first order with respect to both H₂S and SO₂, respectively,

consistent with this scheme because he assumed reaction (5-5) to be the rate-controlling step.

However, our interest in this reaction involves comparatively higher acid concentrations under which conditions little is known regarding its kinetics behavior. A difficulty in studying this reaction is the simultaneous effects of the two reactions in one gas-liquid system. Fortunately, the first reaction occurs negligibly and its rate may be neglected at low acid concentrations. Under the latter conditions, the second reaction rate can be measured by providing a feed mixture of H_2S and SO_2 . In this way, the kinetics of the second reaction, between H_2S and SO_2 , in appropriately dilute sulfuric acid can be obtained.

5.2 Experimental Section

The apparatus and the experimental procedure were nearly identical to those used in Chapter 4. However, the different behavior between the first reaction and the second reaction was taken into account. First, the stoichiometry of the second reaction differs from that of the first reaction. In the second reaction, three moles of gaseous reactants, *i.e.*, two moles of H_2S and one mole of SO_2 , are consumed to give rise to liquid and solid product at temperatures below the melting point of sulfur. As a result, it would seem that the initial rate analysis, which requires much more experimental work, could be avoided; however, some other unpredictable changes occur such as a surface area decrease due to sulfur formation. Second, the total pressure drop is contributed not only by reaction but also by the dissolution of SO_2 in the acid solution and the latter contribution has to be eliminated to measure a reliable reaction rate. In experiments, the acid solution was pre-

saturated with SO_2 such that the SO_2 in both phases was in equilibrium when the reaction started. Third, the second reaction would occur on the surface of solution as well as on the walls inside the reactor, wetted due to the condensation of water vapor. To prevent such condensation of water vapor, the reactor wall above the solution was heated to $10\text{--}15^\circ\text{C}$ higher than the temperature of the solution. Both the temperatures of the gas and solution in the experiments were measured under these circumstances. However, the wall was not heated when condensation did not occur.

The procedure of a run follows the steps described below:

- (1) Charge 200 mL, sometimes 300 mL, of sulfuric acid solution into the reactor.
- (2) Connect the reactor to the feed part of the experiment setup and check for leaks.
- (3) Turn on the impellers in both the solution and gas phases.
- (4) Evacuate the air from the system using an Edwards-5 two-stage vacuum pump.
- (5) Fill the SO_2 reservoir with pure SO_2 to a pre-set pressure.
- (6) Heat the acid solution to the reaction temperature using a warm water bath and heat the wall of the reactor using a heating tape.
- (7) When the temperatures are in equilibrium, record the pressure of the reactor, denoted as P_1 .
- (8) Disconnect the reactor and the vacuum pump. Connect the SO_2 reservoir and the reactor till the pressure does not change 0.1 psi in 20 minutes. Record the pressure, denoted as P_2 . Shut the valve between them. The initial partial pressure of SO_2 is the difference between P_2 and P_1 .
- (9) Suddenly introduce H_2S from its reservoir into the reactor to a certain pressure and shut off the valve between the reactor and the H_2S reservoir. Record the

pressure of the reactor at this moment, denoted as P_3 . The initial partial pressure of H_2S is the difference between P_3 and P_2 .

- (10) Record the subsequent pressure of the reactor every second and obtain the initial pressure drop rate in terms of the slope at $t=0$ of the curve of ΔP , the difference between P and P_3 , against time, t .

The information on the equipment and materials is the same as described in Chapter 4.

5.3 Results and Discussion

5.3.1 Selection of acid concentration range

Two factors determine the selection of the acid concentration range to be used in this chapter. First, the acid concentration range should be located where the rate of the first reaction is insignificant such that the second reaction can be studied separately. Chapter 4 has indicated that the first reaction occurs between H_2S and molecular H_2SO_4 in concentrated sulfuric acid solution and becomes insignificant when acid concentration is less than 88 wt%. Young and Molrafen (1970), and Miller (1990) also showed that the concentration and activity of molecular H_2SO_4 , the active species for the first reaction, are very small when acid concentration is less than 65 wt%. Thus, the acid concentration range in this study was chosen to be no more than 60 wt%. Second, the acid concentration should not change the reaction route. As discussed in section 5.1, the form of dissolved SO_2 determines the path and accordingly, the products of the reaction. The molecular dissolved SO_2 leads to the production of sulfur and water, without the production of polythionic acids. Gold and Tyr (1950) and Govindora and Gopalakrishna

(1993) reported that dissolved SO₂ in sulfuric acid solution remains in the molecular form when acid concentration is greater than 5 wt%. Therefore, the range from 5 wt% to 60 wt% H₂SO₄ meets the requirement for studying the second reaction. In order to avoid the very dilute solution where vapor condensation occurs, this study chose the acid concentration range from 30 wt% to 60 wt%.

5.3.2 Reaction rate measurement and calculation

Similar to the study of the first reaction, the formation of solid sulfur from the second reaction would also block the solution surface and the production of water dilutes the acid solution. Once the reaction commenced, the available surface area and the acid concentration could not be measured. To ensure that the reaction rate is measured under known conditions, the initial rate was obtained by plotting the slope of the pressure-drop versus time curve at time zero, *i.e.*,

$$R_p = \left(\frac{dP}{dt} \right)_{t=0} \quad (5-14)$$

The rate of disappearance of both gaseous reactants was calculated in terms of R_p by the following equation,

$$\frac{dN_s}{dt} = \frac{d}{dt} (N_{H_2S} + N_{SO_2}) = \frac{R_p V_G}{RT} \quad (5-15)$$

From the stoichiometry of the reaction, (5-8), the reaction rate based on H₂S consumption was expressed by

$$r_{H_2S,2} = -\frac{dN_{H_2S}}{dt} = -\frac{2}{3} \frac{dN_s}{dt} \quad (5-16)$$

The rate equation can be described by either Equation (5-17)

$$r_{H_2S,2} = -\frac{dN_{H_2S}}{dt} = k_2 a [H_2S]^m [SO_2]^n \quad (5-17)$$

or Equation (5-18)

$$r_{H_2S,2} = -\frac{dN_{H_2S}}{dt} = k_{P_2} a P_{H_2S}^m P_{SO_2}^n \quad (5-18)$$

depending on whether the partial pressures in the gas phase or the concentrations in the liquid phase of the reactants are known. Because the liquid surface was maintained flat in the experiments, “*a*” in these equations represents the interfacial area or liquid surface area, the cross-sectional area of the reactor. For a gas-liquid reaction, Equation (5-18) is the preferred expression since partial pressures of the reactants are easily determined and thus, k_{P_2} becomes a global rate constant, which includes the effects of reaction temperature, reactant solubility and acid concentration on the reaction rate. These effects sometimes compensate. For instance, rising temperature increases the reaction rate but decreases the solubility of SO_2 which, in turn, should decrease the reaction rate. H_2S does not dissolve in sulfuric acid significantly, as shown by curve 1 in Figure 5-1. To eliminate this effect, the following rate equation form was considered.

$$r_{H_2S,2} = -\frac{dN_{H_2S}}{dt} = k'_{P_2} a P_{H_2S}^m [SO_2]^n \quad (5-19)$$

The reaction rate was measured at equilibrium conditions between P_{SO_2} and $[SO_2]$ and the rate constant, k'_{P_2} , then is a function of temperature when the acid concentration is constant.

5.3.3 SO_2 dissolution

SO_2 dissolves significantly in sulfuric acid at all concentrations. In a closed gas-liquid batch reactor, the change in moles of the gas phase results in a change in the system pressure but the dissolution of SO_2 in the acid will also lead to a pressure change. Curve 1 in Figure 5-1 shows that the pressure drop caused by the interaction between H_2S

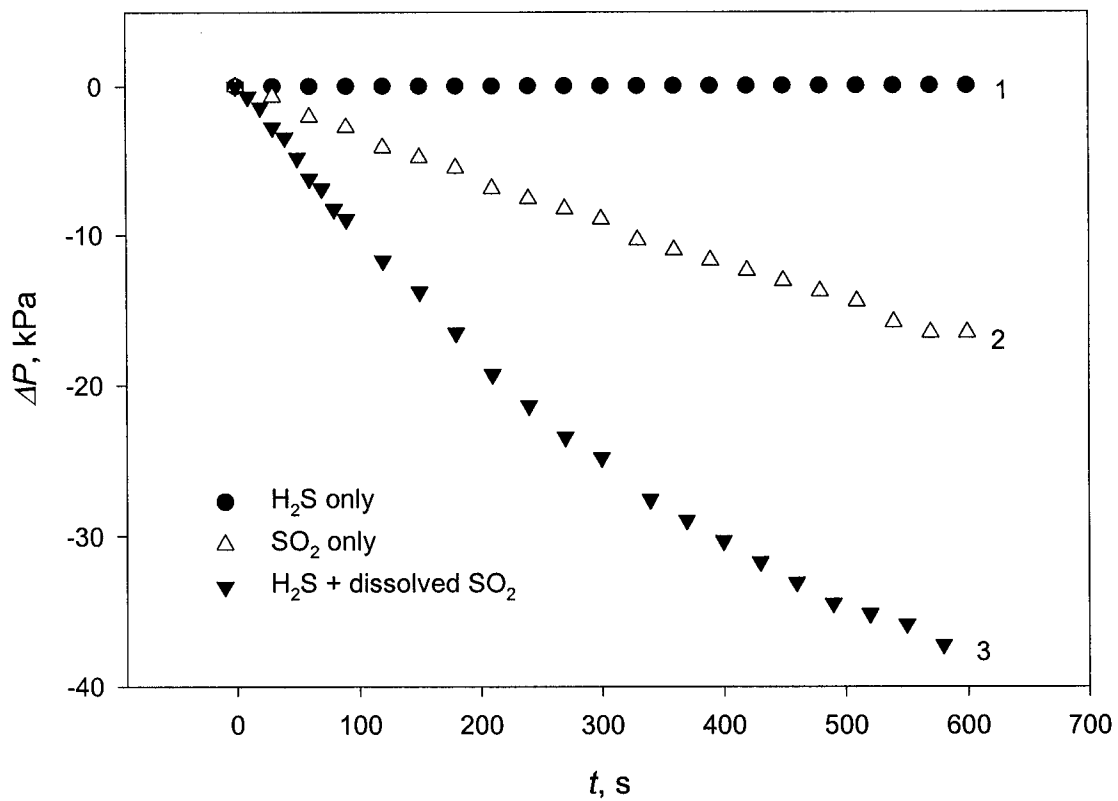


Figure 5-1. Typical curves for pressure-drop versus time. Temperature: 25°C; Acid concentration: 30.16 wt%; Stirring speed: 50 rpm; Run#: pd_test3&5.

and acid solution was negligible. H₂S neither reacts nor dissolves in the dilute sulfuric acid solution to a detectable extent. Curve 2 indicates that the pressure drop caused by SO₂ dissolution is significant. When the equilibrium of SO₂ between the gas and liquid phases has been reached, the pressure drop may be attributed to the reaction, as shown by curve 3. Figure 5-2 shows that the initial rate of SO₂ dissolution is independent of the acid concentration and the same initial pressure of SO₂ leads to the same initial dissolution rate. From the absorption point of view, this is correct because the driving force is only the initial pressure.

In the literature, the interaction of SO₂ with either aqueous solutions or organic solvents was shown to induce the reaction of SO₂ and H₂S. In other words, the intermediates formed by SO₂ in the solutions or the solvents are reactive with H₂S. If the dissolved SO₂ remains in the molecular form, the reaction generates sulfur and water; but if some of the dissolved SO₂ molecules are hydrolyzed and form HSO₃⁻, the reaction also produces polythionic acids. For sulfuric acid solutions, it has been shown (Gold and Tyr, 1950; Govindora and Gopalakrishna, 1993) that dissolved SO₂ exists in the molecular form and as HSO₃⁻ ions when the acid concentration is below 5 wt%, and it takes the molecular form when the acid concentration is at 5 wt% and above. Therefore, in addition to water, both sulfur and polythionic acids would be produced when the reaction occurs in acid solutions below 5 wt% and only sulfur would be obtained above 5 wt%. Tiwari erroneously ignored the effect of the forms of dissolved SO₂ on the reaction routes and therefore, ignored the reaction that leads to polythionic acids in the acid concentration range which he used (from 0.43 wt% to 9.3 wt%). Thus, his results are inconsistent with our measurements, where the reaction only takes the route leading to sulfur and water.

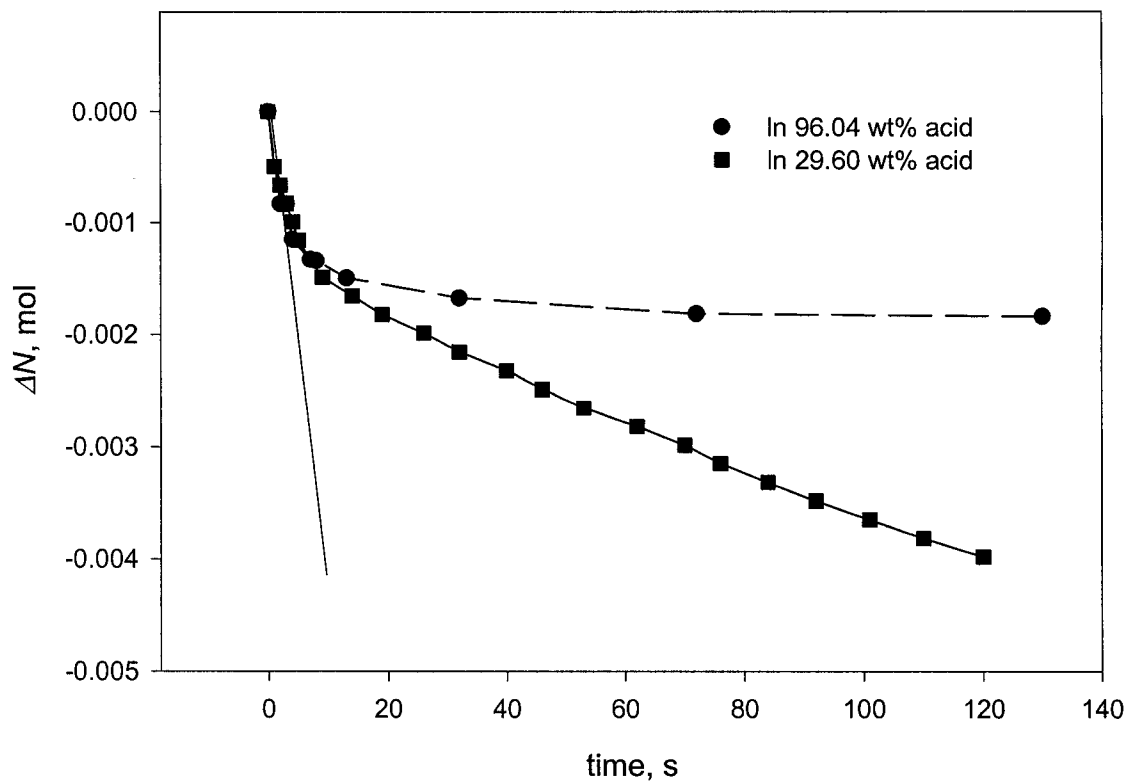


Figure 5-2. SO₂ dissolving rate in sulfuric acid solution of 29.60 wt% and 96.04 wt%. Temperature: 21°C; Initial pressure of SO₂: 80-86.5 kPa; Stirring speed: 50 rpm; Run#: pd_30_s1, pd_96_s4.

5.3.4 Introduction of H₂S

H₂S was introduced into the reactor after the concentrations of SO₂ present in both phases had equilibrated. Either H₂S or an H₂S-SO₂ mixture having a partial pressure equal to the equilibrium pressure of SO₂ in the reactor was introduced, to keep the SO₂ equilibrium unchanged during this introduction. An impeller was installed to improve the mixing between the introduced gas and the gas already present within the reactor. To study the effect of this mixing on the rate measurement, different stirring speeds were used while the other experimental conditions were kept constant. As shown in Figure 5-3, the same initial rate of pressure drop was obtained when the impeller was stirred as fast as 40 rpm. The stirring speed could not be too fast because of the need to maintain a flat surface on the solution. All the other runs were carried out at 50 rpm.

5.3.5 Order of reaction with respect to H₂S and SO₂

For 30.10 wt% sulfuric acid solution, the initial pressure-drop rate was measured at 25°C and various ratios of P_{H_2S} to $[SO_2]$. The results are shown in Table 5-2. The linearization of Equation (5-19) leads to

$$\ln r_{H_2S_2} = \ln(k'_{P_2} a) + m \ln P_{H_2S} + n \ln [SO_2] \quad (5-20)$$

The values of $\ln r_{H_2S_2}$, $\ln P_{H_2S}$ and $\ln [SO_2]$ calculated from Table 5-2 were plotted in a 3-D diagram, as shown in Figure 5-4. The regression analysis yielded values for m and n at 1.22 ± 0.19 and 1.07 ± 0.12 (the regression coefficient \pm the standard deviation), respectively. Rounding these numbers to unity suggests that the reaction could be described by second order kinetics (first order with respect to each of the two reactants, H₂S and SO₂). The value of k'_{P_2} for each run was then calculated by the following equation

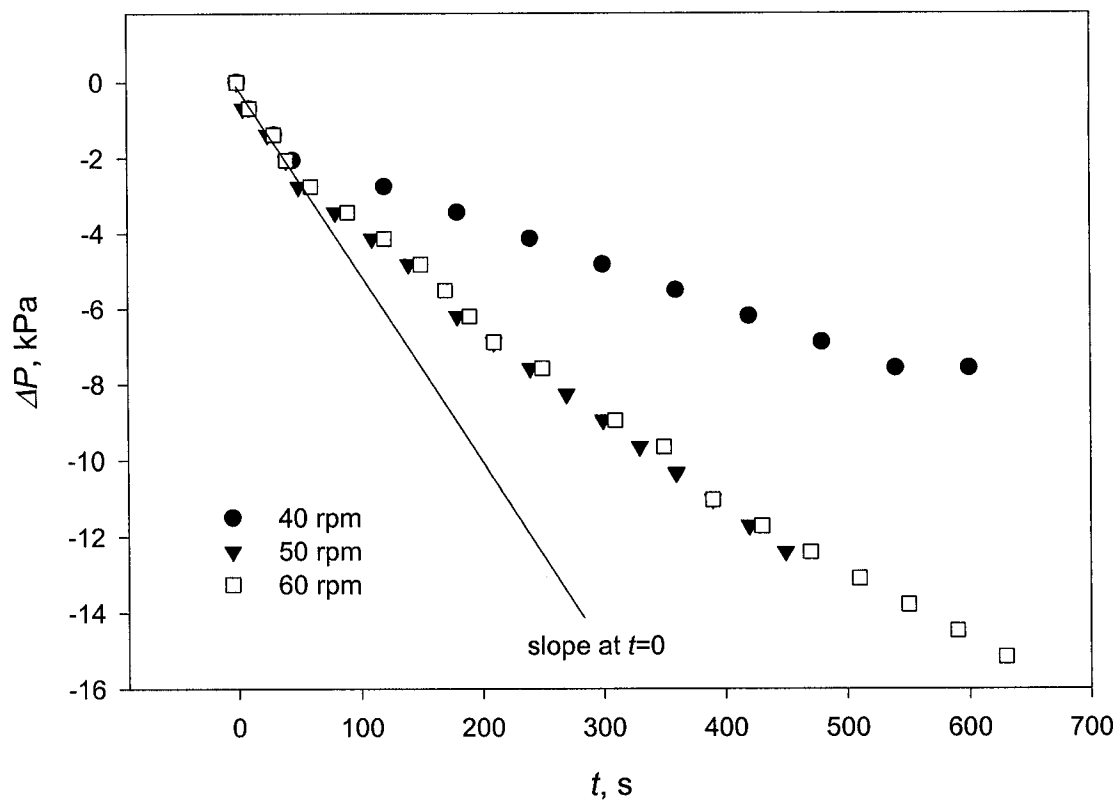


Figure 5-3. Effect of stirring speed. Temperature: 25⁰C; Acid concentration: 30.16 wt%; Run#: pd_st2, pd_p1, pd_st6.

Table 5-2. Experimental results for order of reaction.

Run #	Acid conc. wt%	$V_L \times 10^4$ m^3	$V_G \times 10^4$ m^3	Solution		Gas temp. K	$a \times 10^3$ m^2	P_{H_2S} kPa	$[SO_2]$ $mol L^{-1}$	R_P $kPa s^{-1}$	$k'_{P_2} \times 10^7$ $L s^{-1} m^{-2} Pa^{-1}$
				temp. K	P_{H_2S} kPa						
pd_newp4	30.1	2.00	5.88	298.15	294.15	112	4.42	101	0.667	-0.935	4.54
pd_newp3	30.1	2.00	5.88	298.15	294.15	101	4.42	101	0.695	-0.896	4.63
pd_newp2	30.1	2.00	5.88	298.15	294.15	103	4.42	103	0.804	-0.985	4.31
pd_newp1	30.1	2.00	5.88	298.15	294.15	82.5	4.42	82.5	0.722	-0.689	4.19
pd_new4	30.1	2.00	5.88	298.15	293.15	83.4	4.42	83.4	1.00	-1.03	4.49
pd_newp5	30.1	2.00	5.88	298.15	293.15	73.2	4.42	73.2	1.24	-1.13	4.53
pd_newp6	30.1	2.00	5.88	298.15	293.15	62.5	4.42	62.5	1.55	-1.1	4.13

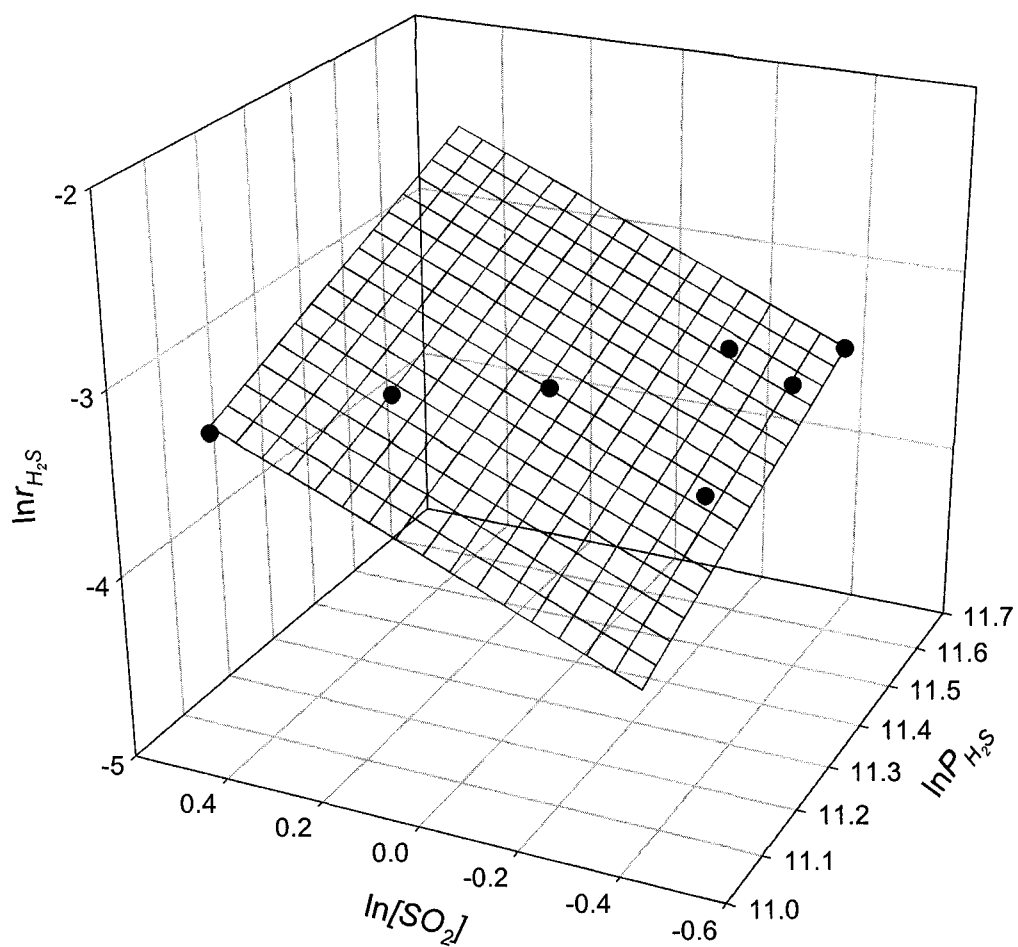


Figure 5-4. Reaction orders with respect to P_{H_2S} and $[SO_2]$. Temperature: 25°C ; Acid concentration: 30.10 wt%; stirring speed: 50 rpm; Run#: see Table 5-2.

$$k'_{p2} = \frac{r_{H_2S,2}}{aP_{H_2S}[SO_2]} \quad (5-21)$$

which is also shown in Table 5-2. The values of k'_{p2} thus obtained are of the same order of magnitude. The average of k'_{p2} is $4.40 \times 10^{-7} \text{ L s}^{-1} \text{ m}^{-2} \text{ Pa}^{-1}$.

5.3.6 Effect of surface area

Because the liquid surface was maintained flat, the interfacial area is equal to the cross sectional area of the reactor. Cylindrical- and conical-shaped reactor vessels were used to measure the reaction rate at different ratios of liquid volume to interfacial area. Figure 5-5 shows that similar values of k'_{p2} were obtained at different surface areas and solution volumes. Because k'_{p2} is based on the unit surface area, this result indicates that the reaction rate is proportional to surface area and not affected by the volume of solution. Figure 5-1 shows that H_2S does not diffuse into the solution of sulfuric acid significantly (curve 1) but reacts rapidly when the solution has been saturated with SO_2 (curve 3). It is reasonable to assume that the reaction of H_2S with the dissolved SO_2 is much faster than the diffusion of H_2S into the solution. Once the H_2S molecules contact the dissolved SO_2 molecules, they react so fast that no H_2S molecules are present at the liquid surface, thus preventing them from diffusing into the bulk solution. Generally, the reaction behavior of a gas-liquid reaction is determined by the relative values of the reaction and diffusion rates of reactants within the liquid phase. In this case, the diffusion rate of H_2S is negligibly small compared with the reaction rate. Therefore, the reaction occurs only at the surface of the acid solution. The initial mechanism of the reaction may be described by the following,

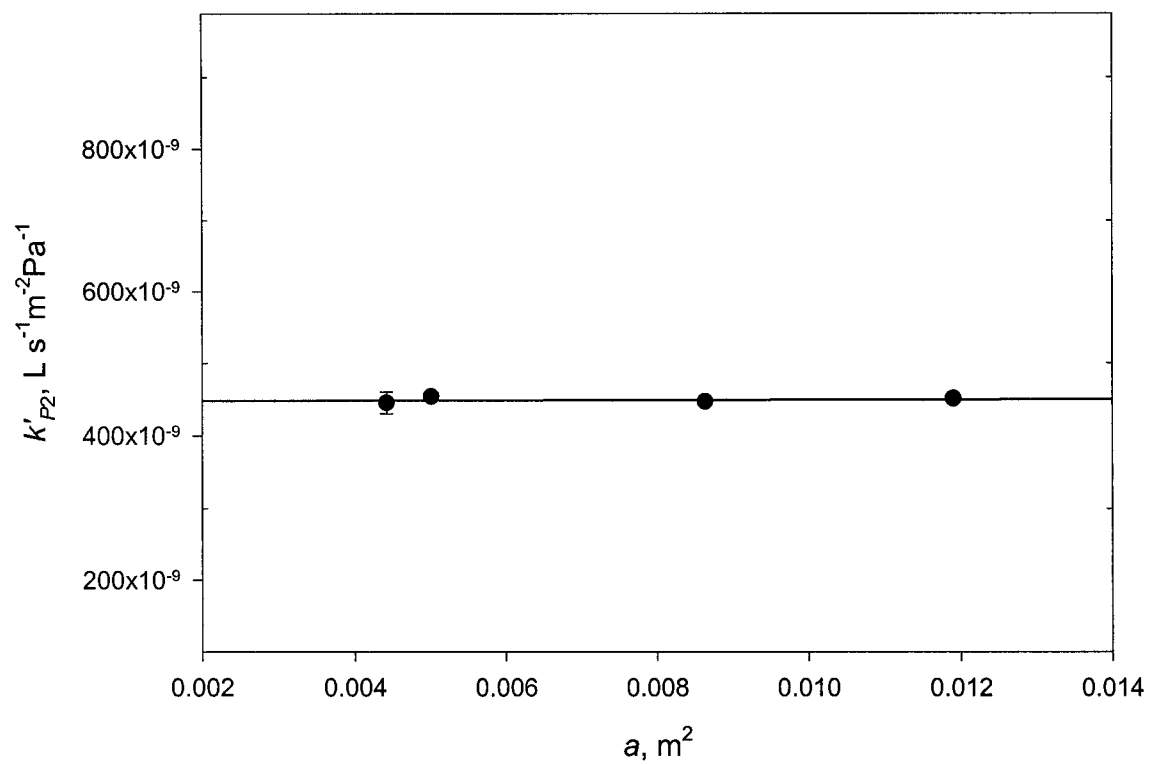
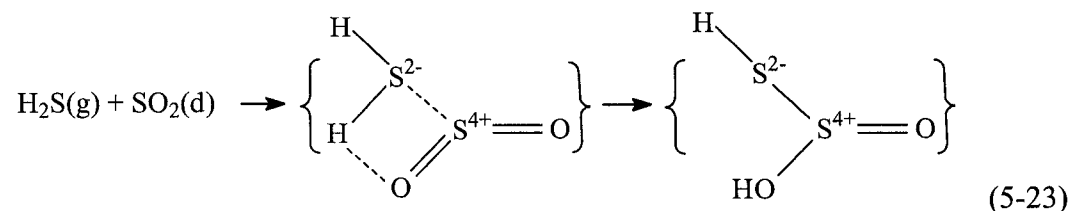
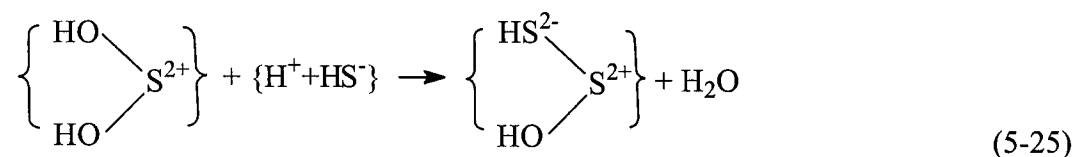
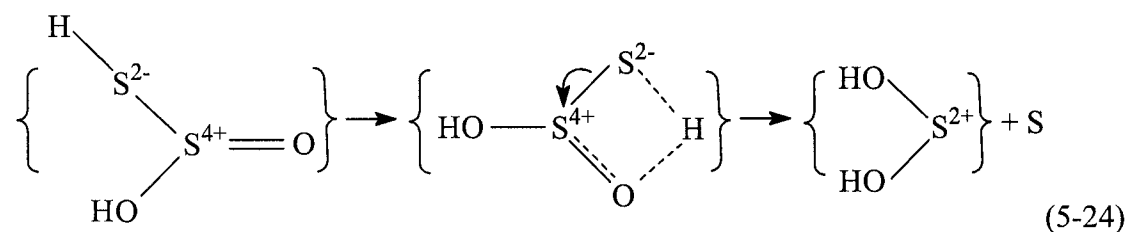


Figure 5-5. Effect of surface area (a) on the reaction rate. Temperature: 25°C; Acid concentration: 30.16 wt%; Stirring speed: 50 rpm; Solution volume: 200, 300, 500, 800 mL, respectively.



where, $\text{SO}_2(\text{d})$ represents dissolved SO_2 in sulfuric acid solutions. Many investigators (Volynskii, 1971) believed that H_2S and dissolved SO_2 in aqueous solutions initially form thiosulfurous acid. Sulfur and water are formed through the following steps, as suggested by Volynskii (1971),



Steps (5-23), (5-25), (5-26) and (5-27) are either physical processes or intermediate transformations, which occur relatively rapidly. Assuming the first step to be rate-controlling, the second order behavior is then in agreement with this mechanism. As pointed out previously, the acid concentration range applied in this chapter ensured that only the reaction route of steps from (5-5) to (5-7) was taken. Therefore, the rate equation

$$r_{H_2S,2} = -\frac{dN_{H_2S}}{dt} = k'_{P2} a_{P_{H_2S}}[SO_2] \quad (5-27)$$

for the second reaction would apply in the acid concentration range from 30 wt% to 60 wt%.

5.3.7 Effect of temperature and acid concentration

The reaction rates were measured at various temperatures from 21°C to 50°C and acid concentrations from 30 wt% to 60 wt%. In addition to Table 5-2, the results for other temperatures and other acid concentrations are listed in Table A-2 in the appendix. The rate constant for each run was also calculated using Equation (5-21). The plot of $\ln k'_{P2}$ against $1/T$ is shown in Figure 5-6, indicating that the relationship between temperature and k'_{P2} for the investigated acid concentrations fits a single Arrhenius equation. In other words, the second reaction has the activation energy, ($E_a = 59.0 \pm 4.3 \text{ kJ mol}^{-1}$), and pre-exponential factor, ($A_0 = 11,790$), which are independent of acid concentration. This is contrary to that observed for the first reaction, in which the activation energy and pre-exponential factor change with acid concentration. The differences may be attributed to the facts that sulfuric acid solution is involved in the first reaction as an oxidant but acts merely as a reaction medium for the second reaction. The reactant in the medium is dissolved SO_2 . The role that the sulfuric acid plays in the reaction also differs from that shown by the organic solvents, in which one SO_2 molecule forms an intermediate with one solvent molecule and accordingly, the concentration of the solvent was included in the kinetic equations (Crean, 1987; Bikbaeva et al., 1988 and 1989).

5.3.8 Extended experiments

Our results suggest that the form of SO_2 dissolved in sulfuric acid determines the path of the reaction. If its structure does not change, neither the reaction mechanism nor

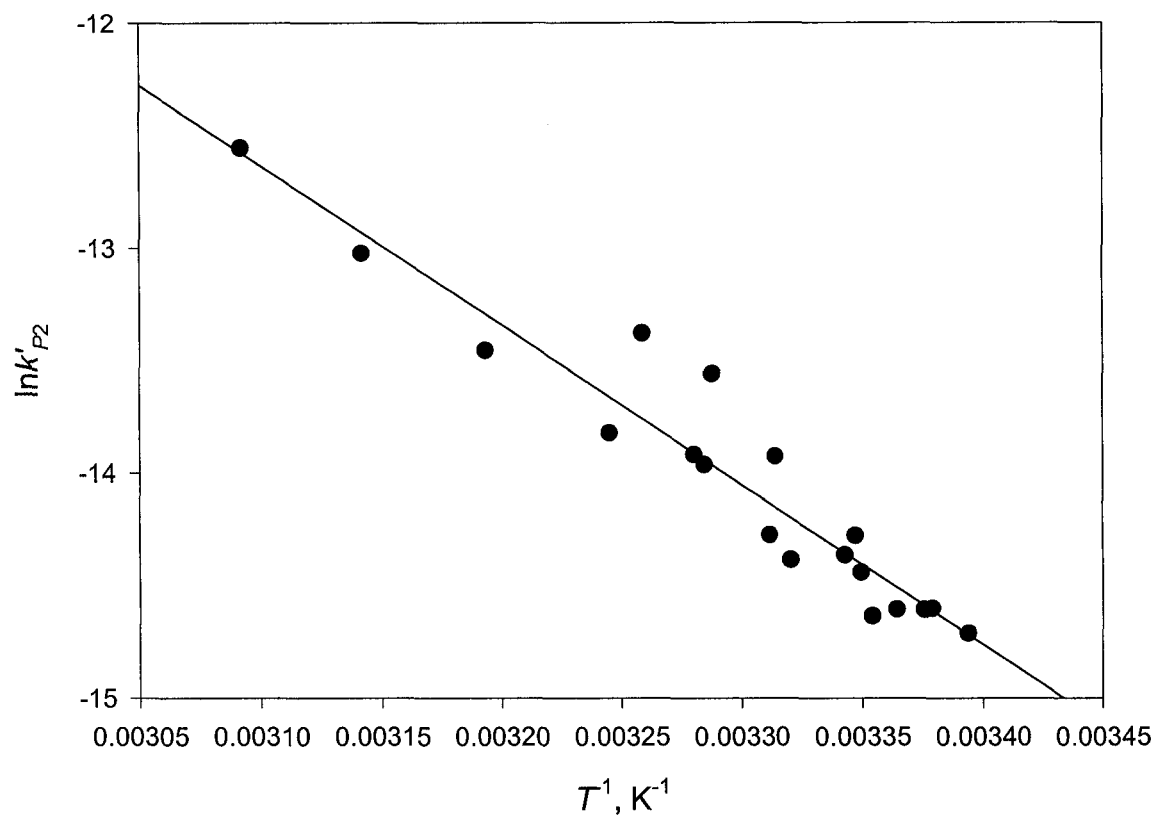


Figure 5-6. Arrhenius plot of reaction in sulfuric acid from 30 wt% to 60 wt%.

its kinetics behavior should change. Dissolved SO₂ maintains its molecular form when acid concentration is in the range from 30 wt% to 60 wt%. Since this molecular form also applies to acid concentrations greater than 60 wt%, it is reasonable that the reaction mechanism and kinetics behavior exhibited in acid concentrations up to 60 wt% may be extrapolated to acid concentrations above 60 wt%.

To confirm the validity of this extrapolation, runs were made to measure the initial reaction rate at acid concentrations of 90 wt% and 96 wt%, where the solutions were pre-saturated with SO₂. When H₂S reacts with the fresh concentrated sulfuric acid, the first reaction causes the reactor pressure to drop because the produced SO₂ tends to stay in the solution. However, when the solution was pre-saturated with SO₂, the first reaction no longer causes a change in total pressure. Thus, the drop in pressure may be attributed to the second reaction. The reaction rate measured under each experimental condition was compared with the value predicted by Equation (5-28)

$$r_{H_2S,2} = k'_{P_2} a_{P_{H_2S}}[SO_2], \text{ mol s}^{-1} \quad (5-28)$$

Figure 5-7 shows that the predictions are in good agreement with the experimental data.

5.3.9 Prediction of conditions to convert all sulfur

The two rate equations should be able to predict the temperature and acid concentration enabling the two reactions to proceed stoichiometrically at any chosen P_{H_2S} and P_{SO_2} under the assumption that the solubility of SO₂ in sulfuric acid obeys Henry's law. The predicted values of k_{P_1} and k'_{P_2} , the two reaction rates, and the ratio $r_{H_2S,1} / r_{H_2S,2}$, at $P_{H_2S} = 1.013$ kPa and $P_{SO_2} = 0.5065$ kPa for temperatures from 25°C to 120°C and acid concentrations from 30 wt% to 96 wt% are shown in Table A-3 in the Appendix. The ratio of $r_{H_2S,1} / r_{H_2S,2}$ is also shown in Figure 5-8. From this estimate it is

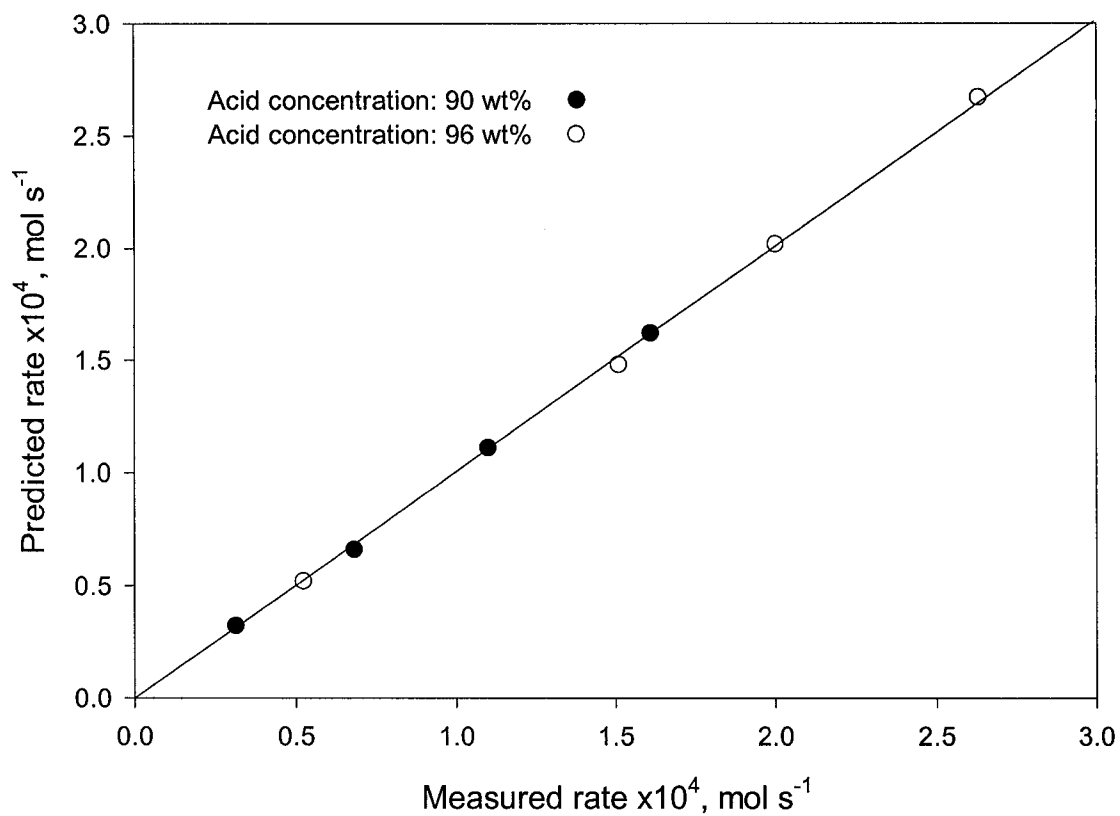


Figure 5-7. Comparison of second reaction rate predicted by Equation (5-28) with that obtained in experiment when two reactions occur simultaneously in 90 wt% and 96 wt% sulfuric acid.

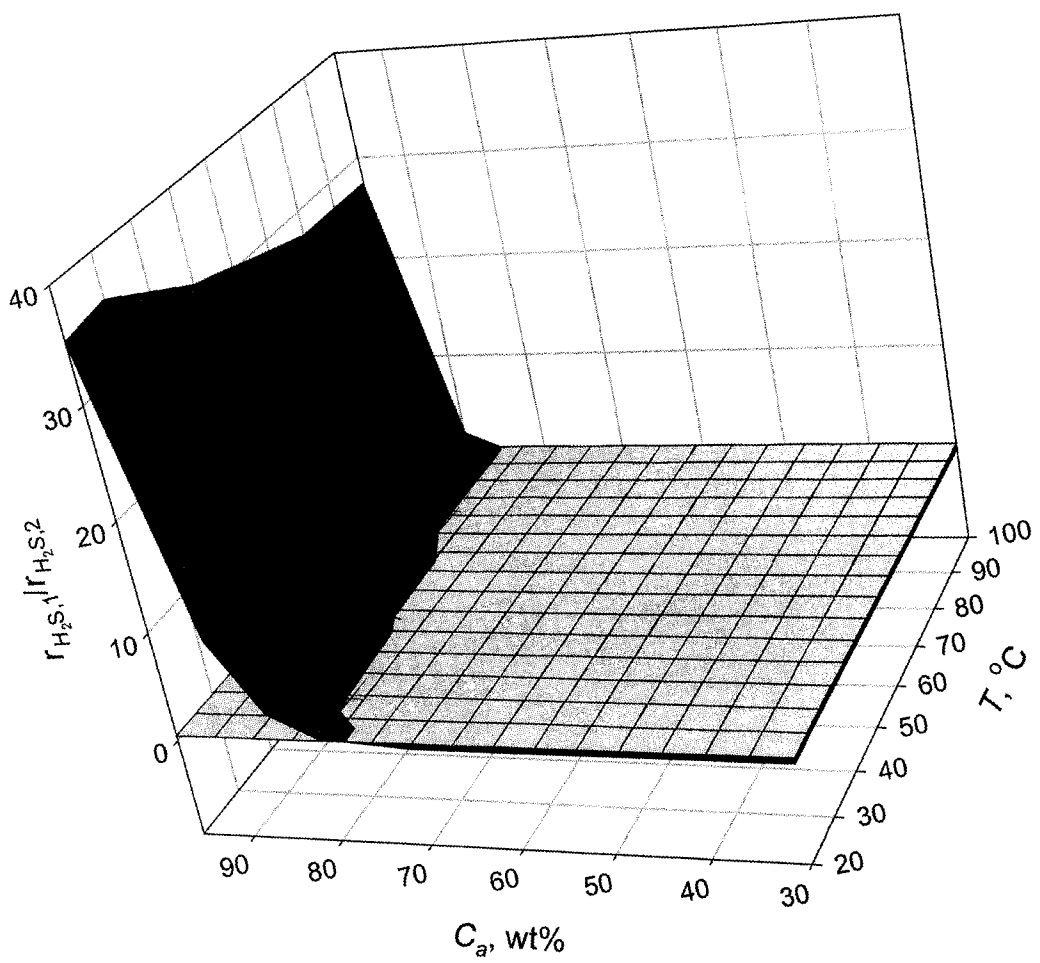


Figure 5-8. Ratio of reaction rate of the first reaction to the second reaction estimated at $P_{H_2S}=1.013$ kPa and $P_{SO_2}=0.5065$ kPa.

seen that H₂S in a gas stream can be consumed completely without SO₂ emission in a single reactor vessel as long as $r_{H_2S,1}/r_{H_2S,2} \leq 0.5$. The temperature and acid concentration that meet this requirement can be easily found in Figure 5-8 where the range of the gray surface (the right part of the plain “z axis” = 0.5) extends. However, under this condition, the relatively slow reaction rate would necessitate use of a large-sized reactor and dilute sulfuric acid, which conditions are economically unjustifiable. The special materials to handle the corrosiveness of dilute acid may add the cost. Nevertheless, the target of the zero sulfur emission requires that SO₂ in both phases be consumed, but a fast second reaction needs high SO₂ solubility in liquid phase. All of these factors render it difficult to consume the entire sulfur from the gas using a single reactor vessel. It seems that the practical choice is likely a two-stage process, where the first stage mainly carries out the first reaction in a relatively small reactor and the second stage conducts the second reaction in a larger reactor.

5.4 Conclusions

The reaction between H₂S and SO₂ in aqueous sulfuric acid solutions from 30 wt% to 60 wt% is first order with respect to both H₂S and SO₂, respectively. The reaction rate is described by the equation

$$r_{H_2S,2} = k'_{P_2} a_{P_{H_2S}} [SO_2], \text{ mol s}^{-1} \quad (5-28)$$

where

$$k'_{P_2} = 11900 \times e^{-7100/T} \quad (5-29)$$

Sulfuric acid merely provides a medium for the reaction which occurs at the interface of the gas-liquid system. Acid concentration does not affect the rate constant and the

reaction has a single activation energy in all solutions. However, the acid concentration affects the reaction rate through the changing SO_2 solubility in various concentrations of acid solution. The dissolution of SO_2 induces the reaction and accordingly, the form of the dissolved SO_2 determines the reaction mechanism. Since the dissolved form of SO_2 does not change in sulfuric acid of concentrations higher than 60 wt%, the reaction should still have the same rate constant.

5.5 Nomenclature

a	Surface area	m^2
A_0	Preexponential factor	$L s^{-1} m^{-2} Pa^{-1}$
C_a	Apparent sulfuric acid concentration	wt%
E_a	Activation energy	$kJ mol^{-1}$
k_{C2}	Specific reaction rate in terms of molarity concentration	
k_{P2}	Specific reaction rate in terms of pressure of reactants	
k'_{P2}	Specific reaction rate defined by Equations (19) and (24)	
N	Number of mole	mol
P	Pressure	Pa or kPa
R	Gas constant	$J mol^{-1} K^{-1}$
R_p	Pressure drop rate	$kPa s^{-1}$ or $Pa s^{-1}$
r	Reaction rate	$mol s^{-1}$
T	Temperature	K
V	Volume of gas phase	m^3
t	Time	s
$[H_2S]$	Molarity concentration of H_2S in solution	$mol L^{-1}$
$[SO_2]$	Molarity concentration of SO_2 in solution	$mol L^{-1}$

Superscripts and Subscripts

d	Dissolving
G	Gas

<i>L</i>	Liquid
<i>m</i>	Reaction order
<i>n</i>	Reaction order
<i>P</i>	Pressure
<i>S</i>	Sulfur
0	Refer to time zero or bulk area
1	Refer to reaction 1
2	Refer to reaction 2

5.6 Literature Cited

- Andreev, E. I., V. V. Zulin, and Yu. N. Sergeeva, "Oxidation Reaction Kinetics of Hydrogen Sulfide with Sulfur Dioxide in Diethylene Glycol Medium," *Tr. Kuibeshev. Nauch.-Issled. Inst. Neft. Prom.*, **44**, 37 (1970).
- Barbieri, R. and G. Faraglia, "Wackenroder reaction. II. Mechanism of Internal Sulfur in Forming Polythionic Acids," *Gazz. Chim. Ital.*, **92**, 660 (1962).
- Bary, P., "Reaction of Sulfur Dioxide and Hydrogen Sulfide in Hydrocarbons," *Rev. gen. Caoutchouc*, **8**, 25 (1931).
- Bikbaeva, G. G., E. M. Baranovskaya, and Yu. E. Nikitin, "Kinetics of Reduction of Sulfur Dioxide with Hydrogen Sulfide in the Presence of Sulfoxide, Pyridine N-Oxide, Trioctylphosphine Oxide, and Tributyl Phosphate," *Kinet. Katal.*, **29**, 794 (1988).
- Bikbaeva, G. G., E. M. Baranovskaya, and Yu. E. Nikitin, "Kinetics of Reduction of Sulfur Dioxide with Hydrogen Sulfide in the Presence of Amines," *Zh. Obshch. Khim.*, **59**, 2162 (1989).
- Crean, D. J., "Kinetics and Corrosion Studies of Hydrogen Sulfide and Sulfur Dioxide in Polyglycol Ethers," MSc Thesis, University of California at Berkeley, Berkeley, California, U.S.A., (1987).
- Dalla Lana, I. G., C. L. Liu, and B. K. Cho, "The Development of a Kinetic Model for Rational Design of Catalytic Reactors in the Modified Claus Process," *Chem React. Eng. Proc. Int. Symp.*, **4th**, 196 (1976).

- Deines, O. v., and H. Grassmann, "Steps in the Reaction between Hydrogen Sulfide and Sulfurous Acid in Aqueous and in Alkaline Solutions and Their Applications," *Z. anorg. Allgem. Chem.*, **220**, 337 (1934).
- Donahue, R. J., and J. S. Hayford, "Liquid Phase Claus Reaction," Eur. Patent Appl. No. EP 142,804 (May 29, 1985).
- Dupasquier, J., "Reactions between Hydrosulfuric and Sulfurous Acids," *Ann. Fac sci. Marseille*, **21**, 155 (1951).
- Franckowiak, S., P. Renault, C. Dezael, and A. Deschamps, "Purification of Gas Containing Sulfur Dioxide with Production of Sulfur," French Demande No. 2,202,714 (May 10, 1974).
- Gold, V, and F. L. Tyr, "The State of Sulfur Dioxide Dissolved in Sulfuric Acid", *J. Am. Chem. Soc.*, **73**, 2932 (1950).
- Govindora, V. M. H., and K. V. Gopalakrishna, "Solubility of Sulfur Dioxide at Low Partial Pressure in Dilute Sulfuric Acid Solutions", *Ind. Eng. Chem. Res.*, **32**, 2111 (1993).
- Klein, D., "The Influence of Organic Liquids upon the Interaction of Hydrogen Sulfide and Sulfur Dioxide", *J. Phys. Chem.*, **15**, 1 (1911).
- Kozak, Z., "Oxidation of Hydrogen Sulfide with Sulfur Dioxide in Solutions," *Pzrem. Chem.*, **59**, 391 (1980).
- Kosak, Z., D. Kozak, and R. Frak, "Production of Polymeric Sulfur by Oxidation of Hydrogen Sulfide with Sulfur Dioxide in methanol Solutions," *Pzrem. Chem.*, **60**, 416 (1981).

- Madenburg, R. S., and T. A. Seese, "Hydrogen Sulfide Reduces Sulfur Dioxide to Desulfurize Flue Gas," *Chem. Eng.*, **87**, 88 (1980).
- Murthy, A. R. V., and B. S. Rao, "Behavior of Sulfur Compounds. III. Kinetics of the Gaseous Reaction between Hydrogen Sulfide and Sulfur Dioxide," *Proc. Indian Acad. Sci.*, **34**, 283 (1951).
- Pagrién, L. S., "Water-soluble Sulfur," French Patent No. 971,913 (Jan. 23, 1951).
- Paj, Z. P., et al., "Manufacture of Sulfur from Sulfur Dioxide-Containing Gases by Chemisorption Using Ammonical Buffer Solution and Reaction with Hydrogen Sulfide," *Izobreteniya*, **30**, 161 (1995).
- Riesenfeld, E. F., and G. W. Feld, "A quantitative Study of the Formation of Polythionic Acids by the Action of Hydrogen Sulfide on Sulfur Dioxide in Water Solution," *Z. anorg. Allgem. Chem.*, **119**, 225 (1921).
- Ross, E. T., and C. B. Welde, "Insoluble Sulfur," U.S. Patent No. 2,534,063 (Dec. 12, 1950).
- Shienk, P. W., and W. Kretschmer, "Intermediate of the Wackenroder Reaction," *Angew. Chem.*, **74**, 695 (1962).
- Taylor, H. A., and W. A. Wesley, "The Gaseous Reaction between Hydrogen Sulfide and Sulfur Dioxide," *J. Phys. Chem.*, **31**, 216 (1927).
- Tiwari, B. L., "The Kinetics of Oxidation of Zinc and Hydrogen Sulfide by Sulfur Dioxide in Aqueous Sulfuric Acid," PhD Thesis, Columbia University, New York, U.S.A., (1976).

- van der Heijde, H. B., and A. H. W. Aten, "Tracer Studies on the Formation of Sulfur from Hydrogen Sulfide and Sulfur Dioxide in Aqueous Solutions," *J. Am. Chem. Soc.*, **75**, 754 (1953).
- Udy, M. J., "Improvements in Sulfur Recovery," British Patent No. 599,073 (Mar. 4, 1948).
- Vilesov, N. G., "Some Characteristics of the reaction of Sulfur Dioxide and Hydrogen Sulfide," *Zh. Prikl. Khim.*, **53**, 2401 (1980).
- Volynskii, N. P., "Mechanism of Wackenroder Reaction," *Russian Journal of Inorganic Chemistry*, **16**, 158 (1971).
- Welde, C. B., "Crystalline Sulfur," U.S. Patent No. 2,562,158 (Jul. 24, 1951).

Chapter 6

Simulation of Operation in Batch Reactor

6.1 Introduction

Up to now, the two reaction rate equations for the H₂S-sulfuric acid system have been described in Chapters 4 and 5, respectively. They are,

$$r_{H_2S,1} = -\frac{dN_{H_2S}}{dt} = k_{P1} a P_{H_2S} \quad (4-6)$$

for reaction 1, and

$$r_{H_2S,2} = -\frac{dN_{H_2S}}{dt} = k'_{P2} a P_{H_2S} [SO_2] \quad (5-22)$$

for reaction 2. In this chapter, a mathematical model based on these two equations is developed to simulate the total pressure-drop changes of the H₂S-sulfuric acid gas-liquid reaction system carried out in a constant-volume batch reactor. The experimental data for this operation was obtained in Chapter 3. When the experiments started with H₂S and fresh sulfuric acid solution, the gas phase in the reactor at reaction initiation contained only H₂S. Once the reaction commenced, part of the SO₂ generated from the first reaction but not converted by the second reaction would desorb from the interfacial reaction site into the gas phase; - the other part may dissolve in the acid solution. The total pressure during the course of reaction was the sum of the partial pressures of H₂S and SO₂, ignoring the vapor pressure of the acid solution, which was very small and did not change

significantly during the reaction. Equation (5-22) contains a term of SO_2 concentration in the acid, which was not monitored in the experiments. It has to be related somehow to the partial pressure of SO_2 in the gas so that the total pressure may be simulated. To do so, it is assumed that the concentration of SO_2 in sulfuric acid and its partial pressure in the gas are in equilibrium at the interface and that the equilibrium obeys Henry's law, that is,

$$P_{SO_2} = H[SO_2] \quad (6-1)$$

where, H is the Henry's law constant. Under this reasonable assumption, Equation (5-22) becomes

$$r_{H_2S,2} = -\frac{dN_{H_2S}}{dt} = k_{P2} a_{P_{H_2S}} P_{SO_2} \quad (6-2)$$

where, k_{P2} is a modified rate constant of the second reaction but incorporates the Henry's law constant.

6.2 Description of Operation

In Chapter 3, when the experiments to determine the mass balances were carried out in a batch reactor vessel of constant volume, the change in total pressure versus time was also recorded. The experimental data are shown by the dark points in Figure 6-1. The experimental procedure can be briefly described as follows: a given volume of sulfuric acid of known concentration was charged into the reactor, which was then connected to a feed system. The acid was stirred and heated to 120°C and the air in the reactor was evacuated using a vacuum pump. After the system pressure reached a steady-state, a known amount of H_2S was introduced instantaneously through bubbling the gas into the liquid. The subsequent change in total pressure in the reactor versus time was recorded.

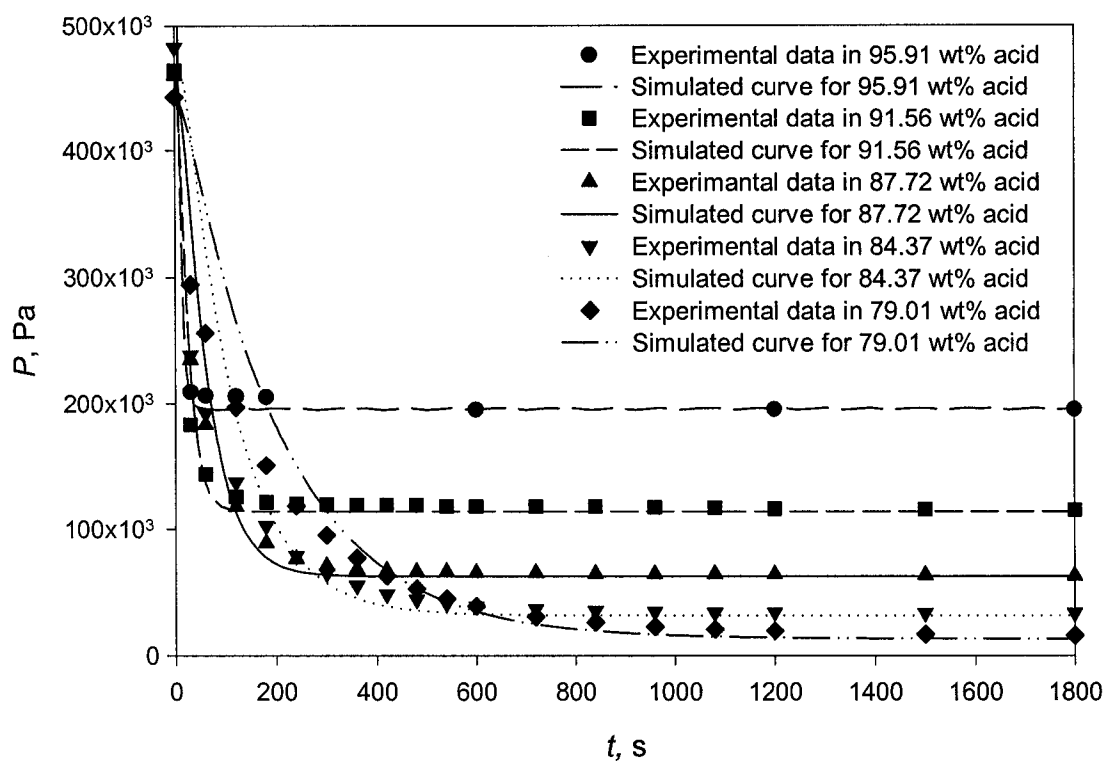


Figure 6-1. Comparison between simulated and experimental data on total P in batch reactor.

6.3 Establishment of the Simulation Model

It has been mentioned that the gas phase during the reaction consists of H₂S, which is introduced, and SO₂, which is produced. H₂S is consumed by both reactions but SO₂ is produced by the first reaction and consumed by the second reaction. Therefore, during the reaction, the partial pressures of H₂S and SO₂ change with time in terms of the following equations,

$$\frac{V_G}{RT_G} \frac{dP_{H_2S}}{dt} = -k_{p1} a P_{H_2S} - k_{p2} a P_{H_2S} P_{SO_2} \quad (6-3)$$

and

$$\frac{V_G}{RT_G} \frac{dP_{SO_2}}{dt} = k_{p1} a P_{H_2S} - \frac{1}{2} k_{p2} a P_{H_2S} P_{SO_2} \quad (6-4)$$

Defining

$$\frac{RT_G a}{V_G} = \kappa \quad (6-5)$$

$$P_{H_2S} = x_1 \quad (6-6)$$

$$P_{SO_2} = x_2 \quad (6-7)$$

Equations (6-3) and (6-4) may be written,

$$\frac{dx_1}{dt} = -\kappa(k_{p1}x_1 + k_{p2}x_1x_2) \quad (6-8)$$

$$\frac{dx_2}{dt} = \kappa(k_{p1}x_1 - \frac{1}{2}k_{p2}x_1x_2) \quad (6-9)$$

The boundary conditions are,

$$\text{When } t = 0, x_1 = \text{initial } P_{H_2S}, \text{ and } x_2 = \text{initial } P_{SO_2} = 0 \quad (6-10)$$

The following assumptions must be satisfied such that κ , k_{p1} and k_{p2} are to be constants.

- (1) The SO_2 concentrations in both phases are in equilibrium and obey Henry's law.
- (2) The effect of the heat of reaction is ignored and the reaction is isothermal.
- (3) The amount of water produced in the reaction is negligible and thus, the concentration of sulfuric acid also changes negligibly.
- (4) The interfacial area of the liquid phase remains constant.
- (5) The mass transfer effect is negligible.

The temperature of the liquid phase was controlled constantly during the measurement except for the first few seconds after the introduction of H_2S , during which period the temperature might jump by 2-3 degrees. But this increase in temperature is not believed to affect the pressure measurement. The interfacial area should not be changing under the mixing conditions. At 120°C , the sulfur produced was in the liquid state and the stirring action dispersed the sulfur droplets in the acid solution. The sulfur did segregate at the liquid surface. The acid concentration can change during the reaction due to the production of water; but the titrations after the runs showed it did not decrease by more than 1 wt%. The equilibrium of SO_2 concentrations between gas and liquid phases might not be reached during the unsteady period. The difference between the experimental data and simulation results attributed to some of the unreasonable assumptions are discussed in next section.

The simulation was conducted using MATLAB's differential equation editor function (version 6.1, 2000).

6.4 Results and Discussion

6.4.1 Simulation of overall pressure-drop

The assumptions made in Section 6.3 presume that the experimental conditions used in obtaining the rate equations (Chapters 4 and 5) are identical to those used for measuring the overall pressure-drop rate when the mass balance was measured (Chapter 3). The purpose of these assumptions is to enable the mathematical model to simulate the experimental results obtained from the batch operation. In fact, differences exist between the conditions used in chapters 4 and 5 to obtain the reaction rate and those in chapter 3 for studying the mass balance. As a result, some parameters in the model were modified such that the simulated and experimental results were comparable.

6.4.1.1 Selection of κ

In an experiment, the temperature and volume of the gas phase, T_G and V_G , were constant and measurable. If the interfacial area, a , were known, κ could be evaluated from Equation (6-5). However, because the H_2S gas was sparged into the acid which was strongly stirred, the interfacial area between gas and liquid was not known. Therefore, the values of κ were also unknown. In the simulation, it was found that the value of κ mainly affects the descending trends of the $P-t$ curves. Accordingly, an appropriate value of κ was selected by trial-and error until the $P-t$ curve best fits the experimental data. The same procedure was conducted for each of acid concentrations. The final values of κ are shown in Table 6-1. The definition in Equation (6-5) indicates that κ should be independent of acid concentration; however, the values of κ changed for various acid concentrations probably due to the variations in liquid density, the bulb size and the different interfacial areas caused by different acid concentrations.

6.4.1.2 Selection of k_{p2}

The values of k_{p1} used in the simulation were obtained directly from Equation (4-10) and the parameters in Table 4-4. However, the values of k_{p2} used were smaller than those obtained from Equation (5-28) and SO₂ solubility data. This suggests that the second reaction, *i.e.*, the reaction between H₂S and dissolved SO₂, occurred more slowly than predicted by Equation (6-2). As pointed out, k_{p2} is the product of k'_{p2} , obtained in terms of Equation (5-28), and the Henry's law constant, H , obtained from the data in Figure (1-3). Because k'_{p2} should not change with operating conditions, the other factor that may change is the SO₂ concentration in the reaction region. This concentration may be lower than the equilibrium value. The values of k_{p1} and k_{p2} used in the simulation and the ratio, k_{p2} in simulation, denoted as $k_{p2,sim}$, to k_{p2} from calculation, denoted as $k_{p2,cal}$, are also shown in Table 6-1. The simulation results are shown by the curves in Figure 6-1. It can be seen that the simulated curves fit the experimental data in the section of steady-state, the flat part of the curves, better than in the unsteady-state, the dropping section of the curves. This means that the experimental conditions during the transient period differed from those assumed. For example, during the transient period, the equilibrium between SO₂ in both phases may not be achieved; the interface area may become less due to the stopping of bubbling; and the acid concentration, although changing slightly, did decrease the reaction rate significantly. In general, the model is able to simulate the process after some modifications.

6.4.2 H₂S and SO₂ partial pressure changes with time

Figures 6-2 and 6-3 show the changes in partial pressures of H₂S and SO₂ during the course of reaction for acid concentrations of 95.91 wt% and 79.01 wt%, respectively.

Table 6-1. Parameters used in simulation.

Acid Conc. wt%	$k_{P1} \times 10^9$ $\text{mol s}^{-1} \text{m}^{-2} \text{Pa}^{-1}$	$k_{P2} \times 10^9$ $\text{mol s}^{-1} \text{m}^{-2} \text{Pa}^{-2}$	$\frac{k_{P2, sim}}{k_{P2, cal}}$	$\kappa \times 10^{-6}$ $\text{Pa m}^2 \text{mol}^{-1}$
79.01	0.49	0.123	0.0006	3.5
84.37	6.91	0.109	0.004	0.5
87.72	36.1	0.117	0.0093	0.2
91.56	240	0.130	0.026	0.09
95.91	2050	0.169	0.09	0.03

The partial pressure of H₂S decreases exponentially with time until it becomes zero; whereas, the SO₂ partial pressure increases exponentially with time until it reaches a constant value. The reaction stops when the partial pressure of H₂S becomes zero. The total pressure change, of course, is the sum of changes in these two partial pressures. For different acid concentrations, the two figures show the same trend. However, in the reaction with 95.91 wt% acid, H₂S is consumed completely in 50 seconds; but with 79.01 wt% acid, 20 minutes are needed to convert all the H₂S charged to the reactor.

6.4.3 Change of each reaction rate vs. time

As shown in Figure 6-4, the pressure-drop rate caused by the first reaction is also an exponential function of time, because the partial pressure of H₂S is an exponential function of time. But the pressure-drop rate caused by the second reaction increases initially, reaches a maximum value at a certain time, t_{max} , and then decreases. This is because the second reaction is a function of the product of both pressures. Before t_{max} , P_{H_2S} is still large, and an increase in P_{SO_2} will make their product increase. After t_{max} , P_{SO_2} is approaching a constant value, whereas P_{H_2S} is continuously decreasing, resulting in a decrease in their product. Figure 6-4 also proves that the first reaction rate dominates when the reaction starts with fresh acid and pure H₂S in batch reactor. This supports the assumption made in Chapter 4, which states that the rate of the second reaction is zero at time zero.

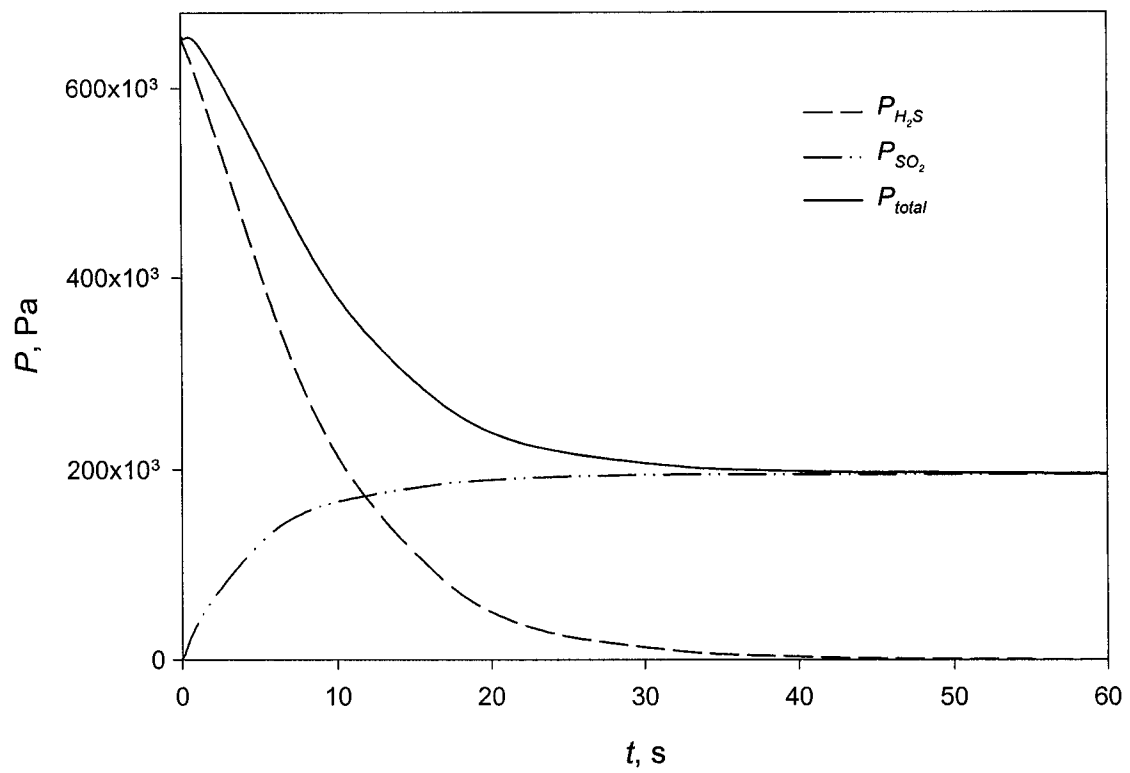


Figure 6-2. Changes in total P and partial P 's for H_2S and SO_2 in 95.91 wt% acid.

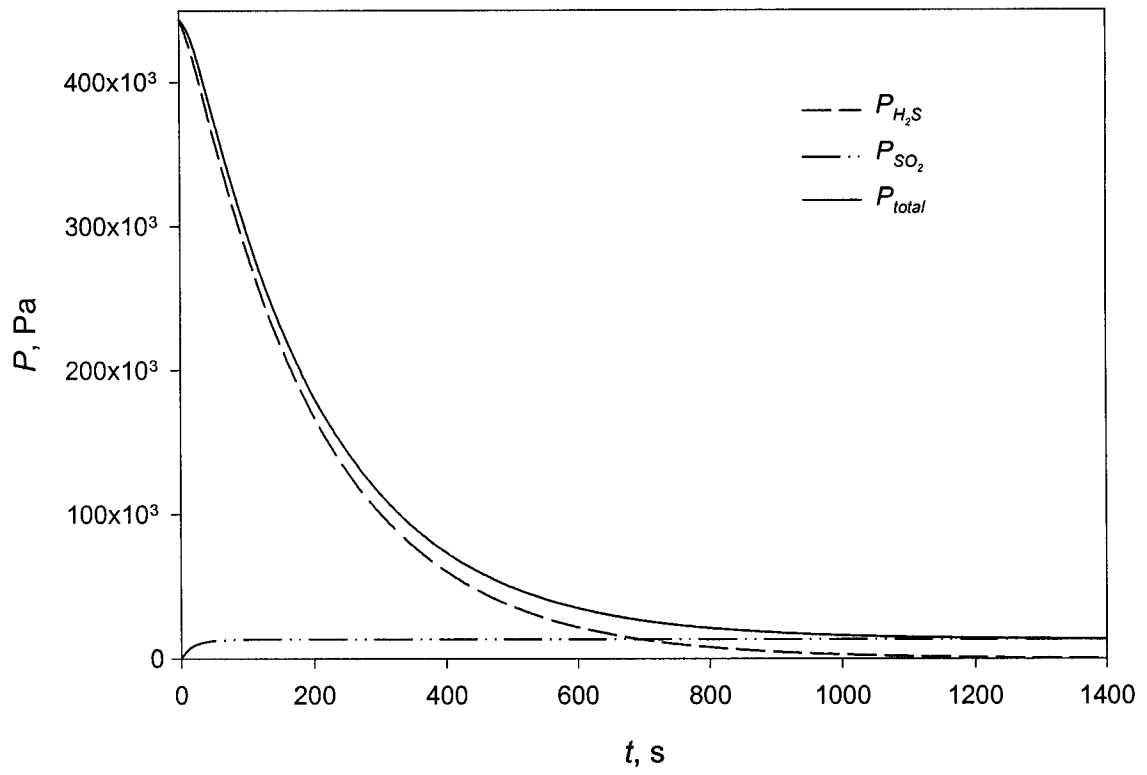


Figure 6-3. Changes in total P and H_2S and SO_2 partial P 's vs. time in 79.01 wt% acid.

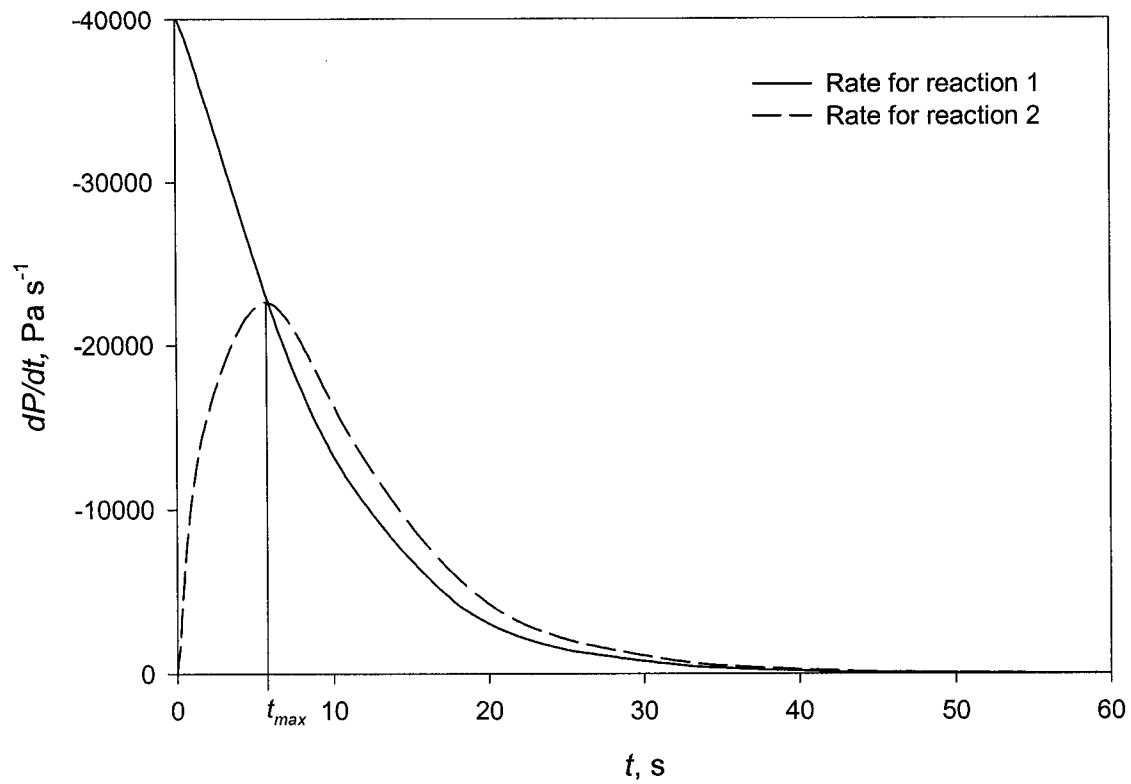


Figure 6-4. Reaction rate vs. time at 120°C and 95.91 wt% of acid concentration.

6.5 Conclusions

The mathematic model established on the basis of the two reaction rate equations from the initial rate measurements is able to simulate the operation of H₂S-sulfuric acid system in a batch reactor. Deviation between the experimental data and the simulated curves could be explained from the differences between the real experimental conditions and the assumptions based on which the model is developed. The simulation discovered that the second reaction was slower in the experiments than predicted by the rate equation (6-2), due to the lower SO₂ concentration at the reaction sites. To increase the second reaction rate, H₂S is suggested to react with the solution pre-saturated with SO₂.

6.6 Nomenclature

<i>a</i>	Interfacial area between gas and liquid	m^2
<i>H</i>	Henry's law constant	$\text{Pa L}^3\text{mol}^{-1}$
<i>k_{P1}</i>	Rate constant for reaction 1	$\text{mol s}^{-1}\text{m}^{-2}\text{Pa}^{-1}$
<i>k_{P2}</i>	Rate constant for reaction 2	$\text{mol s}^{-1}\text{m}^{-2}\text{Pa}^{-2}$
<i>N</i>	Mole number	mol
<i>P</i>	Pressure	Pa
<i>R</i>	Gas constant	$\text{Pa m}^3\text{mol}^{-1}\text{K}^{-1}$
<i>r</i>	Reaction rate	mol s^{-1}
<i>T</i>	Temperature	K, °C
<i>t</i>	Time	s
<i>V</i>	Volume	m^3
<i>x</i>	variable	
<i>[SO₂]</i>	Concentration of SO ₂ in sulfuric acid solutions	mol L^{-1}
<i>Greek</i>		
<i>κ</i>	Constant delivered from Equation (6-5)	$\text{Pa m}^2\text{mol}^{-1}$
<i>Subscripts</i>		
<i>G</i>	Associated with gas	
<i>P</i>	Associated with pressure	
1	Referred as to reaction 1 or for differentiation	
2	Referred as to reaction 2 or for differentiation	

Chapter 7

Reactions of H_2S and H_2SO_4 in a Packed Column Reactor

7.1 Introduction

The kinetic studies described in Chapters 4 and 5 obtained the rate equation for each of the two reactions in the H_2S -sulfuric acid system. With some modifications, the rate equations are capable of predicting the reaction carried out in the batch reactor (Chapter 6). However, the effect of mass transfer has been suppressed intentionally in the experiments described in the preceding chapters. From an engineering point-of-view, mass transfer and chemical reaction simultaneously occur and cannot be easily separated. Consequently, the behavior of mass transfer as well as reaction under continuous operation must be investigated.

The studies on reaction kinetics show that the two reactions occur mainly at the gas-liquid interface. Interfacial area is crucial to these reactions. A packed column reactor is generally chosen for carrying out these reactions in large-scale operations because it is able to provide large interfacial areas. With this consideration, this chapter examines reactions combined with the mass transfer, to evaluate the use of the rate equations in the prediction of the course of the two reactions in a column reactor.

7.1.1 Absorption with chemical reaction in packed columns

A “two-film model”, as shown in Figure 7-1, is usually used to describe the phenomena of a gas-liquid process (Danckwerts, 1970; Shah, 1979). For physical absorption, the soluble gas, A , is transported from the gas phase, across the films and into the liquid phase during a steady-state process. All the resistances are believed to be concentrated within the films, for which the rate can be written as

$$r_A = k_G a (P_A - P_A^i) = k_L a (A^* - A) \quad (7-1)$$

The model supposes that the interfacial partial pressure, P_A^i , is in equilibrium with the interfacial concentration, A^* . For a system obeying Henry's law, that is,

$$P_A^i = HA^* \quad (7-2)$$

the overall rate can then be described as,

$$r_A = K_G a (P_A - HA) = K_L a (P_A / H - A) \quad (7-3)$$

where,

$$\frac{1}{K_G} = \frac{1}{k_G} + \frac{H}{k_L} \quad (7-4)$$

$$\frac{1}{K_L} = \frac{1}{Hk_G} + \frac{1}{k_L} \quad (7-5)$$

7.1.2 Estimation of mass transfer coefficients

The mass transfer during a gas-liquid process in a packed-column reactor has been investigated thoroughly and models for estimating the mass transfer coefficients have been established based on empirical correlations and modifications. Among these models, the most frequently applied are those proposed by Onda, et al. (1959, 1968a, 1968b). First, Onda, et al. suggested replacing the effective interfacial area, a , the very

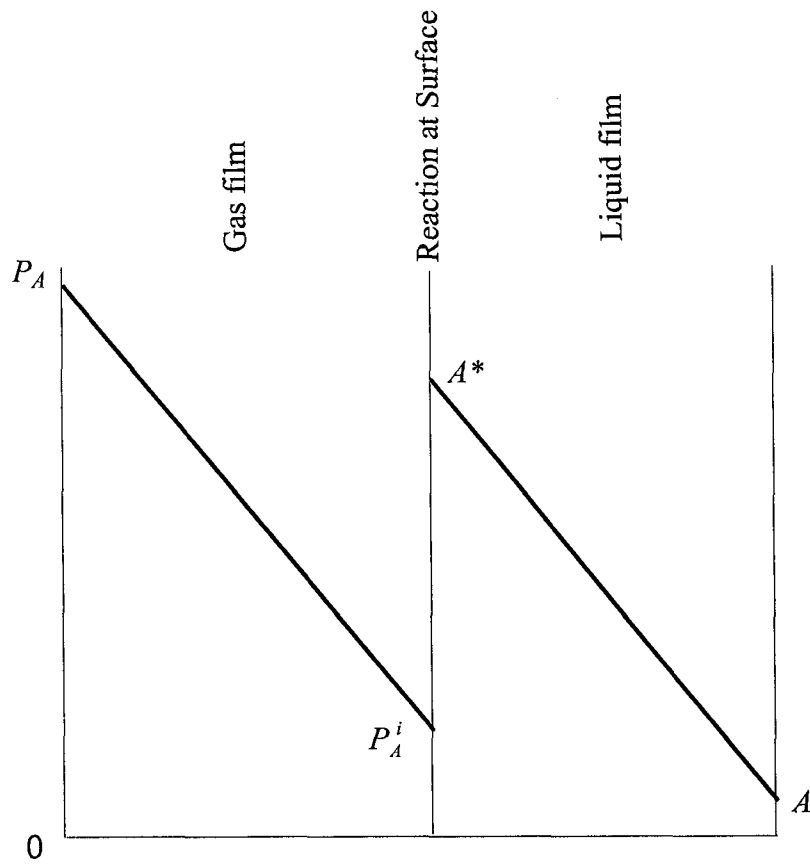


Figure 7-1. Concentration profile for two-film model.

obscure parameter in gas-liquid mass transfer, by a_w , the wetted area of the packing. Because a is not equal to but proportional to a_w , the replacement of a by a_w is convenient but may involve an error which they believe is reasonable. Taking into account the liquid surface tension and the surface energy of packing materials, Onda et al. (1968a) derived a formula as follows:

$$a_w / a_t = 1 - \exp \{ -1.45(\sigma_c / \sigma)^{0.75} (L / a_t \mu_L)^{0.1} (L^2 a_t / \rho_L^2 g)^{-0.05} (L^2 / \rho_L \sigma a_t)^{0.2} \} \quad (7-6)$$

where, a_t is the total surface area of the packing and for Raschig rings $a_t = 4.7 / D_p$ (Onda, et al., 1959). With this equation, it is easy to estimate a_w from a_t . Then, according to the two-film theory, Onda, et al. (1968a) presented a correlation for the liquid-side mass transfer coefficient, k_L :

$$k_L (\rho_L / \mu_L g)^{1/3} = 0.0051 (L / a_w \mu_L)^{2/3} (\mu_L / \rho_L D_L)^{-1/2} (a_t D_p)^{0.4} \quad (7-7)$$

and a correlation equation to predict the gas-side mass transfer coefficient, k_G , in terms of the performance of columns and properties of fluids.

$$k_G RT / a_t D_G = c (G / a_t \mu_G)^{0.7} (\mu_G / \rho_G D_G)^{1/3} (a_t D_p)^{-2.0} \quad (7-8)$$

where $c=5.23$ for Raschig rings and Berl saddles larger than 15 mm and $c=2.00$ for those smaller than 15 mm.

7.2 Two-Film Model Analysis on H₂S-Sulfuric Acid System

Previous chapters have shown that the two reactions occur at the interface between the gas and liquid phases because it is observed that the reaction rate is much faster than the diffusion rate of H₂S in sulfuric acid solution. H₂S diffuses from the bulk

of gas phase to the interfacial surface, as well as H_2SO_4 or SO_2 from the bulk liquid phase. H_2S and H_2SO_4 , or H_2S and SO_2 , react at the interface. Both of the reactions are irreversible due to the formation of a solid product, sulfur. Because the SO_2 involved in the second reaction is provided by the first reaction that takes place at the interface when fresh and concentrated (≥ 90 wt%) sulfuric acid is used, the transportation of sulfur dioxide in liquid phase is likely negligible. Compared to the H_2S concentration in gas streams which contain dilute amounts of H_2S , the concentration of H_2SO_4 is very large ($16-18 \text{ mol L}^{-1}$ vs. $0.392 \times 10^{-3} \text{ mol L}^{-1}$). Therefore, the mass transfer of H_2SO_4 in the liquid phase may be considered to be negligible. Moreover, the use of concentrated sulfuric acid favors the first reaction. Based on these considerations, the system can be simplified to a gas-liquid absorption process accompanied by a single chemical reaction.

In light of the two-film theory, the concentration profile of the reaction of H_2S and H_2SO_4 in a packed column is shown in Figure 7-2. Similar to Equation (7-1), the rate of the process can be expressed as

$$r_{H_2S} = k_G a (P_{H_2S} - P_{H_2S}^i) = k_{p1} a P_{H_2S}^i \quad (7-9)$$

Under this condition, it is difficult to obtain the value of $P_{H_2S}^i$. To eliminate it, following Equation (7-3) and noting that the concentration of H_2S in the liquid phase is zero, one obtains,

$$r_{H_2S} = K_G a P_{H_2S} \quad (7-10)$$

where,

$$\frac{1}{K_G} = \frac{1}{k_G} + \frac{1}{k_{p1}} \quad (7-11)$$

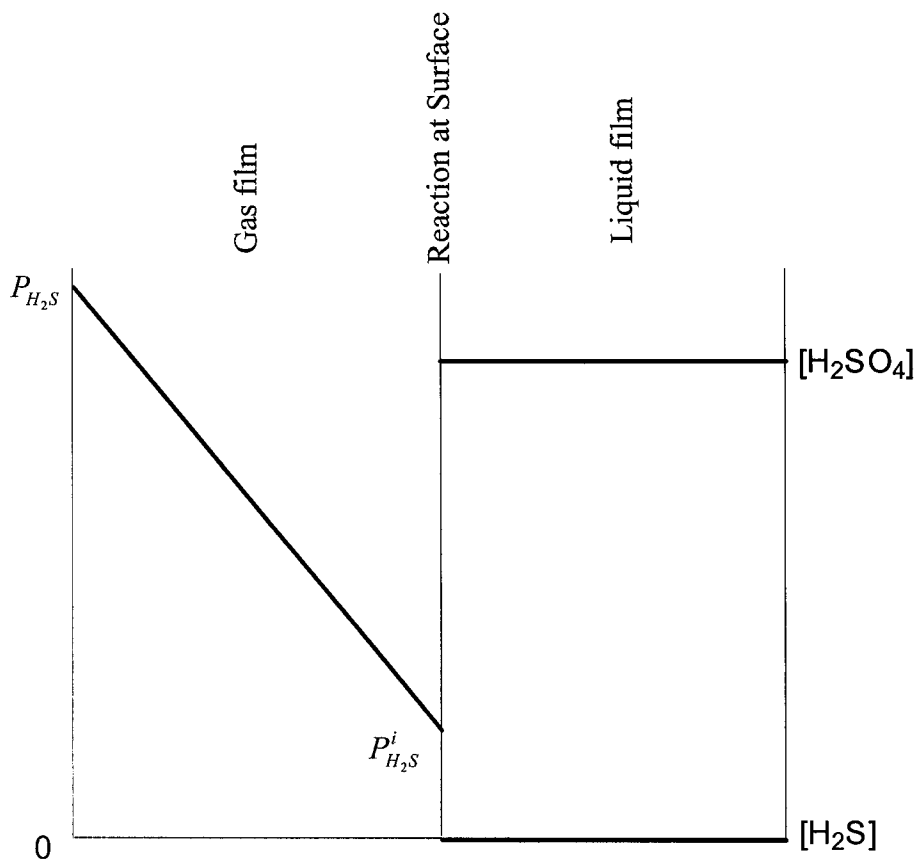


Figure 7-2. Concentration profile for H_2S and H_2SO_4 reaction in packed column.

In general, this idea can be extended to any reaction that occurs at the interfacial surface instead of in the bulk liquid phase. Gaseous reactants do not necessarily diffuse into the liquid and react with the liquid reactants or reactants in the liquid. Instead, they react with the reactants from the liquid at the interface. In this case, Equations (7-9), (7-10) and (7-11) are able to describe the process without considering the behavior of reactants in the liquid phase. There should be two extremes. If mass transfer in the gas side is the controlling step and H₂S transferred to the surface is completely consumed by the reaction, then, $P_{H_2S}^i = 0$, and as shown in Figure 7-3, the rate equation is simplified to be

$$r_{H_2S} = k_G a (P_{H_2S} - P_{H_2S}^i) = k_G a P_{H_2S} \quad (7-12)$$

For this extreme condition, analogous to instant and irreversible reaction, one has $k_{p1} \gg k_G$, i.e., $K_G \approx k_G$. Equation (7-10) also leads to Equation (7-12). And if reaction is the controlling step, all of the gas phase is homogeneous, i.e., $P_{H_2S}^i = P_{H_2S}$. The rate equation becomes

$$r_{H_2S} = k_{p1} a P_{H_2S}^i = k_{p1} a P_{H_2S} \quad (7-13)$$

Similarly, Equation (7-10) also leads to Equation (7-13) when considering $k_G \gg k_{p1}$ or $K_G \approx k_{p1}$. The concentration profile is shown in Figure 7-4.

Many criteria are available to estimate the operation regime for the reaction in a column. For example, $K_G a$ can be obtained from a measurement of the mole fractions of H₂S at the top and bottom of the column using Equation (7-14),

$$\ln \frac{y_b}{y_t} = \frac{K_G a P z}{G} \quad (7-14)$$

where, both y_b and y_t are much less than unity. If $K_G a$ increases significantly as the temperature increases and vice versa, but does not change as the gas flow rate changes,

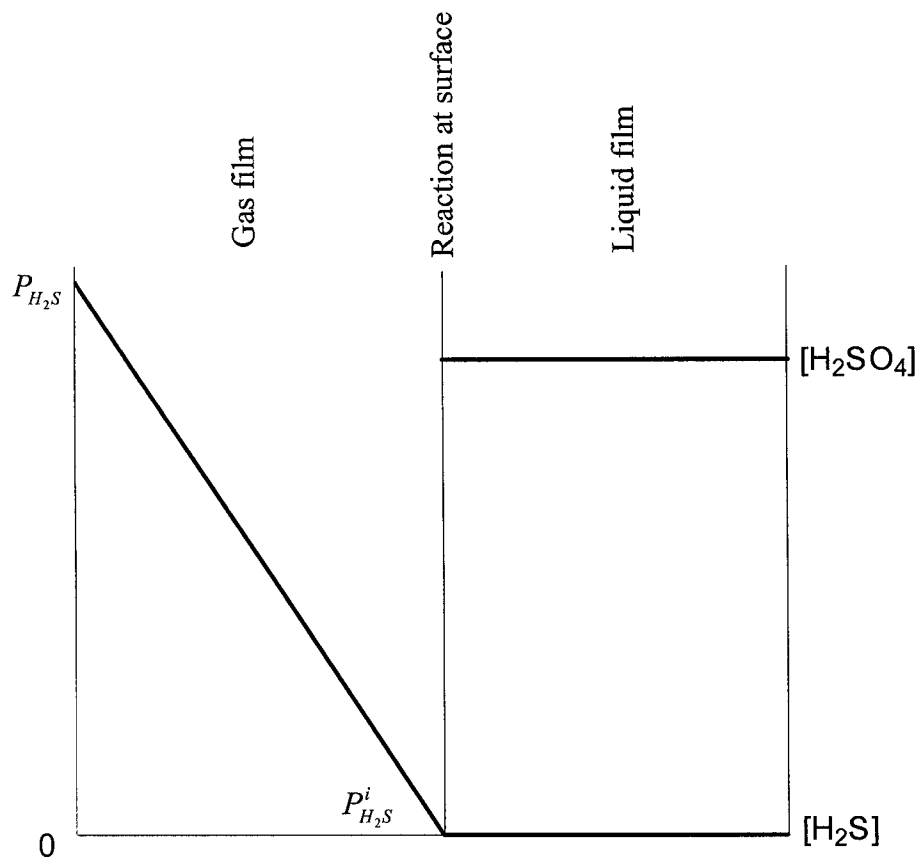


Figure 7-3. Concentration profile for H_2S and H_2SO_4 reaction in packed column when mass transfer is rate-controlling step.

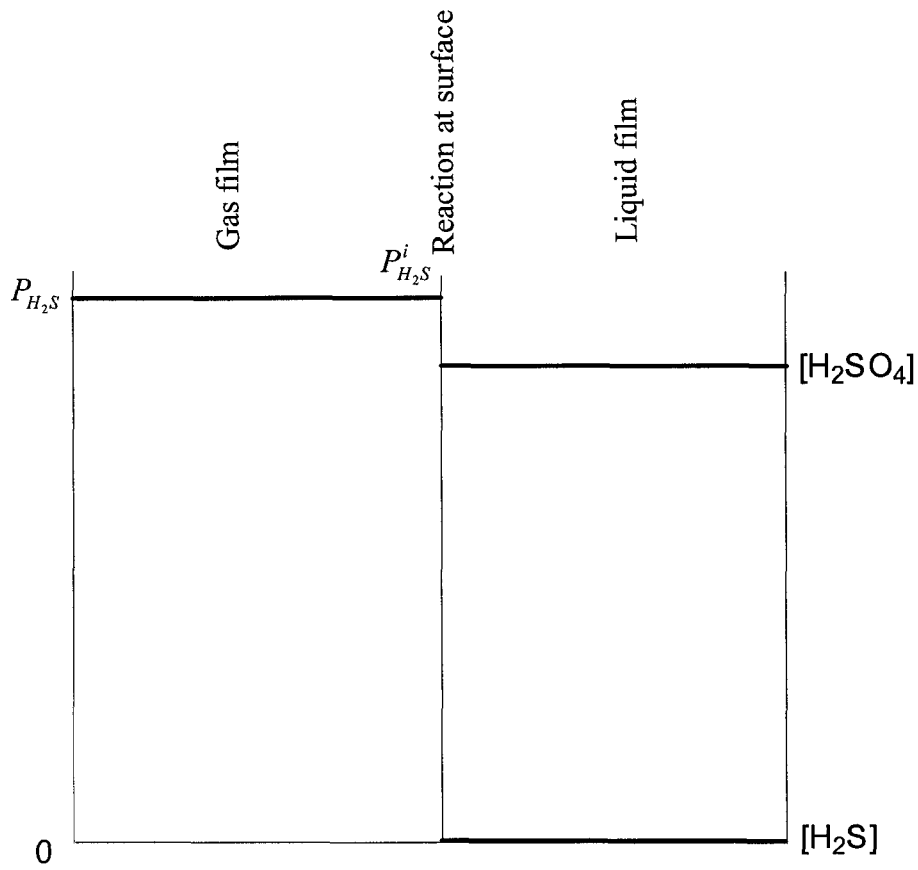


Figure 7-4. Concentration profile for H_2S and H_2SO_4 reaction in packed column when reaction is rate-controlling step.

the operation must fall into the reaction-controlling regime. However, if it changes with gas flow rate but does not change with the temperature, the operation is in mass transfer control. The other way to check the rate-controlling regime is to compare the experimental rate coefficient, K_G , respectively with the calculated k_{p1} from Equation (4-10) and k_G from Equation (7-8). When K_G is comparable to k_{p1} , the process is controlled by the chemical reaction; when K_G is comparable to k_G , it is controlled by mass transfer.

7.3 Physicochemical Properties

Physicochemical properties of the fluids are necessary and important to the estimation of the mass transfer parameters such as a_w , k_G and k_L using Equations (7-6), (7-7) and (7-8). Some properties such as density and the gravitational constant are available in handbooks; and others such as viscosity and diffusivity need to be estimated at operating parameters. The units of a property from various sources or used in different equations may be different and need to be converted accordingly. The properties worth discussion on their determination are mentioned in the following sections.

7.3.1 Surface tension

The critical surface tension, σ_c , of ceramic rings is found in Table 18-11 in *Perry's Chemical Engineers' Handbook* (Perry, et al., 1997), which is 56 dyn cm⁻¹. And the surface tension, σ_L , of sulfuric acid is reported by Myhre, et al. (1998). Although the surface tension for a liquid varies with temperature, its dependence is not significant. For example, the surface tension of 96 wt% sulfuric acid changes from 0.05544 N m⁻¹ at 0°C to 0.05308 N m⁻¹ at 50°C. The value of surface tension at a particular temperature is estimated by interpolation or extrapolation using the data available.

7.3.2 Viscosity

The viscosity of sulfuric acid solution at a temperature may be chosen from the nomograph for viscosities of liquids (Perry, et al., 1997). The viscosity of gases such as nitrogen can be found in *CRC Handbook of Chemistry and Physics* (80th edition, 1999-2000).

7.3.3 Diffusivity

The diffusivity of H₂S in water is calculated by the Wilke-Chang correlation (Geankoplis, 1993),

$$D_{H_2S,L} = 1.173 \times 10^{-16} (\phi M_L)^{0.5} \frac{T}{\mu_L V_{H_2S}^{0.6}} \quad (7-15)$$

This equation is also used to calculate the H₂S diffusivity in sulfuric acid solutions by supposing that H₂S is very dilute in the solution. In this case, $D_{H_2S,L}$ is the diffusivity of H₂S diffusing through sulfuric acid solution, L, m² s⁻¹; ϕ is an “association parameter” of the solution which is assumed to be equal to 2.6, the value for water; M_L is the molar average molecular weight of sulfuric acid solution, g mol⁻¹; μ_L is the viscosity of the solution, Pa s or kg m⁻¹s⁻¹; and V_{H_2S} is the molar volume of H₂S at the boiling point, 0.0329 L mol⁻¹. Equation (7-15) simplifies to,

$$D_{H_2S,L} = 1.339 \times 10^{-14} \frac{T}{\mu_L} \quad (7-16)$$

when the liquid is sulfuric acid of 96 wt%.

The diffusivity of H₂S in the gas phase is determined by the Fuller Equation (Geankoplis, 1993),

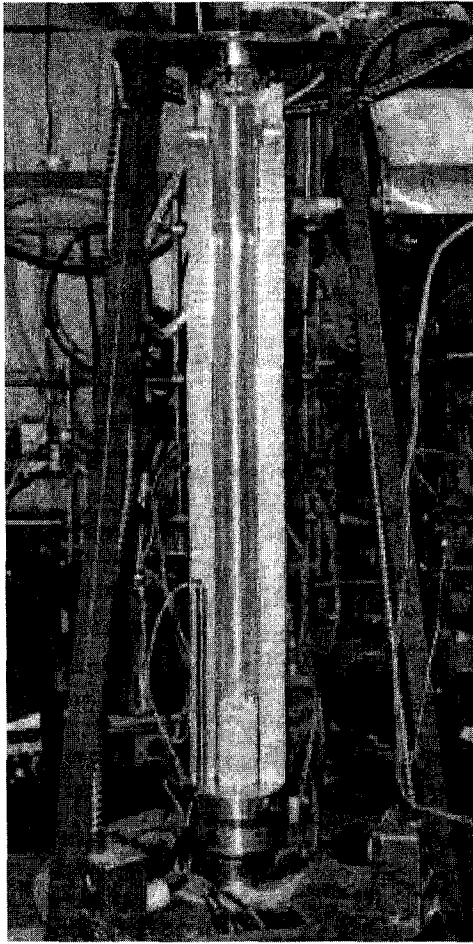
$$D_{AB} = \frac{1 \times 10^{-7} T^{1.75} (1/M_A + 1/M_B)^{1/2}}{P[(\sum v_A)^{1/3} + (\sum v_B)^{1/3}]^2} \quad (7-17)$$

where, A represents H_2S , and B represents N_2 for most of the runs in this study; D_{AB} is the diffusivity, m^2s^{-1} ; T is temperature, K; M_A and M_B are the molar weights of A and B, respectively, g mol $^{-1}$; P the total pressure, atm; and $\sum v_A$ and $\sum v_B$ are the sum of structural volumes of A and B, respectively. For the binary system of H_2S and N_2 ,

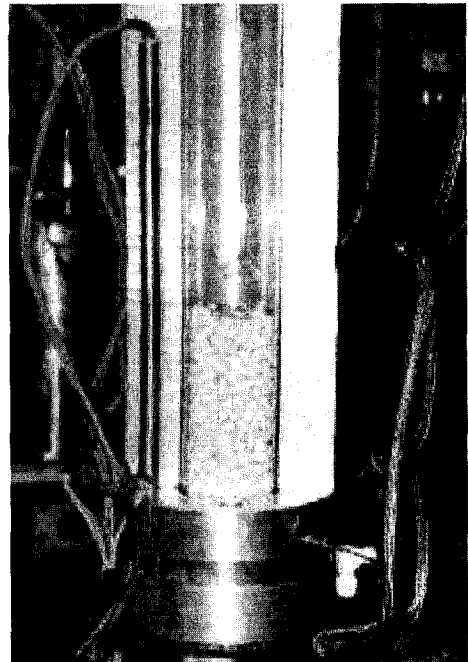
$$D_{AB} = 8.840 \times 10^{-10} T^{1.75} / P \quad (7-18)$$

7.4 Experimental Section

Because both liquid (sulfuric acid) and gas (containing H_2S) involved in this study are corrosive, ceramic Raschig rings with a normal size of 6 mm were used as the packing. The column was made of Pyrex glass, with an inner diameter of 0.06 m and a height of 1 meter. Figure 7-5 shows a photo of the column. The bottom section of the column consisted of a packing holder made of Teflon, a gas-liquid separation chamber, a liquid exiting flow-controlling valve, and a gas inlet/outlet tube. The top section consisted of a liquid inlet tube connected with a liquid distributor and a gas inlet/outlet tube. The three sections were joined together by two standard joints and sealed with Teflon gaskets. The joints were clasped using flanges of aluminum alloy. The aluminum blocks, inside which the cartridge heaters were installed, heated the column. The temperature was controlled by an Omron temperature controller, model E5CX (Omron Corporation, Tokyo, Japan) and can be read to 0.1°C. Since the thermocouples that measure the temperature of the column touched the outside skin of the column, two other thermocouples with glass covers were placed in the inlet and outlet acid solutions to monitor the temperature inside the column. The depth of the packing bed was varied by installing different heights of packing in the column. The liquid distributor could be

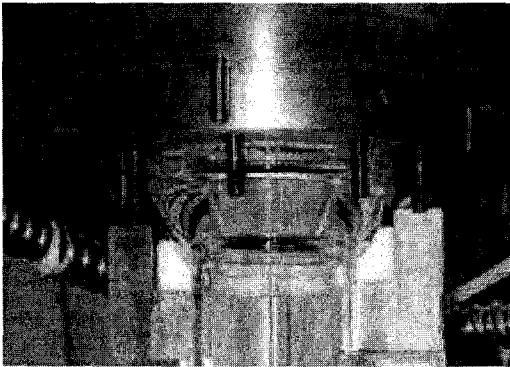


(a)

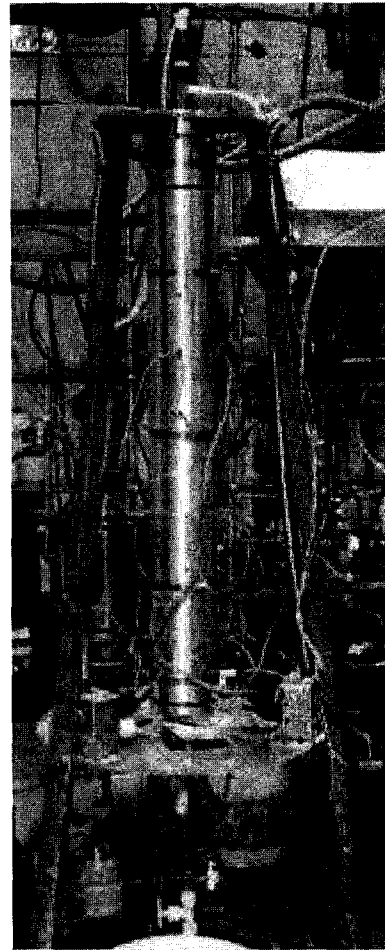


(b)

Figure 7-5. Photos of column reactor. (a) Inside column and block heater; (b) packing section.



(c)



(d)

Figure 7-5. Photos of column reactor. (c) joint and clasp; (d) ready to be used.

adjusted just above the packing. The gas stream could be introduced into the column either from the top or from the bottom so that either co-current or counter-current operation was possible. Most of the runs were carried out in co-current flow. The flow rates of the cylinder gases were regulated by mass flow controllers (Sierra Instruments, Inc., Monterey, CA), which were calibrated using a BIOS primary air flow meter, Model DryCal DC-2M (BIOS International Corporation, Pompton Plains, NJ). The fresh acid solution was stored in a 5 L tank of Pyrex glass, which was heated to a preset temperature by a hot plate (Model 200T, Fisher Scientific). The heated acid solution was pumped into the column using a variable-speed acid pump (Cole Parmer Instruments Co., Chicago, IL). The preheater was used if temperatures higher than 100°C were required because the acid pump could not be operated above 100°C.

The used acid solution was collected in another 5 L tank. The flowsheet of the experimental setup is shown in Figure 7-6.

For a typical run, sulfuric acid solution of a desired concentration was prepared and heated to a preset temperature. The inlet gas mixture was prepared based on the chosen composition and flow rate. The composition was also analyzed using a GC coupled with TCD and SCD. Then, the solution was pumped into the column at a set flow rate. The gas mixture was directed to the column once the steady acid flow had been established. After the reaction, both gas and liquid were directed to the gas-liquid separation chamber below the packing bed (for co-current flow). A valve was used to control the liquid level in the chamber. When a steady-state was reached, the composition of the exiting gas was analyzed three times using the same GC.

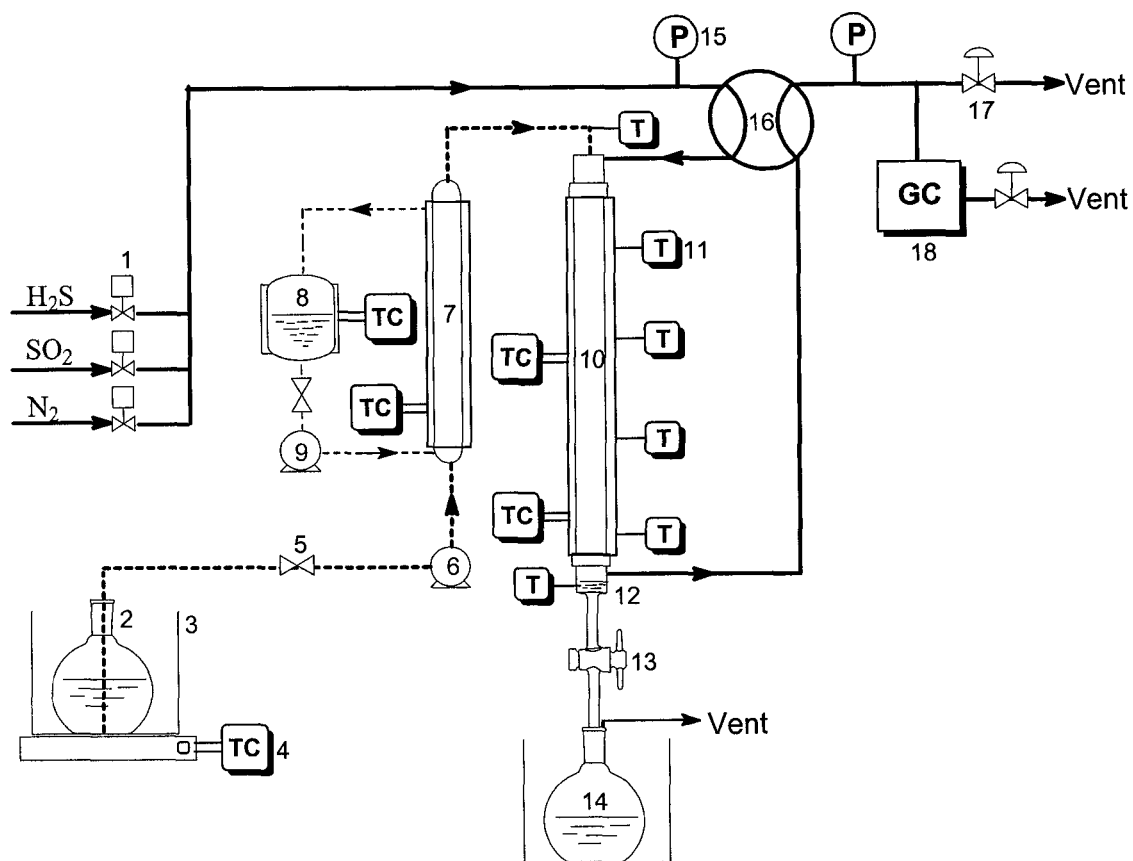


Figure 7-6. Schematic diagram of experimental setup for column reactor. 1. mass flow controller; 2. Tank for fresh acid; 3. protecting holder; 4. temperature controller; 5. valve; 6. acid pump; 7. acid preheater; 8. tank for heating oil; 9. oil pump; 10. column reactor; 11. temperature reader; 12. gas-liquid separator; 13. valve; 14. tank spent acid; 15. pressure gauge; 16. 4-way valve; 17. valve; 18. gas chromatograph coupled with TCD and SCD.

7.5 Results and Discussion

7.5.1 Estimation of liquid-side mass transfer coefficient

Although it has been indicated that the liquid-side mass transfer can be ignored in this system, the mass transfer in the liquid side in packed column was studied using an H₂S-water system. The purpose of these runs was to evaluate the applicability of Onda's correlations to this reactor system. To measure the mass transfer in the liquid side, the ideal experiment should meet three conditions: (1) pure soluble gas is used such that the gas-side mass transfer effect can be eliminated; (2) the concentrations of soluble gas on both sides are in equilibrium at the interfacial surface; and (3) the concentration of the soluble gas in the liquid is measured directly. However, this experiment used H₂S (soluble) and nitrogen (inert) gas mixture instead of pure H₂S for safety reasons. Thus, the concentration of H₂S in the gas phase will change along the packing from top to the bottom. The concentration of H₂S at the surface of the liquid phase will change accordingly but it is believed to be in equilibrium with the corresponding gas composition. The content of H₂S in the existing water was estimated from a mass balance for H₂S across the gas phase. Although the effects of mass transfer in both gas side and liquid side would co-exist under this operation, the resistance to mass transfer in the gas side is small compared with that in the liquid side. Under this circumstance, the liquid-side mass transfer coefficient can be measured.

Table 7-1 lists the value of $k_L a$ measured under various conditions. If the wetted surface area calculated by Equation (7-6) is taken as the effective surface area, the value of liquid-side mass transfer coefficient of H₂S-water system can be obtained by dividing $k_L a$ by this a_w . The values of k_L so obtained and of k_L estimated by Equation (7-7) are also

Table 7-1. Measured and estimated values of k_L for H₂S-water system

Run#	H ₂ S in gas	G	L	$k_L a$	k_L	$k_L(\text{est})$
	%	kg m ⁻² s ⁻¹	kg m ⁻² s ⁻¹	s ⁻¹	m s ⁻¹	m s ⁻¹
MS-3c	0.988	0.00341	0.764	0.00549	1.31×10 ⁻⁵	1.47×10 ⁻⁵
MS-4a	0.988	0.00341	0.764	0.00588	1.33×10 ⁻⁵	1.47×10 ⁻⁵
MS-6	0.905	0.00682	0.764	0.00605	1.44×10 ⁻⁵	1.47×10 ⁻⁵
MS-7a	2.51	0.00682	0.764	0.00518	1.23×10 ⁻⁵	1.47×10 ⁻⁵
MS-5	0.988	0.00341	1.27	0.0101	2.12×10 ⁻⁵	1.90×10 ⁻⁵

listed in Table 7-1. The experimental values of k_L deviated from the estimated value by $\pm 11\%$. In fact, the estimation of k_L by Equation (7-7) has an error range of $\pm 20\%$. It turns out that Onda's correlations are applicable to our packed column system. Table 7-1 also shows that the value of k_L is significantly affected by the liquid flow rate. When the superficial liquid flow rate increased from 0.764 to 1.27 kg m⁻²s⁻¹, k_L increased from about 1.33×10^{-5} to 2.12×10^{-5} m s⁻¹. However, it was obtuse to the gas flow rate. As the gas flow rate doubled, the k_L value almost remained unchanged.

7.5.2 H₂S absorption companied with reaction

The conversion of H₂S in 96 wt% sulfuric acid was too rapid to be useful in the determination of rate coefficients. Even when the packing height was reduced to 0.2 m, the conversion of H₂S at room temperature could reach as high as 90%. When the temperature $\geq 60^\circ\text{C}$, complete conversion was obtained at all gas flow rates and H₂S concentrations tested. Therefore, a lower acid concentration was chosen for this study.

First, the end effect was investigated by varying the packing height. At 25°C, sulfuric acid of 90 wt% was pumped at 130 mL/min into the column. It was dispersed over the packing bed inlet through a liquid distributor. The gas stream containing 1% of H₂S was directed into the column top at 1500 mL/min (STP). The H₂S concentrations in the inlet and outlet gas streams were measured using the GC coupled with TCD and SCD (Wang, et al., 1998). From the concentration changes, an overall rate coefficient, K_{Ga} , was calculated using Equation (7-14). The values of K_{Ga} were plotted against the packing height, z , in Figure 7-7 and the result shows that no significant end effects during these experiments. The fluctuation in K_{Ga} values may be attributed to the slight variations in acid concentration or temperature during various runs.

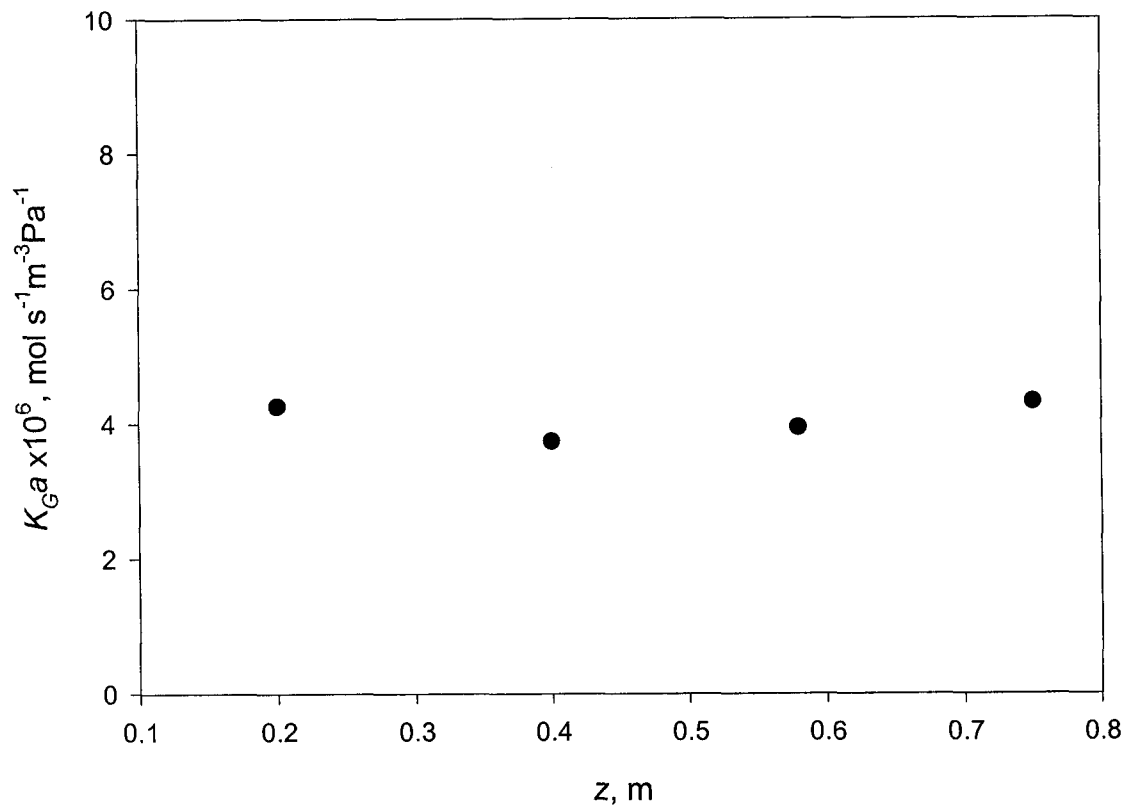


Figure 7-7. Rate Coefficient, $K_G a$, vs. height of packing, z .

MS_18: $z=0.2\text{m}$, 90.13 wt%, 24.2°C;

MS_13: $z=0.4\text{m}$, 89.2 wt%, 23.9°C;

MA_14: $z=0.58\text{m}$, 89.2 wt%, 24.7°C;

MS_15: $z=0.75\text{m}$, 89.6 wt%, 23.9°C.

To determine the rate-controlling regime for the H₂S-sulfuric acid gas-liquid reaction system in the packed column reactor, $K_G a$ were measured at different temperatures. The values of K_G were obtained by dividing $K_G a$ by the effective interfacial area, a_w , estimated using Equation (7-6). As discussed previously, if the system is in gas-side mass transfer control, then K_G approximates k_G , which should be independent of temperature; however, when the system is in chemical reaction control, then K_G can be approximated by k_{p1} , which depends on temperature, as predicted by Equation (4-10). Figure 7-8 shows that K_G is significantly temperature-dependent but slightly less than the value of k_{p1} , estimated from Equation (4-10). This comparison suggests that the chemical reaction in the process is likely the rate-controlling step. However, an appropriate explanation is worthwhile for the question, why is K_G measured from the experiments using the column reactor less than k_{p1} from the rate equation?

7.5.3 Discussion on effective surface area

When the process is controlled by the rate of chemical reaction the local overall rate should equal the reaction rate, *i.e.*,

$$r_{H_2S} = K_G a_w P_{H_2S} = k_{p1} a P_{H_2S} \quad (7-19)$$

The a_w estimated from Equation (7-6) is probably too large and this leads to a smaller value for K_G because K_G was obtained by dividing the measured rate by a_w . The value of a_w so obtained may be 10% larger than the real interface area. Actually, when a_w is introduced to replace a , the real interfacial area, an error would also have been introduced. If a_w is estimated from a_t using Equation (7-6), another error is introduced. Onda, *et al.* (1968a) proposed that the total error would be $\pm 20\%$ for packings including the ceramic Raschig rings, used in this study. It is evident that the error in our experiment is within

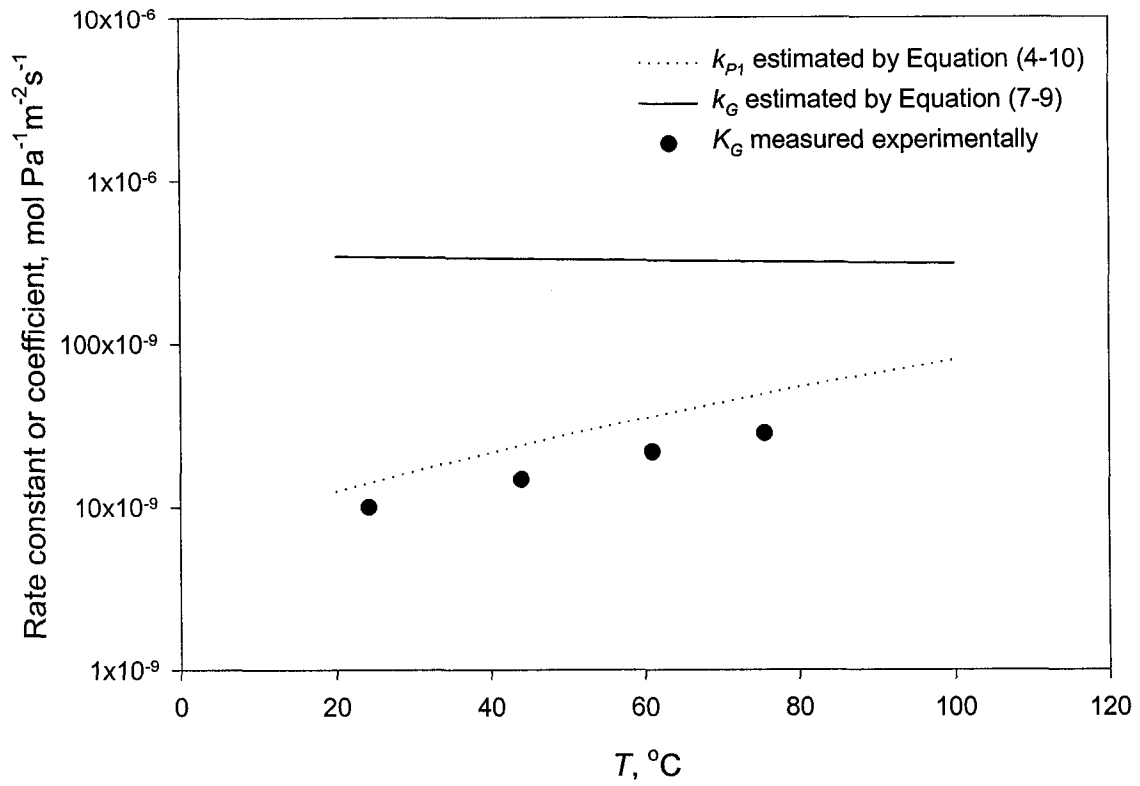


Figure 7-8. Dependence of estimated k_G and k_{p1} and measured K_G for reaction of H_2S and 90 wt% acid.

MS_18: 24.2°C, 90.13 wt%;

MS_21: 44.0°C, 90.07 wt%;

MS_20: 61.0°C, 90.09 wt%;

MS_19: 75.5.0°C, 90.10 wt%.

the error range suggested for Equation (7-6). In spite of this, some physical factors can also explain why the real interfacial area was smaller. The first factor that makes the interface smaller could be poor liquid distribution on the packing surface. This phenomenon may occur with an inadequate liquid distributor, heterogeneous packing density, or poor liquid flow pattern inside the bed. For example, much liquid is driven to the wall creating a shortcut. The second factor could be the produced sulfur that blocks the liquid surface. This phenomenon would happen when the production of sulfur is large and/or liquid flow is small. We were aware of this effect and tried to make it as insignificant as possible. The measure we took was to apply a large liquid flow rate under reaction conditions ensuring a small sulfur production. The molar ratio of our most sulfur production rate to the acid flow rate was 3.5×10^{-5} . Under this circumstance, the coverage of the interface area by solid sulfur was estimated using the wetted area and the particle size of the produced sulfur. It is known that the modification of sulfur is complicated and varying. Thus, the particle size of the produced sulfur from the reaction is difficult to estimate. However, literature (Schmidt and Siebert, 1973) shows that sulfur from the oxidation of H_2S tends to keep S_8 allotropy, which forms orthorhombic crystals with a unit structure consisting of 128 sulfur atoms (Meyer, 1968). Suppose that all the sulfur forms unit cells and that all the cells float at the surface of sulfuric acid solution. Calculation using the wetted surface area, the liquid hold-up, the liquid flow rate, the sulfur production rate and the average cross sectional area of a unit cell indicates that the coverage of the liquid surface by produced sulfur is 13.3%. In fact, this number could be much smaller because larger sulfur crystals might form, which makes the overall cross sectional area of sulfur particles smaller, and sulfur colloids tend to stay in the liquid

phase, which makes the surface coverage smaller. The experiments in Chapter 4 have shown that sulfur colloids stayed in the acid solution when visible amounts of sulfur were formed as pure H₂S was reacted with concentrated sulfuric acid. The current study in this chapter could not prove which of the three factors: the error from a_w estimation, the poor liquid distribution in the packing, and the sulfur block at the interface, to affect the effective interface area more significantly.

Now, it is believed from this study that the reaction of H₂S and 90 wt% acid in the column reactor is in the reaction-controlling regime. In other words, the bulk of the resistance comes from the reaction, and the reaction rate constant, k_{p1} , calculated from Equation (4-10) should approximate the overall mass transfer coefficient, K_G . Thus, from another point of view, the surface area available for the reaction may also be estimated by dividing the measured $K_G a$ obtained using the column reactor, by k_{p1} , the reaction rate constant. The value of a thus obtained may better approximate the real surface area than the value calculated using Equation (7-8). However, in reactor design, estimation of the value of effective area from Equation (7-8) is more convenient because it does not need experimental verification. If a reasonable safety factor is taken into consideration, the error arising from this method could be kept within an acceptable range.

7.5.4 Analysis on reaction in 96 wt% sulfuric acid

It has also been mentioned that the rate of the reaction of H₂S in 96 wt% sulfuric acid is too rapid for it to be used to evaluate the behavior in the packed column reactor. At room temperature, the H₂S conversion could reach as high as 96%. When higher temperatures were used, complete H₂S conversion was obtained no matter how other parameters such as flow rate and feed H₂S concentration were adjusted. One value of the

rate coefficient based on the 96% H₂S conversion was plotted in Figure 7-9. However, the plot of the values of k_{P1} and k_G predicted by Equations (4-10) and (7-8), respectively, also suggested a profile of rate-controlling regime for reactions in this acid. As shown in Figure 7-9, when the temperature is below *ca.* 60°C, the process is controlled by reaction but when the temperature exceeds 60°C mass transfer becomes the controlling step.

7.5.5 Reactor design

Some assumptions can be made before developing the equations and procedures for packed column reactor design. First, the process is assumed to have no radial concentration gradients in the column. Second, the SO₂ in both phases is in equilibrium only at the interfacial surface. Although the previous analysis assumed that the first reaction rate dominates, the produced SO₂ will be consumed to some extent by the second reaction as long as H₂S is still available. Considering SO₂ consumption in the second reaction, the mass balance with respect to H₂S and SO₂ leads to differential equations similar to those obtained for the batch reactor (Chapter 6),

$$\frac{dP_{H_2S}}{dz} = -\frac{PA}{G} a(K_G P_{H_2S} + k_{P2} P_{H_2S} P_{SO_2}) \quad (7-20)$$

$$\frac{dP_{SO_2}}{dz} = \frac{PA}{G} a(K_G P_{H_2S} - \frac{1}{2} k_{P2} P_{H_2S} P_{SO_2}) \quad (7-21)$$

where, K_G is k_G under mass transfer control and K_G is k_{P1} under reaction control. The height of the packing in the reactor may be obtained by solving the equations simultaneously for z at an expected value of P_{H_2S} (Exit requirement). Accordingly, the procedure for designing a packed column reactor to be used to carry out the H₂S-sulfuric acid reaction system is suggested as the follows:

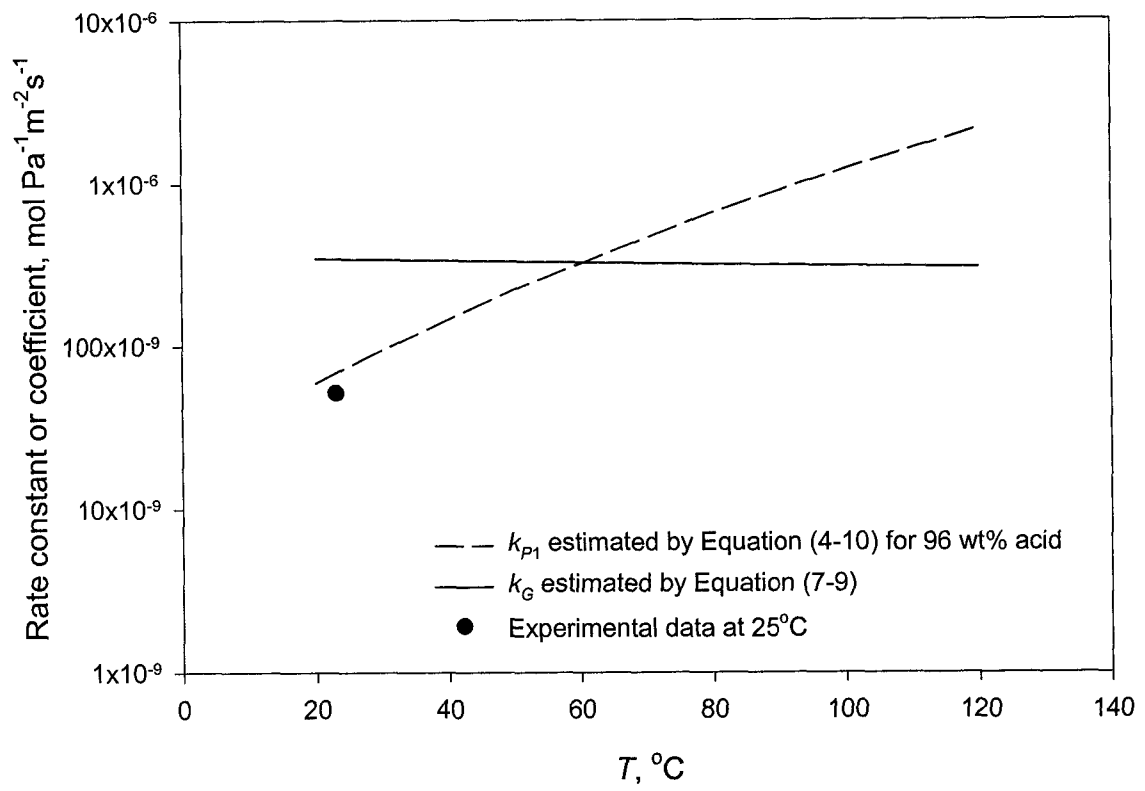


Figure 7-9. Analysis of rate controlling regime for reaction in 96 wt% acid.

- (1) Choose the temperature and acid concentration at which the reaction is to be carried out.
- (2) Analyze the rate-controlling regime by drawing a plot like Figure (7-8) or (7-9).
- (3) According to the rate-controlling regime, choose k_{P1} or k_G as the overall mass transfer coefficient, K_G .
- (4) Choose the diameter of the column. If mass transfer controls the rate, take superficial gas flow into account when the diameter is chosen.
- (5) Use Equation (7-7) to estimate the surface area available for the reaction after the liquid flow rate is selected.
- (6) For a particular H₂S exit requirement, simultaneously solve Equations (7-19) and (7-20) for the height of packing, which in turn determines the height of column.

7.6 Conclusions

The “two-film” theory analysis on H₂S-sulfuric acid system results in a concentration profile, based on which the mass transfer regime is obtained. The mass transport resistance consists of two consecutive steps: gas-side mass transfer and surface reaction. The overall rate coefficient could be either the mass transfer coefficient or the reaction rate constant depending on which is the rate-controlling step. Using the H₂S-water system, mass transfer in the liquid side was determined, indicating that Onda’s correlations can be used to estimate the effective interfacial area and liquid-side mass transfer coefficient for the operation of the packed column reactor used in this study. The reaction of H₂S and 90 wt% sulfuric acid in the column falls into the chemical reaction rate-controlling regime. The rate coefficient measured from column operations

approximates the values of the rate constant obtained in Chapter 4. Using the differential equations to model the column operation, a basis for a design procedure is proposed.

7.7 Nomenclature

A	Concentration of A in liquid	mol L^{-1}
A^*	Equilibrium concentration of A at interfacial surface	mol L^{-1}
a	Effective surface area	$\text{m}^2 \text{m}^{-3}$ or m^{-1}
a_t	Total surface area of packing	$\text{m}^2 \text{m}^{-3}$ or m^{-1}
a_w	Wetted surface area	$\text{m}^2 \text{m}^{-3}$ or m^{-1}
D	Diffusivity	$\text{m}^2 \text{s}^{-1}$ or $\text{m}^2 \text{h}^{-1}$
D_G	Diffusivity in gas phase	$\text{m}^2 \text{s}^{-1}$ or $\text{m}^2 \text{h}^{-1}$
D_L	Diffusivity in liquid phase	$\text{m}^2 \text{s}^{-1}$ or $\text{m}^2 \text{h}^{-1}$
D_p	Normal size of packing	m
G	Gas flow rate	mol s^{-1}
G	Superficial mass flow rate of gas (Equation (7-8))	$\text{kg m}^{-2} \text{h}^{-1}$
g	Gravitational constant	m h^{-2}
H	Henry law constant	L Pa mol^{-1}
K_G	Overall coefficient in gas phase	$\text{mol s}^{-1} \text{m}^{-2} \text{Pa}^{-1}$
K_L	Overall coefficient in liquid phase	m s^{-1}
k_G	Gas phase mass transfer coefficient	$\text{mol s}^{-1} \text{m}^{-2} \text{Pa}^{-1}$
k_L	Liquid phase mass transfer coefficient	m s^{-1}
k_{p1}	Rate constant for reaction 1	$\text{mol s}^{-1} \text{m}^{-2} \text{Pa}^{-1}$
k_{p2}	Rate constant for reaction 2	$\text{mol s}^{-1} \text{m}^{-2} \text{Pa}^{-2}$
L	Superficial mass flow rate of liquid (Equation (7-6,7))	$\text{kg m}^{-2} \text{h}^{-1}$
M	Molecular weight	g mol^{-1}
M_L	Molecular weight of liquid component	g mol^{-1}

<i>P</i>	Pressure of partial pressure	Pa
<i>Pⁱ</i>	Pressure of partial pressure at interfacial surface	Pa
<i>R</i>	Gas constant	$\text{m}^3\text{PaK}^{-1}\text{mol}^{-1}$
<i>T</i>	Absolute temperature	K
<i>V</i>	Solute molar volume at boiling point (Equation (7-15))	L mol^{-1}
<i>v</i>	Structural volume of a molecule (Equation (7-17))	
<i>y</i>	Mole fraction of a component in gas phase	
<i>z</i>	Height of packing	m

Subscripts

<i>A</i>	A soluble gas component
<i>B</i>	Another component
<i>b</i>	Bottom
<i>c</i>	Critical
<i>G</i>	Gas
<i>L</i>	Liquid
<i>p</i>	Packing units (rings, spheres, <i>etc.</i>)
<i>t</i>	Total, Top
<i>w</i>	Wetted
<i>1</i>	Refer to reaction 1
<i>2</i>	Refer to reaction 2

Greek

<i>μ</i>	Viscosity	Pa s or $\text{kg m}^{-1}\text{s}^{-1}$
<i>ρ</i>	Density	kg m^{-3}

σ	Surface tension	dynes cm^{-1} or kg h_2
ϕ	Association parameter (Equation (7-17))	

7.8 Literature Cited

- Al-Ghawas, H. A., D. P. Hagewiesche, G. Ruiz-Ibanez, and O. C. Sandall, Physico-chemical Properties Important for Carbon Dioxide Absorption in Aqueous Methyl-diethanolamine, *J. Chem. Eng. Data.*, **34**, 385 (1989).
- Danckwerts, P. V., *Gas-Liquid Reactions*. McGraw-Hill Book Company: New York (1970).
- Geankoplis, C. J., *Transport Processes and Unit Operations*, 3rd Ed., Prentice Hall, Englewood Cliffs, New Jersey, p396, p401 (1993).
- Lide, D. R. (Ed-in-Chief), *CRC Handbook of Chemistry and Physics*, CRC (1999-2000).
- Meyer, B., Elemental Sulfur in *Inorganic Sulfur Chemistry*, ed. by G. Nickless, Elsevier Publishing Company, Amsterdam, p252 (1968).
- Myhre, C. E. L., C. J. Nielsen, and O. W. Saastad, Density and Surface Tension of Aqueous H₂SO₄ at Low Temperature, *J. Chem. Eng. Data.*, **41**, 617 (1998).
- Onda, K., E. Sada, and Y. Murase, "Liquid-side Mass Transfer Coefficients in Packed Towers", *AIChE J.*, **5**, 235 (1959).
- Onda, K., H. Takeuchi, and Y. Okumoto, "Mass Transfer Coefficients between Gas and Liquid Phases in Packed Columns", *J. Chem. Eng. Jpn.*, **1**, 56 (1968a).
- Onda, K., E. Sada, and H. Takeuchi, "Gas Absorption with Chemical Reaction in Packed Columns", *J. Chem. Eng. Jpn.*, **1**, 62 (1968b).
- Perry, H. P., D. W. Green, and J. O. Maloney (Editors), *Perry's Chemical Engineers' Handbook*, McGraw-Hill, New York (1997).
- Rinker, E. B., O. T. Hanna, and O. C. Sandall, "Asymptotic Models for H₂S Absorption into Single and Blended Aqueous Solution", *AIChE Journal*, **43**, 1 (1997).

Shah, Y. T., *Gas-Liquid-Solid Reactor Design*, McGraw-Hill International Book Company, New York (1979).

Schmidt, M. and W. Siebert, Sulfur in *Comprehensive Inorganic Chemistry* vol. 2, ed. by Bailar, I. C., *et al.*, Pergamon Press, Oxford, pp803-807 (1973).

Chapter 8

Suggested Applications and Recommendations

8.1 Introduction

The previous studies have clarified which independent reactions occur in the H₂S-sulfuric acid gas-liquid reaction system. The rate equations for each of the two independent reactions were obtained using the initial-rate analysis. The two rate equations for the reaction system were applied to analyzing a batch reactor and a packed-column reactor. The models based on these equations were used to estimate the size of the column. In this chapter, we apply this technology by proposing two different sulfur removal cases: H₂S removal from flare gas, where the gas flow rate and the H₂S concentration are small, and sulfur recovery from sour gas, where the production scale and H₂S concentration may be larger.

8.2 Application to Flare Gas Recovery

8.2.1 Flare gas problems

In natural gas and oil industries and their processing plants, hydrocarbon-containing gas, mainly methane, is produced in such a way that it cannot be processed or sold or it is not worth doing so. Flaring in a controlled manner is the traditional way to dispose of this so-called unwanted gas. According to Alberta Energy and Utilities Board (Bott, 2000), about 1,900 million cubic meters of gas were flared in Alberta in 1998,

among which 77% was solution gas, natural gas contained in crude oil which is burned at oil battery sites. Complete combustion during flaring releases mainly carbon dioxide, water vapor and small amounts of sulfur dioxide. However, recent field research (Harvie and Dixon, 2000) found that the efficiency of gas flaring could be significantly lower than previously assumed. As a result, carbon monoxide, unburned hydrocarbons, particulate matter, volatile organic compounds such as benzene, toluene and xylene, other organic compounds known as polycyclic aromatic hydrocarbons, and other sulfur compounds such as carbon disulfide and carbonyl sulfide may also be found in the emissions. These substances are toxic and hazardous to the environment. On the other hand, flaring is a waste of energy resources. Therefore, attempts to reduce and recover the flare gas become more attractive, one such example being the generation of electric power from solution gas (Kline, 2000). Gas turbine generators can work at the flare sites and the electricity produced can be transferred to the provincial power pool. Both vapor and hydrogen sulfide need to be removed from the solution gas to protect long-term use of generators. (Williams, 1999).

8.2.2 Suggested application for sulfur removal from flare gas

Figure 8-1 shows the flowsheet of a process which uses the H₂S-sulfuric acid gas-liquid reaction system to remove hydrogen sulfide and water vapor from flare gas. Four basic unit operations are involved: reaction in a packed-column reactor, filtration, stripping and adsorption. Solution gas (G1) containing H₂S and vapor enters the reactor column from the bottom. Concentrated sulfuric acid (>90 wt%) (L2) enters the column from the top. Counter-current flow is established inside the column where H₂S and sulfuric acid react. SO₂ produced from the reaction is adsorbed in the down-coming

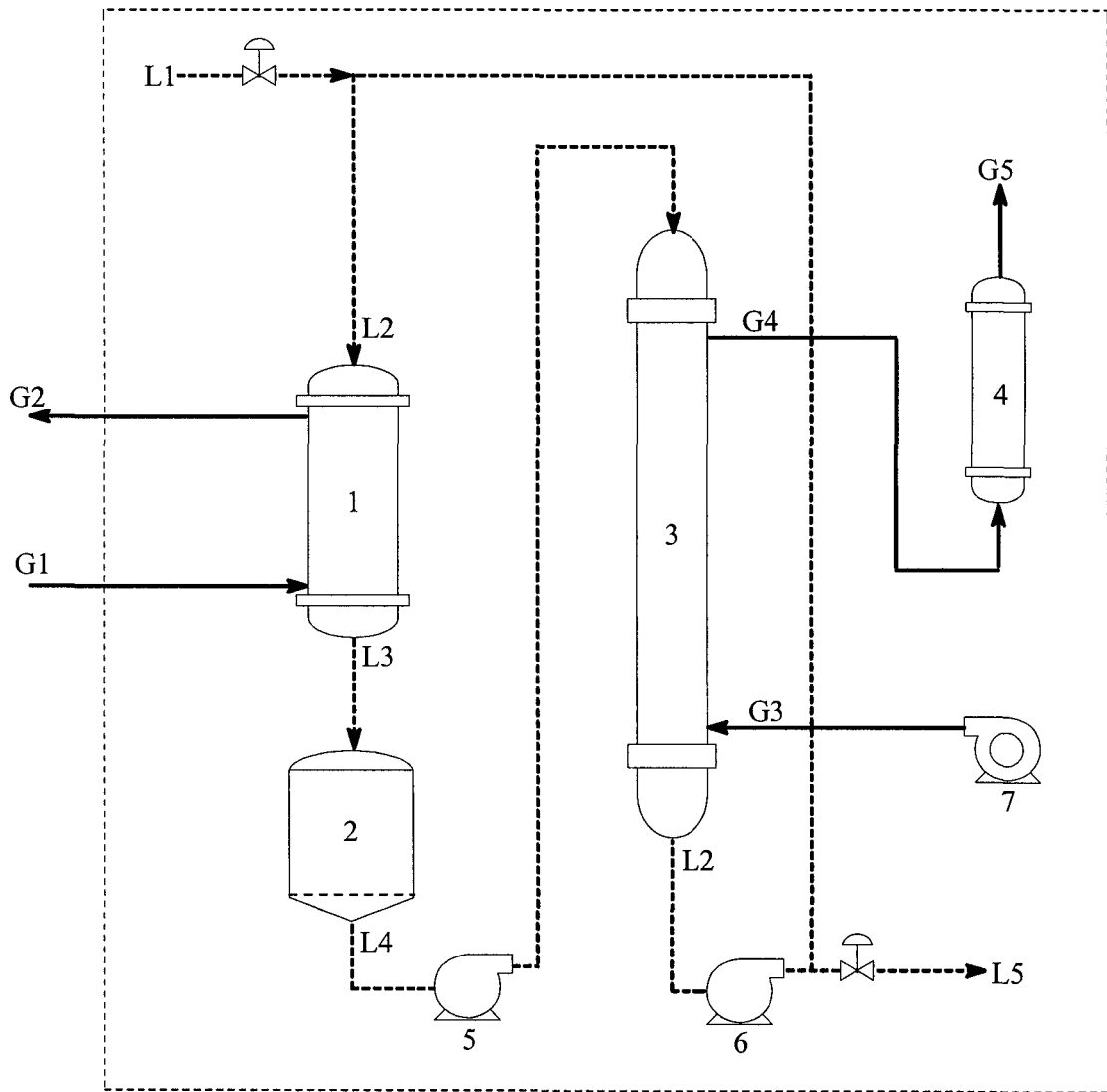


Figure 8-1. Flowsheet of suggested application in flar gas recovery. 1. Packed column reactor; 2. Filter; 3. Stripper; 4. Adsorber; 5 & 6, Pumps; 7, Blower.

liquid acid in the upper section of the column and reacts with H_2S in the lower section. The sweetened and dry solution gas (G2) comes from the top of the column and goes to the turbine for power generation. The acid together with the produced sulfur and unreacted SO_2 (L3) exits from the bottom of the column, going through a filter to remove the solid sulfur and then to a stripping column to remove the SO_2 . The lean solution (L2) is recycled and SO_2 in the stripping gas (air) is adsorbed by an adsorbent installed in a tower. Over a certain period of operation, some of the downgraded sulfuric acid is removed from the system and replaced with fresh solution. The filter bed also needs to be replaced periodically. The acid concentration is suggested to be 96 wt% and higher, such that a fast reaction and a high SO_2 solubility can be provided at atmospheric temperature. The column is to be run counter-currently to have the unreacted SO_2 scrubbed in the upper section. This design also enables more SO_2 to be reacted in the lower section because SO_2 is pre-dissolved in the acid. Operation at a high L/G ratio and low temperature will also improve the efficiency in SO_2 scrubbing. The use of packing with a smooth surface will keep the produced sulfur away from the packing surface and prevent the packing bed from being blocked by solid sulfur.

8.2.3 Column reactor design

The main operating unit shown in Figure 8-1 is a packed column reactor, which is to be operated counter-currently. The column plays not only the role of a reactor, in which H_2S reacts with H_2SO_4 and SO_2 , but also the role of an absorber, in which the unreacted SO_2 in the gas is scrubbed into the liquid phase which is sulfuric acid. Because the designed working temperature is the room temperature, chemical reaction will be the rate-controlling step according to Figure 7-9. Equations (7-19) and (7-20) are used to

determine the size of the reaction section and k_{P1} is taken as the rate coefficient. The Kremser method (Wankat, 1988) is used to calculate the number of equilibrium stages required to absorb SO_2 to a certain exit concentration. Figure 8-2 shows the required number versus various SO_2 exit “ppm” values. The column size is finally determined by adding the two sections together.

A sample calculation for a solution gas stream with a flow rate of 708 scm/day and H_2S content of 0.25% (information provided by Mercury Electric Corporation) shows that the process generates 3.16 kg of sulfur and 1.26 kg of SO_2 every day. After a 30-day operation, 5000 kg of sulfuric acid will be downgraded from 96 wt% to 94.7 wt%, without considering the effect of vapor content in the solution gas stream. To upgrade the acid concentration to 96 wt% and keep 5000 kg acid solution in the system, 1230 kg of 94.7 wt% acid needs to be removed from the system and the same mass of 100 wt% acid to be added.

8.2.4 Discussion and recommendations

Flare gas power generators (the fuel turbines) are designed for working at the sites of oil wells, batteries, satellites and gas plants. The flow rate of the gas varies from site to site, most of them being very small. Because of this, microturbines have been invented. Accordingly, flexibility in the sulfur removal technology is most important for this purpose. The suggested technology based on Figure 8-1 exactly meets this requirement because the size of the operation units can be designed based on the gas flow rate with few restrictions. It is also simple because it can be operated with little care. The capital and operating cost should not be significant. The other advantage of this sulfur removal process is that it can remove water vapor, which is hazardous to the microturbine

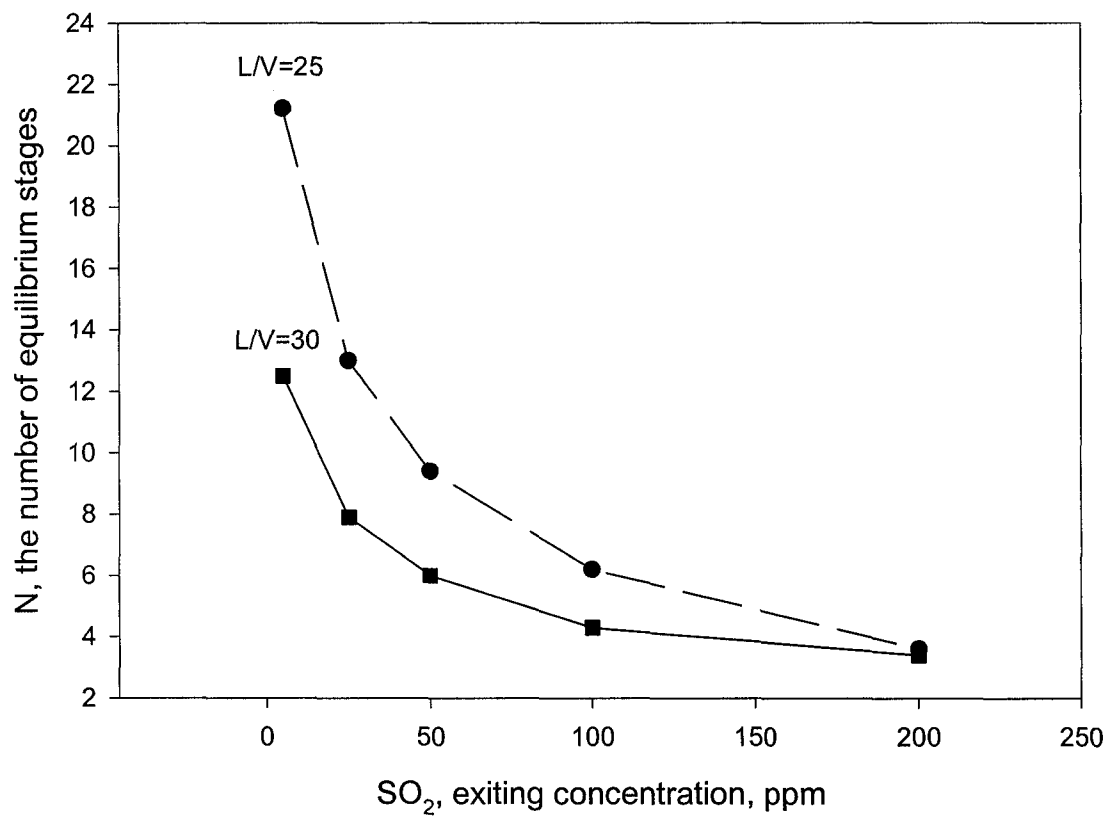


Figure 8-2. Equilibrium stages needed vs. exit SO₂ concentrations.

generator and which needs to be removed before the flare gas enters the generator.

The reuse or disposal of used sulfuric acid poses a problem. The used acid may contain sulfur and the oxidation products of the organic components in the gas stream. It can be shipped back to sulfuric acid manufacturing plants for complete oxidation to SO₂. Before being upgraded, it can also be used as the catalyst for alkylation of aromatic hydrocarbons. Sulfuric acid catalyzed alkylation accounts for 50% of all alkylation processes (Hammershaimb, et al., 1992). The demand of sulfuric acid must be large. Moreover, the concentration range for sulfuric acid to be used as the catalyst is above 90 wt%. If sulfur contamination in sulfuric acid does not matter, the filtration unit could be avoided. This will make the process even more economical.

8.3 Sulfur Recovery Process

8.3.1 Claus process and its suitability

The modified Claus process works on the reaction of hydrogen sulfide and sulfur dioxide in terms of the following equation (Kohl and Riesenfeld, 1985),



This process is widely used for sulfur recovery from sour gases; however, it is not a process for removing H₂S from the sour gas for gas purification purpose. It cannot be “plugged” into the gas stream that requires H₂S removal, because its furnace unit would burn the fuel components in the gas stream as it burns H₂S into SO₂. Extra operations such as H₂S absorption and stripping using alkaline or amine solutions have to be supplemented. Therefore, Claus process is economically justifiable only if the sulfur intake is large. In addition, due to the equilibrium of the reactions involved in the process,

complete conversion of sulfur compounds in the gas stream to elementary sulfur is precluded. Other sulfur compounds like carbonyl sulfide and carbon disulfide would be produced in the process. The process, in many instances, is not able to reduce the sulfur emission to the atmosphere to the level that the air pollution control authorities permit. It needs to be supplemented with processes specially designed for removing residual sulfur compounds from the Claus plant tail gases. This makes the process very costly both in investment and operation.

8.3.2 Suggested application for sulfur recovery

Figure 8-3 shows the flowsheet of a sulfur removal and recovery process based on the hydrogen sulfide-sulfuric acid gas-liquid reaction system, to be used where the modified Claus process is used. It indicates that the system is able to work with sour gas without any prior supplement such as absorption-regeneration unit. Suppose the SO_2 selectivity of column 1, the molar ratio of the SO_2 concentration of G2 to the H_2S concentration of G1, to be 50%. To meet the stoichiometric requirement for reaction (8-1) in the liquid-phase Claus reaction unit, half of the sour gas stream feed, (G1a), is directed into the reactor. Concentrated sulfuric acid is also fed into the reactor column from its top (L2). The two reactions are carried out in the reactor at a temperature above 120°C , to keep the produced sulfur in liquid state, totally converting H_2S . The only sulfur-containing compound in the exit gas stream (G2) is SO_2 . The exiting acid from column 1, (L3), contains sulfur and dissolved SO_2 . This sulfuric acid needs to be treated with two options, depending on the acid concentration. If its concentration is high enough for it to be recycled back to the column, sulfur needs to be removed. The dissolved SO_2 remains, for more dissolved SO_2 in the acid will result in more conversion of H_2S by the second

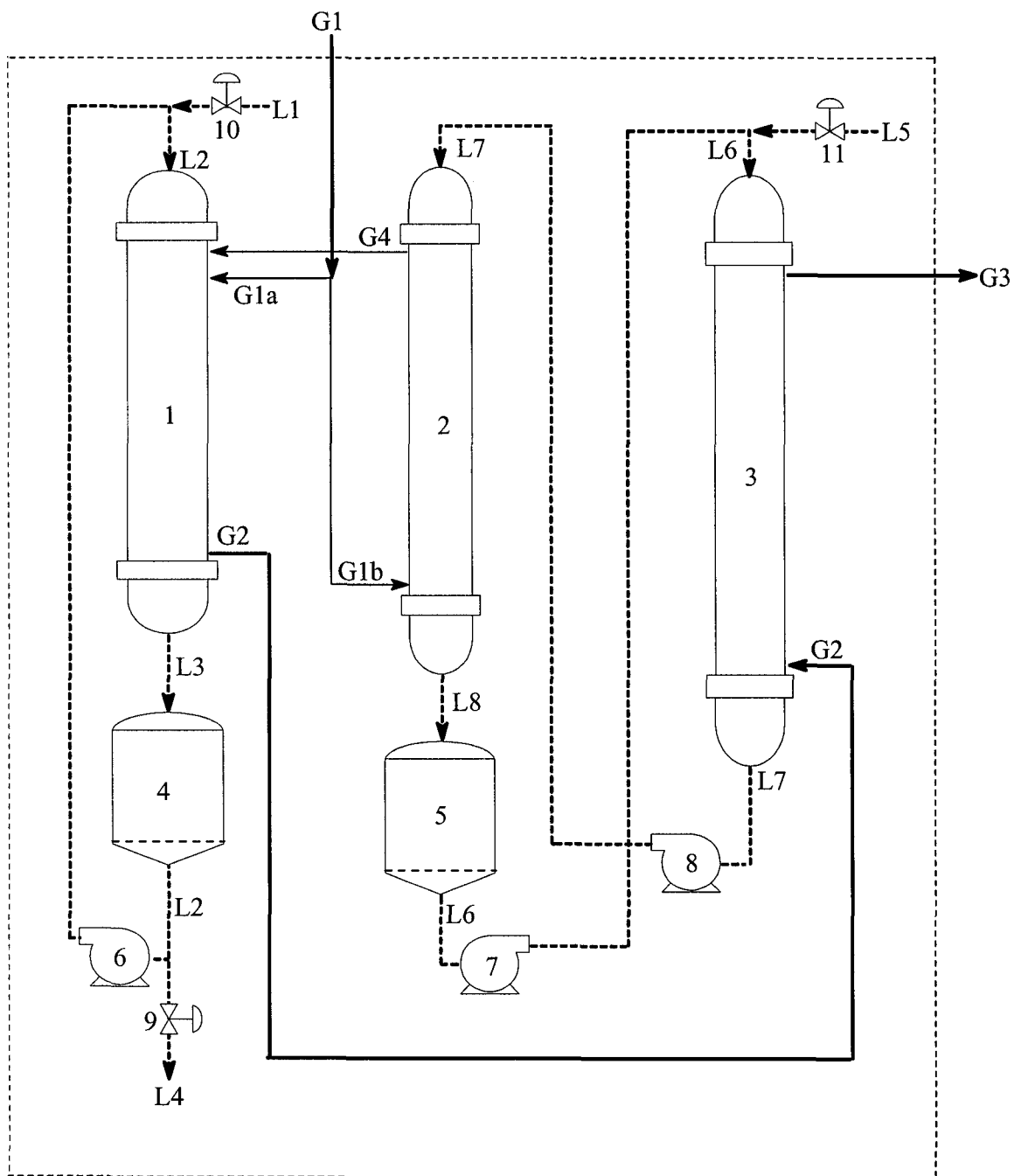


Figure 8-3. Flowsheet of suggested application for sulfur recovery from sour gas. 1. reactor column; 2. column for liquid-phase Claus reaction; 3. column for SO_2 absorption; 4 and 5. sulfur separators; 6, 7 and 8. pumps; 9, 10 and 11. valves.

reaction, which, in turn, decreases the consumption of acid for a unit of converted H_2S . If the exit acid is too dilute, it is shipped to the sulfuric acid manufacturing plant for upgrading without circulating. Distillation on site would be an alternative to upgrade the acid, but the large consumption of energy in distillation has to be taken into consideration.

The SO_2 -containing gas stream (G2) is then fed into an SO_2 absorption column (column 3), where SO_2 is scrubbed by a solution, for example, sodium citrate (Madengurg and Seese, 1980). The S-free gas stream (G3) from the absorber goes to the user. The SO_2 -rich solution (L7) is directed into the second reactor column where SO_2 in the solution reacts with the H_2S from the other half of the sour gas stream (G1b) fed from the bottom of the reactor, resulting in regeneration of the solution. After removing the produced sulfur, the lean solution is fed back to the absorption column for reuse. The amount of H_2S in the gas stream (G1b) is kept slightly larger than that required by the stoichiometry of reaction (7-1) such that SO_2 is consumed completely. The resulting gas (G4), containing a small amount of H_2S , is fed back to the first reactor. Fresh sulfuric acid (L1) and sodium citrate solution (L5) need to be added to make up the loss in consumption and downgrading. Also the downgraded acid will be removed from the circulation.

8.3.3 Case study

The purpose of this application is to recover sulfur from sour gas that contains a large amount of H_2S . Much sulfur will be produced and retained in the acid solution; thus, to prevent the packed bed from being plugged by solid sulfur, it is suggested that the process be run above the melting point of sulfur ($\sim 120^\circ\text{C}$). However, the operating temperature cannot be higher than 150°C so as to avoid sulfur being oxidized into SO_2 . A

Table 8-1. Specifications of sour gas from a gas plant
(provided by Colt Engineering Corporation).

<u>Plant conditions</u>	
Temperature	120°F (<i>ca.</i> 50°C)
Pressure	900 psig (61.2 atm, 6.20 MPa)
Flow rate	97.74×10 ⁶ ft ³ /day (2.64×10 ⁶ m ³ /day) @STP
<u>Compositions</u>	
	% v/v
H ₂ S	11.88
C ₁	73.29
C ₂	4.42
C ₃	1.39
iC ₄	0.30
nC ₄	0.44
iC ₆	0.16
nC ₆	0.13
C ₆₊	0.26
N ₂	1.10
CO ₂	6.63
O ₂	-

Table 8-2. Outputs from simulations of a reactor column.

L/G molar ratio	10	5	1	0.5
L, kg h ⁻¹	2142×10 ³	1071×10 ³	214.2×10 ³	107.1×10 ³
L, m ³ h ⁻¹	1170×10 ³	585.1×10 ³	117.0×10 ³	58.51×10 ³
Acid downgrade to %	95.6	95.2	91.9	87.5
S production, kg h ⁻¹	12.23×10 ³	12.23×10 ³	12.23×10 ³	12.23×10 ³

sample calculation was conducted at 120°C for a specific sour gas (the plant information, as shown in Table 8-1, was provided by Colt Engineering Corporation, Calgary, Alberta). As suggested, half of the total gas flow goes into the column reactor. The flow rate of sulfuric acid, the acid downgrading and sulfur production for each ratio were estimated based on L/G molar flow ratios of 10, 5, 1 and 0.1, respectively. The simulation results are shown in Table 8-2. It is seen that a large liquid flow rate is required to run the process at a relatively stable acid concentration (L/G=10). If a smaller liquid flow rate is used, acid concentration will drop dramatically. In this case, it is better not to circulate the acid. Instead, the dilute acid should be upgraded. The simulation also shows that the acid requirement is very large. Because the recovered sulfur is mostly used to make sulfuric acid, a sulfuric acid plant with this sulfur recovery process may be practical. Compared to a Claus plant and a separate sulfuric acid plant, this joint technology may also be more economical. The flexibility in scale of operation will be its second advantage, making the technology suitable for treating the sour gas over a broad range of flow rates and H₂S content of sour gas feed. Due to the irreversible reactions involved in the process, sulfur emissions may be quite low.

8.4 Conclusions and Recommendations

The case studies describing the application of the sulfur recovery technology using H₂S-sulfuric acid gas-liquid reaction system indicate that this technology is more suitable for treating gas streams that are small in flow rate and H₂S content. The commercialization in this area will be easier. In fact, the intention of this study is to develop a sulfur removal and recovery technology suitable for gases that contained small

amounts of H₂S and for the locations that are remote and isolated. From this point of view, the process may become successful when a practical sulfur filtration method and the reuse of downgraded sulfuric acid are possible.

However, the use of this technology for recovering sulfur from sour gas containing large amounts of H₂S seems to have more difficulty where the transportation of a large amount of sulfuric acid to and from the recovery site will be the biggest issue. More detailed work is expected not only on the unit operations such as sulfur separation and the reuse of the downgraded sulfuric acid but also on the economical assessment. Because it generates no sulfur emission into the atmosphere, the hope for it to replace Claus plants remains if the replacement can be proven to be more economical.

8.5 Literature Cited

- Bott, R., *Flaring: Questions and Answers*, Petroleum Communication Foundation, Calgary, (2000).
- Harvie, A., and Macleod Dixon, *Gas Flaring: The Environmental and Legal Impacts, Gas Flaring: Guide 60 and Its Impact on the Petroleum Industry*, Insight Information Co., Toronto, (2000).
- Hammershaimb, H. U., T. Imai, G. J. Thompson, B. V. Vora, "Alkylation", *Kirk-Othmer Encyclopedia of Chemical Technology*, John Wiley and Sons, Inc., New York (1992)
- Kline, R. H., "Flare Gas Power Generation: New Technology and Options", *Gas Flaring: Guide 60 and Its Impact on the Petroleum Industry*, Insight Information Co., Toronto, (2000).
- Kohl, A. L., and F. C. Riesenfeld, *Gas Purification*, 4th Ed., Gulf Publishing Company, Huston, (1985).
- Madenburg, R. S., and T. A. Seese, "Hydrogen Sulfide Reduces Sulfur Dioxide to Desulfurize Flue Gas", *Chem. Eng.*, **87**, 88 (1980).
- Wankat, P. C., *Equilibrium Staged Separations: Separations in Chemical Engineering*, PTR Prentice Hall (1988).
- Williams, R. L., "Role of Power Generation in Combating Gas Flaring", *Dealing with the Gas Flaring Problem in the Petroleum Industry – Conference Reports*, Insight Information Co., Toronto (1999).

Chapter 9

Summary and Conclusions

The study of the gas-liquid reaction system, H₂S and sulfuric acid, has focused on both theoretical aspects such as chemical stoichiometry, chemical kinetics, and mass transfer, and practical application aspects such as the effect of other components in the to-be-treated gas streams, reactor design, and process development. The objectives of the theoretical part were

- To find out the independent reactions that are involved in H₂S-sulfuric acid system and the dependence of their overall stoichiometry on acid concentration.
- To establish the rate equation for each of the involved reactions and the dependence of the kinetic parameters on acid concentration and temperature.
- To determine the mass transfer regime and to establish the mathematical models that can be used for reactor design.

The objectives of the application part were

- To get to know how sulfuric acid in various concentrations reacts with possible components other than H₂S in the gas stream to be treated.
- To suggest the potential applications of this technology.
- To suggest a flowsheet for the particular potential uses.
- To simulate the process, especially the reactor unit, at plant conditions.
- To address practical issues in the use of this technology.

9.1 Literature Review on H₂S-Sulfuric Acid Reaction System

A thorough literature survey on the reaction between hydrogen sulfide and sulfuric acid was conducted. The profiles of the H₂S-sulfuric acid reaction system before this study are summarized as the follows.

- The reaction between H₂S and sulfuric acid was first reported in the middle of 19th century. Since then, no systematical research on this reaction system has been conducted.
- Snurnilov observed that elemental sulfur, sulfur dioxide and water are the products of the reaction between H₂S and sulfuric acid and Tiwari studied the reaction of H₂S and SO₂ in dilute sulfuric acid. No connection was found between these two studies.
- No literature has been found describing the possible reactions, the reaction stoichiometry and its dependence on temperature and acid concentration, the reaction kinetics, and the mass transfer behavior of this reaction system.

9.2 Reactions of Sulfuric Acid with Components other than H₂S

The objective of this study is to develop a sulfur removal and recovery technology. Whether and how sulfuric acid interferes with components such as methane, ethylene, carbon monoxide, carbon dioxide, and nitrogen, and reacts with other sulfides such as carbonyl sulfide, carbon disulfide, thiophene, and mercaptan were the major concern before the systematic studies were started. The experiments at 120°C using a semi-batch reactor answered these questions with the following results.

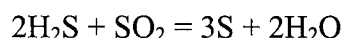
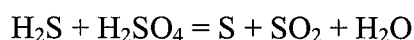
- Sulfuric acid does not react with methane, carbon monoxide, carbon dioxide, and nitrogen. It is inferred that it will not react with other saturated hydrocarbons.

- Sulfuric acid of 96 wt% converts ethylene by *ca.* 98 % but the acid of 80 wt% only converts it by less than 50 %. The results indicate that the technology will be limited for removing H₂S from gas streams which contain ethylene or other olefins as valuable components.
- Sulfuric acid shows little chemical reactivity to COS and CS₂. However, it converts thiophene and mercaptan nearly completely.

An important by-product of this section is the establishment of means for simultaneous analysis of sulfur and non-sulfur containing compounds and the sulfides both in large and small concentrations using a single GC couple with thermal conductivity and sulfur chemiluminescence detectors in parallel.

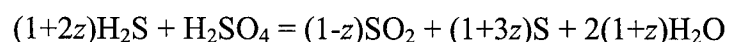
9.3 Reaction Scheme and Overall Stoichiometry

- Thermodynamic analysis and experiments found that the following two independent reactions are involved in H₂S-sulfuric acid system:



These two reactions are independent.

- When starting with H₂S and fresh sulfuric acid, the two reactions are parallel with respect to H₂S but consecutive for SO₂.
- Mass balance measurement shows that the overall stoichiometry of H₂S-sulfuric acid system is usually not the sum of the stoichiometry of the two reactions. Instead, the overall reaction is,



where, the overall stoichiometric coefficient, z , changes with acid concentration.

- The further oxidation of sulfur by concentrated sulfuric acid was not observed.

9.4 Kinetics of Two Reactions

The dominant part of this thesis was to measure the rate of the two reactions and to establish a rate equation for each of them. The initial reaction rate was recorded by measuring the pressure drop rate in a constant-volume batch reactor under specified conditions. The major results are obtained as follows.

- The rate equation for each reaction:

$$r_{H_2S,1} = k_{P1} a_{P_{H_2S}}$$

$$r_{H_2S,2} = k'_{P2} a_{P_{H_2S}} [SO_2]$$

- The dependence of the apparent rate constants on temperature and acid concentration was determined.
- Comparing the rate constant for the first reaction with the activity and concentration of molecular H_2SO_4 in sulfuric acid solutions suggests that sulfuric acid molecules are the only species that oxidizes H_2S .
- Because SO_2 dissolves in sulfuric acid in molecular form when acid concentration is 5 wt% or more, the reaction between H_2S and dissolved SO_2 takes the route that only produces sulfur and water. No polythionic acids were observed.
- Because the diffusion of H_2S into sulfuric acid solutions is negligibly slow, both reactions occur at the interface between gas and liquid.

9.5 Simulation for Batch Reactor Operation

Based on the rate equations obtained, differential equation models were established for batch reactor operation with strong stirring. The operation starts with fresh sulfuric acid solution and pure H₂S. Under particular assumptions described in Chapter 6, the models are

$$\frac{V_G}{RT_G} \frac{dP_{H_2S}}{dt} = -k_{P1} a P_{H_2S} - k_{P2} a P_{H_2S} P_{SO_2}$$

and

$$\frac{V_G}{RT_G} \frac{dP_{SO_2}}{dt} = k_{P1} a P_{H_2S} - \frac{1}{2} k_{P2} a P_{H_2S} P_{SO_2}$$

The total pressure and partial pressures of H₂S and SO₂ during the reaction course were simulated using MATLAB. The agreement between the simulated result and the result obtained experimentally in Chapter 3 indicates that the rate equations obtained in Chapters 4 and 5 are reliable and applicable. Modification made to the rate constant of the second reaction indicates that SO₂ is not in equilibrium in the batch operation. Its concentration in the acid should be far less than the equilibrium value. It also suggests that improving the dissolution of SO₂ in sulfuric acid is crucial to the second reaction

9.6 Mass Transfer and Reaction Behaviors in Packed Column

- Considering the observation that H₂S diffuses negligibly slow in sulfuric acid, the “two film theory” analysis indicates that the mass transportation process for H₂S in the reaction consists of two steps: H₂S transferring from gas phase to the liquid surface and H₂S reacting at the surface. Gas-phase mass transfer and interfacial reaction coexist and the resistance to the transportation of liquid reactants is ignored.

This situation is encountered when the reaction between H₂S in gas and concentrated sulfuric acid as the liquid is carried out in a packed column reactor.

- The overall rate equation for the process can be described as

$$r_{H_2S} = K_G P_{H_2S}$$

The overall resistance to the mass transportation is composed of two parts shown as

$$\frac{1}{K_G} = \frac{1}{k_G} + \frac{1}{k_{p1}}$$

when the first reaction predominates.

- A packed column was made to study the reactions in continuous operation, where reaction and mass transfer co-exist. Raschig ceramic rings were used as packing. H₂S-water absorption process in the column shows that Onda's correlations for the effective interfacial area and liquid-side mass transfer coefficient can be used to predict the operation in this column.
- Experiment results indicate that the reaction between H₂S and sulfuric acid of 90 wt% in the column reactor is reaction rate-controlling. The rate-controlling regime was analyzed for the reaction in 96 wt% sulfuric acid.
- Mathematical models were suggested for column design.

9.7 Application Suggestions and Recommendations

- Two flowsheets are proposed for applying this technology to two typical circumstances. One is H₂S removal from gas streams, such as flare gas or solution gas, that contains small amount of H₂S and are relatively small in flow rate. The other is

sulfur removal and recovery from sour gas that is large both in flow rate and H₂S content.

- Calculation based on plant information shows that the use of the suggested technology is practical for the first circumstance but difficult for the second.
- Further work is suggested which focuses on the separation of sulfur from sulfuric acid and the reuse of the downgraded sulfuric acid. An assessment on economics with respect to the application in sulfur recovery from the sour gas is also required.

Appendix A

Calibrations of Apparatus

A.1 Calibration of Mass Flow Controllers

Although well-designed mass flow controllers can maintain a constant flow within 1% of the full scale-flow with a repeatability of 0.2% of the full scale, they need to be calibrated while being in use because errors exist between their readings and the real flowrates. The errors are severe when solid contaminants plug their capillary tube. This occurs very often when they are used to control the flow of sulfur-containing gases.

A DryCal DC-2M Primary Air Flow Meter, made by BIOS International Corporation, was used to calibrate the mass flow controllers. This meter was designed for the air/gas flow calibration due to its high accuracy. According to its menu, the error is $\pm 2\%$ for a single reading and $\pm 1\%$ for an average reading, corresponding to ± 0.05 mL/min. When the readings are transferred to those at standard temperature and pressure, the volumetric accuracy is $\pm 0.6\%$ at 20-30°C.

Because corrosive gases are harmful to the flow calibrator, all the mass flow controllers were calibrated using nitrogen and the data were converted by an equation mentioned below. The calibration procedures are:

1. Connect the mass flow controller to be calibrated with nitrogen cylinder.
2. Connect the flow calibrator downstream of the mass flow controller.
3. Establish the gas flow.

4. Check leaking.
5. Set the mass flow controller.
6. Read 3 sets of 10-reading-average standardized flowrate.
7. Calculate the average value of the three numbers.

For the nitrogen mass flow controller, the flowrate read from the calibrator is directly used for drawing the flow-rate vs. setting diagram (Figure A I-1). For mass flow controllers for other gases, the flowrate of N₂ has to be converted to the flowrate of a particular gas according to the equation as follows,

$$Fl_c = \frac{c.f.c}{c.f.m} Fl_m \quad (A-1)$$

where, Fl_c and Fl_m represent the flowrate of the gas being calibrated and of the gas measured, respectively; $c.f.c$ and $c.f.m$ represent the gas conversion factor of the gas being calibrated and of the gas measured, respectively. Then the flow-rate vs. setting diagram was drawn, for example, Figure A I-2 for H₂S, and Figure A I-3 for SO₂. Similar figures were also drawn for gases such as CH₄, CO, CO₂ and ethylene.

For experiments where mass flow controllers were used, the flowrate of each gas was determined from the total flowrate and composition. The corresponding setting value was found from the diagram. Normally, the mass flow controllers are calibrated every 3 months.

A.2 Calibration of GC Detectors

Actually, the calibration of GC detectors has been mentioned in Chapter 2. The responses of the detector, *i.e.*, peak area, at different concentrations for particular gases, are measured intermittently, say, every 6 months, or when GC operation parameters, for

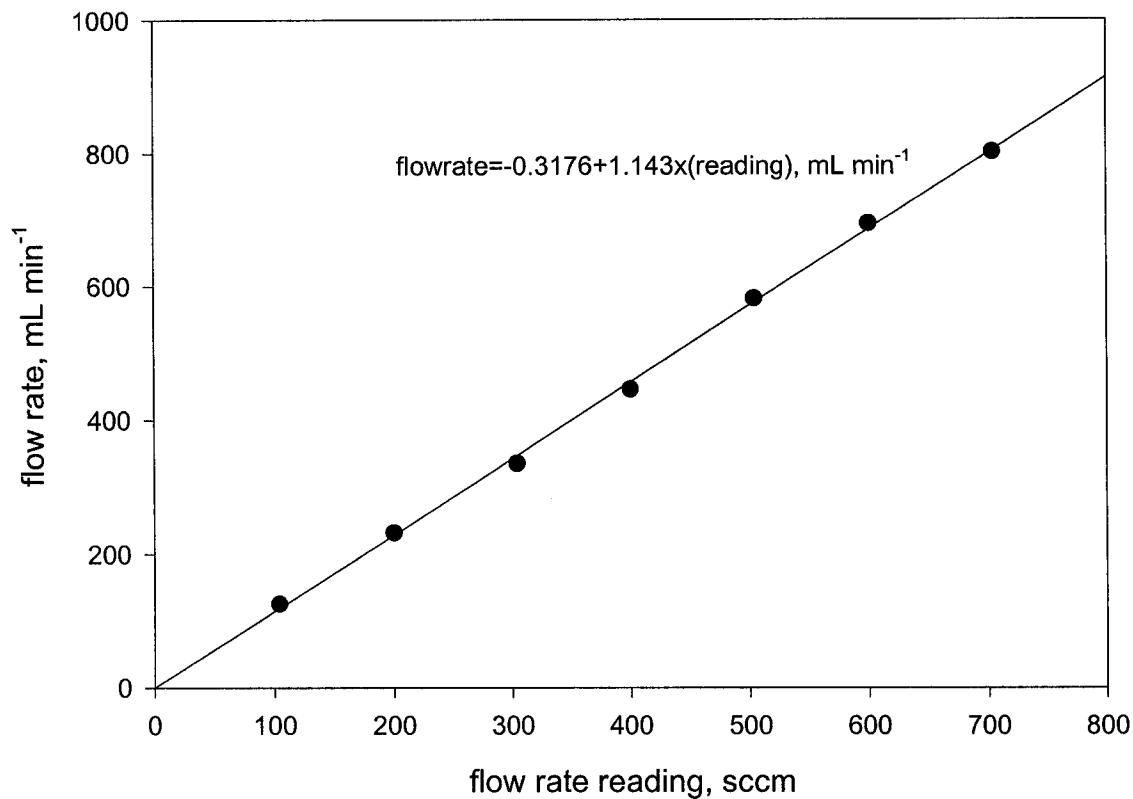


Figure A-1. Mass flowrate calibration for N₂ (old MFC, channel 3).
Calibration date: February 12, 2002.

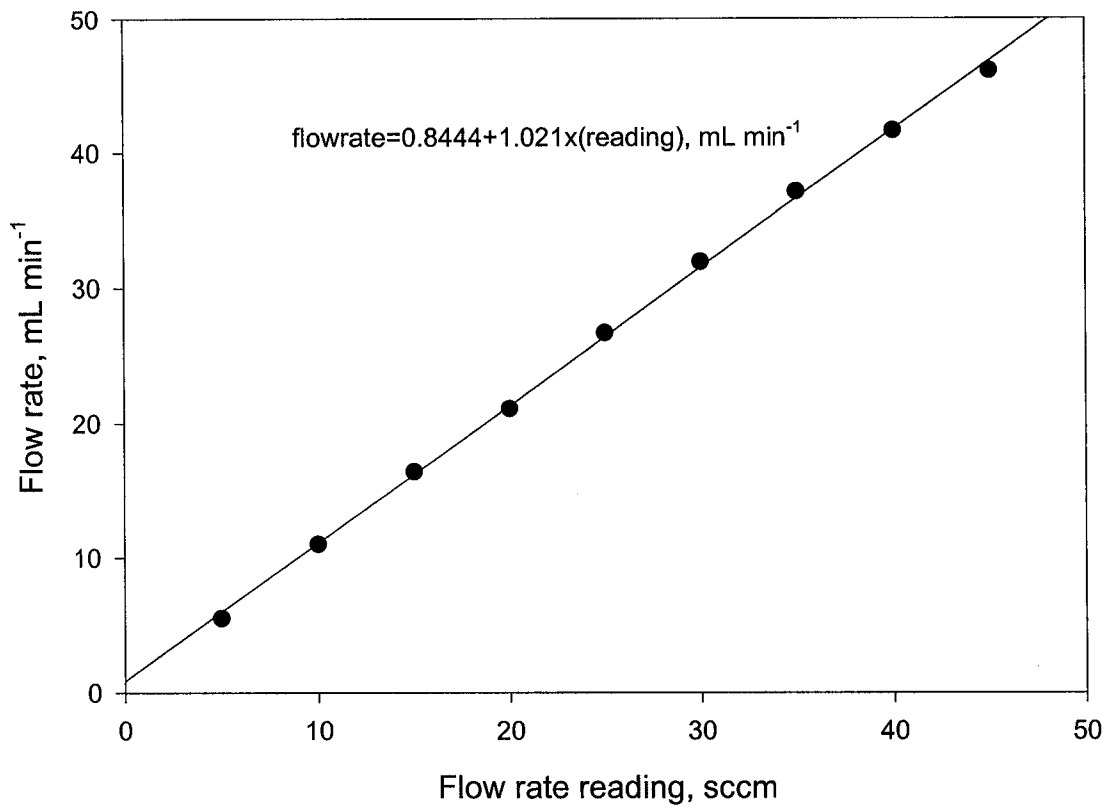


Figure A-2. Mass flowrate calibration for H₂S (old MFC, channel 2).
Calibration date: February 12, 2002.

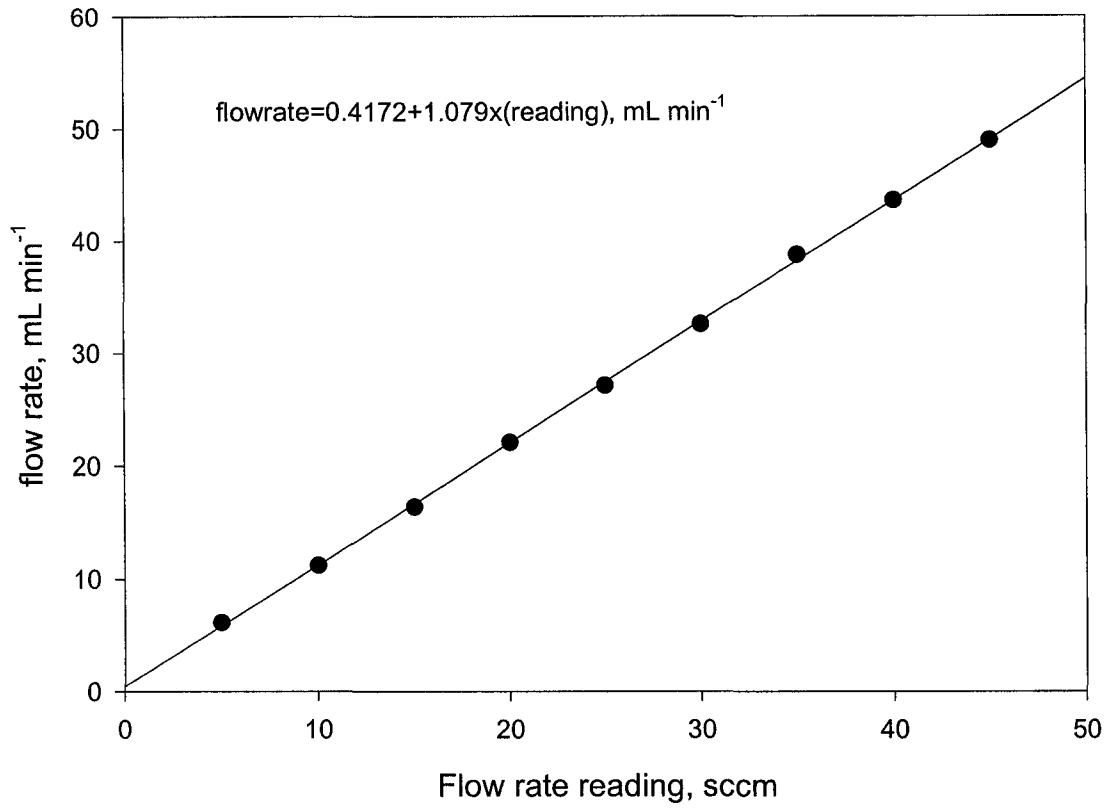


Figure A-3. Mass flowrate calibration for SO₂ (old MFC, channel 1).
Calibration date: February 12, 2002.

example, the size of the sampling loop, are changed. Usually, a linear relationship between the response and concentration, which passes through the origin in Cartesian coordinates, is obtained, shown in Figure A I-4 as an example.

In experiments, two methods, the internal standard and the external standard, are used to calculate the exiting concentration or conversion of a particular gas in flowing stream. When the conversion is large and changes the total flowrate significantly, the internal standard method is used; otherwise, the external standard method is good enough to be used. The *internal standard method* calculates the flowrate of each component in the exit gas stream. It assumes that the flowrate of the inert gas will not change after passing through the reactor. Since the reacting gas is consumed significantly, the relative concentrations of the inert gas and of the reacting gas in the exit stream will change and so will the corresponding peak areas, even the peak for the inert gas. In this study, the inert gas is N₂. Based on the flowrates and peak areas for the components in the feed gas, a factor known as the Effective Factor for the reacting component, say, H₂S, is calculated in terms of the following equation,

$$Eff(H_2S) = \frac{Fl(H_2S)_{feed} * A(N_2)_{feed}}{Fl(N_2)_{feed} * A(H_2S)_{feed}} \quad (A-2)$$

The flowrate of this reacting gas in the exit stream is calculated from this equation,

$$Fl(H_2S)_{exit} = Eff(H_2S) \frac{Fl(N_2) * A(H_2S)}{A(N_2)} \quad (A-3)$$

The *external standard method* calculates the concentrations of components in a gas stream. It assumes that the concentration of the inert gas does not change significantly due to the consumption of reacting components. The concentration of each component can be determined from the calibration curve and corresponds to its flowrate.

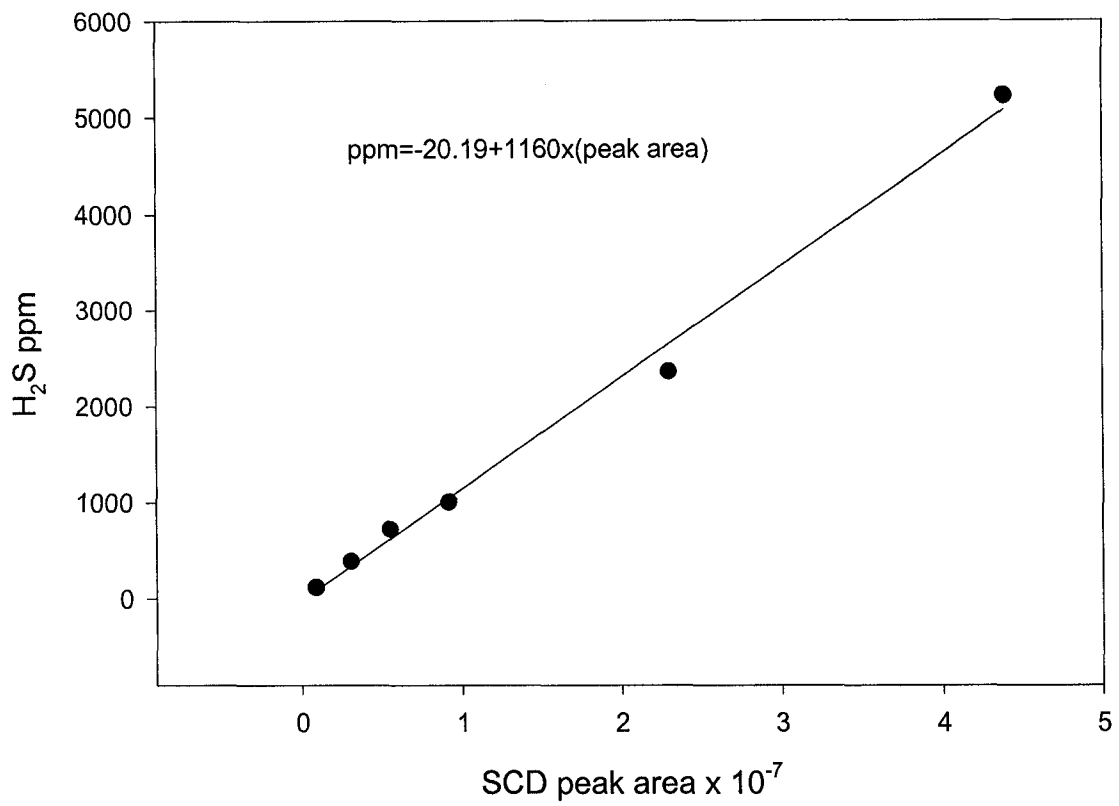


Figure A-4. SCD calibration for H₂S. Calibration date: April 20, 2001.

A.3 Verification of Thermocouples

Type K thermocouples are used in this study. After the thermocouples were purchased, the electrical technicians in the department verify them to check the error of their readings from the real temperatures of a thermo-bath. It was found the errors for all the thermocouple fell within 1°C in the range of temperature this study used.

Appendix B

Tables for Kinetics Data

B.1 Example of Rate Calculation for Reaction (4-1)

Take the runs for 96 wt% sulfuric acid and 21.5°C as an example. The plot of the pressure drop against time was plotted in the figures such as Figure 4-2. The pressure drop rate was obtained from the regression over the initial linear section of the plot, denoted as R_p . The values of R_p at different initial H₂S pressures are shown in Table A-1. They are -0.0110 kPa s⁻¹ at 13.1 kPa of H₂S pressure; -0.0171 kPa s⁻¹ at 25.5 kPa; -0.0282 kPa s⁻¹ at 37.2 kPa; -0.0391 kPa s⁻¹ at 49.6 kPa; and -0.0475 kPa s⁻¹ at 62.0 kPa, respectively. Substituting these numbers into Equation (4-5), respectively, and dividing the rate by interface area, a , the reaction rate per unit interface area is calculated, *i.e.*,

$$RPA = -\frac{dN_{H_2S}}{dt} \frac{1}{a} = \frac{V}{\delta a RT} \frac{dP_T}{dt} = \frac{V}{\delta a RT} R_p \quad (\text{A-4})$$

where, V is the volume of gas phase in m³; δ is 1 for reaction (4-1) at the initial time; R is 8.314×10⁻³ kPa m³ K⁻¹ mol⁻¹; and T is the absolute temperature in K. Corresponding to the above H₂S pressure levels, the reaction rates are 0.920×10⁻³, 1.43×10⁻³, 2.36×10⁻³, 3.27×10⁻³, and 3.97×10⁻³ mol s⁻¹m⁻², respectively. Correlating these reaction rates with H₂S pressures, as shown in Figure 4-5, indicated a linear relationship between them, meaning that the reaction is first order with respect to H₂S. The correlation also evaluated k_{p1} , the overall rate constant, which was the slope of the line.

Table A-1. Data for the rate of reaction 1 (88 wt% acid).

Run #	Acid conc. wt%	$V_L \times 10^3$ m^3	$V_G \times 10^3$ m^3	Solution		Gas temp. K	$a \times 10^3$ m^2	P_{H_2S} kPa	R_P kPa s ⁻¹	$RPA \times 10^3$ mol s ⁻¹ m ⁻²
				temp. K	temp. K					
pd_88_t4	87.68	0.200	0.588	311.35	293.15	4.42	48.25	-0.0112	0.611	
pd_88_t4	87.68	0.200	0.588	311.35	293.15	4.42	68.79	-0.0162	0.884	
pd_88_t4	87.68	0.200	0.588	311.35	293.15	4.42	78.58	-0.0178	0.972	
pd_88_t4	87.68	0.200	0.588	311.35	293.15	4.42	82.36	-0.0192	1.05	
pd_88_t6	87.68	0.200	0.588	324.05	293.15	4.42	47.56	-0.0142	0.775	
pd_88_t6	87.68	0.200	0.588	324.05	293.15	4.42	61.35	-0.0174	0.950	
pd_88_t6	87.68	0.200	0.588	324.05	293.15	4.42	64.2	-0.0184	1.00	
pd_88_t6	87.68	0.200	0.588	324.05	293.15	4.42	81.67	-0.0228	1.24	
pd_88_t5a	87.68	0.200	0.588	330.45	293.15	4.42	47.56	-0.0204	1.03	
pd_88_t5a	87.68	0.200	0.588	330.45	293.15	4.42	61.35	-0.0189	1.11	
pd_88_t5a	87.68	0.200	0.588	330.45	293.15	4.42	77.2	-0.0261	1.42	
pd_88_t5a	87.68	0.200	0.588	330.45	293.15	4.42	95.12	-0.0333	1.82	
pd_88_t5b	87.68	0.200	0.588	335.15	293.15	4.42	46.87	-0.018	0.982	
pd_88_t5b	87.68	0.200	0.588	335.15	293.15	4.42	62.73	-0.0233	1.27	
pd_88_t5b	87.68	0.200	0.588	335.15	293.15	4.42	77.89	-0.0285	1.56	
pd_88_t5b	87.68	0.200	0.588	335.15	293.15	4.42	93.74	-0.0349	1.90	

Table A-1. Continued (90 wt% acid).

Run #	Acid conc. wt%	Solution				Gas temp. K	$a \times 10^3$ m^2	P_{H_2S} kPa	R_p kPa s ⁻¹	$RPA \times 10^3$ mol s ⁻¹ m ⁻²
		$V_L \times 10^3$ m^3	$V_G \times 10^3$ m^3	temp. K	temp. K					
pd_90_t1	90.13	0.200	0.588	302.75	294.15	4.42	46.87	-0.0103	0.560	
pd_90_t1	90.13	0.200	0.588	302.75	294.15	4.42	64.79	-0.0135	0.734	
pd_90_t1	90.13	0.200	0.588	302.75	294.15	4.42	78.58	-0.0173	0.941	
pd_90_t1	90.13	0.200	0.588	302.75	294.15	4.42	90.27	-0.0224	1.22	
pd_90_t2	90.13	0.200	0.588	313.35	294.15	4.42	43.43	-0.0138	0.751	
pd_90_t2	90.13	0.200	0.588	313.35	294.15	4.42	55.83	-0.0168	0.914	
pd_90_t2	90.13	0.200	0.588	313.35	294.15	4.42	71.69	-0.0212	1.15	
pd_90_t2	90.13	0.200	0.588	313.35	294.15	4.42	86.16	-0.0263	1.43	
pd_90_t2	90.13	0.200	0.588	313.35	294.15	4.42	100.64	-0.0314	1.71	
pd_90_t3	90.13	0.200	0.588	321.65	294.15	4.42	40.67	-0.0146	0.794	
pd_90_t3	90.13	0.200	0.588	321.65	294.15	4.42	55.83	-0.0204	1.11	
pd_90_t3	90.13	0.200	0.588	321.65	294.15	4.42	71.69	-0.0261	1.42	
pd_90_t3	90.13	0.200	0.588	321.65	294.15	4.42	86.85	-0.0323	1.76	
pd_90_t3	90.13	0.200	0.588	321.65	294.15	4.42	98.57	-0.0377	2.05	
pd_90_t5	90.13	0.200	0.588	333.21	294.15	4.42	41.36	-0.0198	1.08	
pd_90_t5	90.13	0.200	0.588	333.21	294.15	4.42	56.52	-0.0274	1.49	
pd_90_t5	90.13	0.200	0.588	333.21	294.15	4.42	73.06	-0.0357	1.94	
pd_90_t5	90.13	0.200	0.588	333.21	294.15	4.42	88.23	-0.0471	2.56	

Table A-1. Continued (91.5 wt% acid).

Run #	Acid conc. wt%	$V_L \times 10^3$ m^3	$V_G \times 10^3$ m^3	Solution		Gas temp. K	$a \times 10^3$ m^2	P_{H_2S} kPa	R_P kPa s ⁻¹	$RPA \times 10^3$ mol s ⁻¹ m ⁻²
				temp. K						
pd_91_t1	91.53	0.200	0.588	297.65	293.15	4.42	34.46	-0.0137	0.748	
pd_91_t1	91.53	0.200	0.588	297.65	293.15	4.42	45.49	-0.0199	1.09	
pd_91_t1	91.53	0.200	0.588	297.65	293.15	4.42	62.04	-0.0268	1.46	
pd_91_t1	91.53	0.200	0.588	297.65	293.15	4.42	90.99	-0.0381	2.08	
pd_91_t2	91.53	0.200	0.588	305.15	293.15	4.42	34.46	-0.0147	0.802	
pd_91_t2	91.53	0.200	0.588	305.15	293.15	4.42	46.18	-0.0212	1.16	
pd_91_t2	91.53	0.200	0.588	305.15	293.15	4.42	60.66	-0.0269	1.47	
pd_91_t2	91.53	0.200	0.588	305.15	293.15	4.42	74.44	-0.0339	1.85	
pd_91_t2	91.53	0.200	0.588	305.15	293.15	4.42	91.68	-0.0421	2.30	
pd_91_t3	91.53	0.200	0.588	313.15	294.15	4.42	32.4	-0.0199	1.08	
pd_91_t3	91.53	0.200	0.588	313.15	294.15	4.42	45.49	-0.0251	1.37	

Table A-1. Continued (91.5 wt% acid).

Run #	Acid conc. wt%	$V_L \times 10^3$ m^3	$V_G \times 10^3$ m^3	Solution		Gas temp. K	$a \times 10^3$ m^2	P_{H_2S} kPa	R_P $kPa\ s^{-1}$	$RPA \times 10^3$ $mol\ s^{-1}\ m^{-2}$
				temp. K	temp. K					
pd_91_t3	91.53	0.200	0.588	313.15	294.15	4.42	61.35	-0.038	2.07	
pd_91_t3	91.53	0.200	0.588	313.15	294.15	4.42	75.82	-0.0463	2.52	
pd_91_t3	91.53	0.200	0.588	313.15	294.15	4.42	90.99	-0.0613	3.33	
pd_91_t4	91.53	0.200	0.588	322.75	294.15	4.42	35.15	-0.0271	1.47	
pd_91_t4	91.53	0.200	0.588	322.75	294.15	4.42	46.18	-0.0357	1.94	
pd_91_t4	91.53	0.200	0.588	322.75	294.15	4.42	61.35	-0.0487	2.65	
pd_91_t4	91.53	0.200	0.588	322.75	294.15	4.42	75.82	-0.0617	3.36	
pd_91_t4	91.53	0.200	0.588	322.75	294.15	4.42	90.3	-0.0756	4.11	
pd_91_t5	91.53	0.200	0.588	331.05	294.15	4.42	37.91	-0.0391	2.13	
pd_91_t5	91.53	0.200	0.588	331.05	294.15	4.42	46.87	-0.0521	2.83	
pd_91_t5	91.53	0.200	0.588	331.05	294.15	4.42	62.73	-0.071	3.86	
pd_91_t5	91.53	0.200	0.588	331.05	294.15	4.42	78.58	-0.0873	4.75	
pd_91_t5	91.53	0.200	0.588	331.05	294.15	4.42	93.05	-0.101	5.49	

Table A-1. Continued (93 wt% acid).

Run #	Acid conc. wt%	$V_L \times 10^3$ m^3	$V_G \times 10^3$ m^3	Solution		Gas temp. K	$a \times 10^3$ m^2	P_{H_2S} kPa	R_P $kPa\ s^{-1}$	$RPA \times 10^3$ $mol\ s^{-1}\ m^{-2}$
				temp. K	temp. K					
pd_93_t1	92.97	0.200	0.588	294.65	294.15	294.15	4.42	33.76	-0.0184	1.00
pd_93_t1	92.97	0.200	0.588	294.65	294.15	294.15	4.42	49.63	-0.0251	1.37
pd_93_t1	92.97	0.200	0.588	294.65	294.15	294.15	4.42	61.35	-0.0322	1.75
pd_93_t1	92.97	0.200	0.588	294.65	294.15	294.15	4.42	75.82	-0.0378	2.06
pd_93_t2	92.97	0.200	0.588	301.95	294.15	294.15	4.42	20.68	-0.0159	0.86
pd_93_t2	92.97	0.200	0.588	301.95	294.15	294.15	4.42	31.37	-0.0205	1.12
pd_93_t2	92.97	0.200	0.588	301.95	294.15	294.15	4.42	45.92	-0.0273	1.49
pd_93_t2	92.97	0.200	0.588	301.95	294.15	294.15	4.42	59.97	-0.0342	1.86
pd_93_t2	92.97	0.200	0.588	301.95	294.15	294.15	4.42	75.13	-0.0429	2.33
pd_93_t3	92.97	0.200	0.588	312.95	294.15	294.15	4.42	21.37	-0.0232	1.26
pd_93_t3	92.97	0.200	0.588	312.95	294.15	294.15	4.42	31.71	-0.033	1.80
pd_93_t3	92.97	0.200	0.588	312.95	294.15	294.15	4.42	47.56	-0.0465	2.53

Table A-1. Continued (93 wt% acid).

Run #	Acid conc. wt%	$V_L \times 10^3$ m^3	$V_G \times 10^3$ m^3	Solution		Gas temp. K	$a \times 10^3$ m^2	P_{H_2S} kPa	R_p $kPa\ s^{-1}$	$RPA \times 10^3$ $mol\ s^{-1}m^{-2}$
				temp. K						
pd_93_t3	92.97	0.200	0.588	312.95	294.15	4.42	62.04	-0.0596	3.24	
pd_93_t3	92.97	0.200	0.588	312.95	294.15	4.42	75.82	-0.0667	3.63	
pd_93_t4	92.97	0.200	0.588	321.25	294.15	4.42	20.68	-0.0249	1.35	
pd_93_t4	92.97	0.200	0.588	321.25	294.15	4.42	31.02	-0.036	1.96	
pd_93_t4	92.97	0.200	0.588	321.25	294.15	4.42	45.49	-0.0531	2.89	
pd_93_t4	92.97	0.200	0.588	321.25	294.15	4.42	62.04	-0.075	4.08	
pd_93_t4	92.97	0.200	0.588	321.25	294.15	4.42	75.82	-0.0886	4.82	
pd_93_t6	92.97	0.200	0.588	331.35	293.15	4.42	19.99	-0.0357	1.95	
pd_93_t6	92.97	0.200	0.588	331.35	293.15	4.42	31.71	-0.052	2.84	
pd_93_t6	92.97	0.200	0.588	331.35	293.15	4.42	46.18	-0.0746	4.07	
pd_93_t6	92.97	0.200	0.588	331.35	293.15	4.42	60.65	-0.0987	5.03	
pd_93_t6	92.97	0.200	0.588	331.35	293.15	4.42	75.13	-0.122	6.66	

Table A-1. Continued (96 wt% acid).

Run #	Acid conc. wt%	$V_L \times 10^3$ m^3	$V_G \times 10^3$ m^3	Solution		Gas temp. K	$\alpha \times 10^3$ m^2	P_{H_2S} kPa	R_P kPa s ⁻¹	$RPA \times 10^3$ mol s ⁻¹ m ⁻²
				temp. K	temp. K					
pd_96_t1	96.04	0.200	0.910	294.65	296.15	296.15	4.42	13.1	-0.0110	0.920
pd_96_t1	96.04	0.200	0.910	294.65	296.15	296.15	4.42	25.5	-0.0171	1.43
pd_96_t1	96.04	0.200	0.910	294.65	296.15	296.15	4.42	37.22	-0.0282	2.36
pd_96_t1	96.04	0.200	0.910	294.65	296.15	296.15	4.42	49.63	-0.0391	3.27
pd_96_t1	96.04	0.200	0.910	294.65	296.15	296.15	4.42	62.04	-0.0475	3.97
pd_96_t2	96.04	0.200	0.910	302.15	296.15	296.15	4.42	13.1	-0.0183	1.53
pd_96_t2	96.04	0.200	0.910	302.15	296.15	296.15	4.42	25.5	-0.0288	2.41
pd_96_t2	96.04	0.200	0.910	302.15	296.15	296.15	4.42	37.91	-0.0387	3.24
pd_96_t2	96.04	0.200	0.910	302.15	296.15	296.15	4.42	50.32	-0.0504	4.21
pd_96_t2	96.04	0.200	0.910	302.15	296.15	296.15	4.42	64.1	-0.0696	5.82

Table A-1. Continued (96 wt% acid).

Run #	Acid conc. wt%	$V_L \times 10^3$ m^3	$V_G \times 10^3$ m^3	Solution		Gas temp. K	$a \times 10^3$ m^2	P_{H_2S} kPa	R_P $kPa s^{-1}$	$RPA \times 10^3$ $mol s^{-1} m^{-2}$
				temp. K						
pd_96_t3	96.04	0.200	0.910	310.15	296.15	4.42	13.1	-0.0226	1.89	
pd_96_t3	96.04	0.200	0.910	310.15	296.15	4.42	25.5	-0.0388	3.24	
pd_96_t3	96.04	0.200	0.910	310.15	296.15	4.42	37.71	-0.0555	4.64	
pd_96_t3	96.04	0.200	0.910	310.15	296.15	4.42	50.31	-0.0685	5.73	
pd_96_t3	96.04	0.200	0.910	310.15	296.15	4.42	63.41	-0.0849	7.10	
pd_96_t4	96.04	0.200	0.910	326.75	296.15	4.42	11.72	-0.0406	3.39	
pd_96_t4	96.04	0.200	0.910	326.75	296.15	4.42	11.72	-0.0394	3.29	
pd_96_t4	96.04	0.200	0.910	326.75	296.15	4.42	24.81	-0.0741	6.20	
pd_96_t4	96.04	0.200	0.910	326.75	296.15	4.42	37.91	-0.102	8.53	
pd_96_t4	96.04	0.200	0.910	326.75	296.15	4.42	50.31	-0.132	11.0	
pd_96_t4	96.04	0.200	0.910	326.75	296.15	4.42	63.41	-0.149	12.5	

Table A-1. Continued (100 wt% acid).

Run #	Acid conc. wt%	$V_L \times 10^3$ m ³	$V_G \times 10^3$ m ³	Solution			P_{H_2S} kPa	R_P kPa s ⁻¹	$RPA \times 10^3$ mol s ⁻¹ m ⁻²
				temp. K	Gas temp. K	$a \times 10^3$ m ²			
pd_99_t1	99.97	1.00E-04	1.01E-03	294.45	294.15	4.42E-03	19.3	-0.0361	3.37
pd_99_t1	99.97	1.00E-04	1.01E-03	294.45	294.15	4.42E-03	28.26	-0.0583	5.45
pd_99_t1	99.97	1.00E-04	1.01E-03	294.45	294.15	4.42E-03	42.05	-0.0817	7.63
pd_99_t2	99.97	1.00E-04	1.01E-03	298.55	294.15	4.42E-03	15.85	-0.0442	4.13
pd_99_t2	99.97	1.00E-04	1.01E-03	298.55	294.15	4.42E-03	28.95	-0.0756	7.06
pd_99_t2	99.97	1.00E-04	1.01E-03	298.55	294.15	4.42E-03	42.05	-0.102	9.53
pd_99_t3	99.97	1.00E-04	1.01E-03	303.35	294.15	4.42E-03	15.85	-0.0594	5.55
pd_99_t3	99.97	1.00E-04	1.01E-03	303.35	294.15	4.42E-03	28.95	-0.0969	9.05
pd_99_t3	99.97	1.00E-04	1.01E-03	303.35	294.15	4.42E-03	43.43	-0.143	13.4
pd_99_t4	99.97	1.00E-04	1.01E-03	308.65	294.15	4.42E-03	16.54	-0.0823	7.69
pd_99_t4	99.97	1.00E-04	1.01E-03	308.65	294.15	4.42E-03	28.26	-0.126	11.8
pd_99_t4	99.97	1.00E-04	1.01E-03	308.65	294.15	4.42E-03	42.05	-0.193	18.0

Table A-2. Data for the rate of reaction 2.

Run #	Acid conc.		Solution							
	C_a wt%	$V_L \times 10^4$ m^3	$V_G \times 10^4$ m^3	temp., T K	Gas temp. K	$a \times 10^3$ m^2	P_{H_2S} kPa	$[SO_2]$ mol L ⁻¹	R_P kPa s ⁻¹	$k'_{P2} \times 10^7$ L s ⁻¹ m ⁻² Pa ⁻¹
pd_t1	30.26	2.00	5.88	298.15	294.15	4.42E-03	99.9	0.532	-0.645	4.40
pd_t6	30.26	2.00	5.88	301.15	297.15	4.42E-03	86.9	0.532	-0.73	5.67
pd_t7	30.26	2.00	5.88	301.15	297.15	4.42E-03	86.9	0.552	-0.754	5.64
pd_t2	30.26	2.00	5.88	303.15	294.15	4.42E-03	88.2	0.502	-1.13	9.26
pd_t3	30.26	2.00	5.88	308.15	309.82	4.42E-03	84.8	0.463	-1.13	9.91
pd_t11	30.26	2.00	5.88	313.15	310.59	4.42E-03	89.6	0.394	-1.47	14.3
pd_t12	30.26	2.00	5.88	318.28	308.22	4.42E-03	94.4	0.315	-1.93	22.5
pd_t13	30.26	2.00	5.88	318.28	314.76	4.42E-03	88.2	0.345	-1.95	21.7
pd_t14	30.26	2.00	5.88	323.42	314.42	4.42E-03	90.3	0.276	-2.61	35.5
pd_t15	30.26	2.00	5.88	323.42	314.49	4.42E-03	83.4	0.315	-2.71	35.0

Table A-2. (Continued).

Run #	Acid conc.		Solution					R_p kPa s ⁻¹	$k'_{p2} \times 10^7$ L s ⁻¹ m ⁻² Pa ⁻¹	
	C_a wt%	$V_L \times 10^4$ m ³	$V_G \times 10^4$ m ³	temp., T K	Gas temp. K	$a \times 10^3$ m ²	P_{H_2S} kPa			[SO ₂] mol L ⁻¹
pd_40_a1	40.9	2.00	5.88	294.65	296.15	4.42E-03	51.7	0.477	-0.279	4.08
pd_40_a2	40.9	2.00	5.88	296.25	296.15	4.42E-03	41.4	0.703	-0.366	4.53
pd_40_a3	40.9	2.00	5.88	298.55	296.15	4.42E-03	53.1	0.438	-0.345	5.34
pd_40_a5	40.9	2.00	5.88	304.45	296.15	4.42E-03	49.6	0.407	-0.483	8.62
pd_50_a1	51.17	2.00	5.88	297.25	296.15	4.42E-03	49.6	0.463	-0.285	4.53
pd_50_a2	51.17	2.00	5.88	299.15	296.15	4.42E-03	48.3	0.440	-0.345	5.78
pd_50_a3	51.17	2.00	5.88	301.75	296.15	4.42E-03	51.0	0.409	-0.483	8.94
pd_50_a4	51.17	2.00	5.88	304.15	295.15	4.42E-03	52.4	0.400	-0.689	12.9
pd_40_a5	51.17	2.00	5.88	306.85	296.15	4.42E-03	49.6	0.338	-0.689	15.4

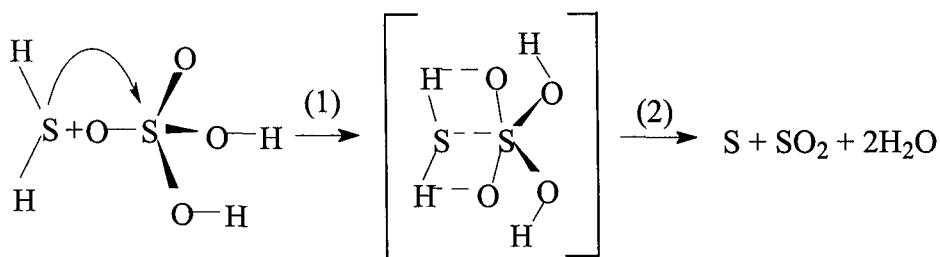
Table A-2. (Continued).

Run #	Acid conc.		Solution		Gas temp. K	a×10 ³ m ²	P _{H₂S} kPa	[SO ₂] mol L ⁻¹	R _P kPa s ⁻¹	k' _{P2} ×10 ⁷ L s ⁻¹ m ⁻² Pa ⁻¹
	C _a wt%	V _L ×10 ⁴ m ³	V _G ×10 ⁴ m ³	temp., T K						
pd_60_a1	59.78	2.00	5.88	295.95	296.15	4.42E-03	51.7	0.438	-0.286	4.55
pd_60_a2	59.78	2.00	5.88	298.75	296.15	4.42E-03	53.1	0.372	-0.345	6.29
pd_60_a3	59.78	2.00	5.88	301.95	296.15	4.42E-03	49.6	0.397	-0.345	6.31
pd_60_a4	51.17	2.00	5.88	304.85	296.15	4.42E-03	53.8	0.322	-0.433	9.00

Appendix C

More Discussion on Reaction (4-1)*

Thermodynamic analysis in Chapter 3 and discussions in Chapter 4 indicate that molecular H_2SO_4 may be the active species present in sulfuric acid solutions which reacts with hydrogen sulfide. When hydrogen sulfide is oxidized, its sulfur atoms increase their oxidation number by transferring their electrons to the molecules of the oxidizing agent (Weil and Randler, 1997). When the gas, H_2S , contacts the concentrated sulfuric acid, it attacks the H_2SO_4 molecule and forms an active intermediate, through which the electrons are transferred and the products, sulfur, sulfur dioxide and water, are formed. Such an interaction is illustrated by the consecutive route (A-5),



(A-5)

Durant (1970) pointed out that, for the molecule H_2S , the distance, H-S, is 1.34 Å and the angle of HSH is 92.2°; and for H_2SO_4 , the length of the π d bonds between O and S is 1.40 Å and the angle between the two π d bonds is 124°. The values of these structure

* Because it does not fully agree with the rate equation obtained in Chapter 4, the discussion on reaction mechanism of reaction (4-1) is presented in Appendix, as suggested by the examining committee.

parameters also support the view that the attack in step (1) in Equation (A-5) is reasonable and stereo-favorable. After an effective collision, an intermediate forms, through whose deformation the electrons are transferred directly from the sulfur atom in H_2S to the sulfur atom in H_2SO_4 and as a result, the products are formed. It should be emphasized that Equation (A-5) is not a mechanism illustration of elementary processes but of a possible interaction route between H_2S and H_2SO_4 molecules. However, it agrees the observation that the reaction is first order with respect to hydrogen sulfide if step (1) is the rate-controlling step.

Literature Cited

Durrant, P. J., and B. Durrant, *Introduction to Advanced Inorganic Chemistry*, 2nd Ed.

John Wiley & Sons, New York, pp842-843, pp853-854 (1970).

Weil, E. D., and S. R. Randler, "Sulfur Compounds", *Kirk-Othmer Encyclopedia of*

Chem. Eng. 4th Ed. John Wiley & Sons (Web version, 1997).

Appendix D

Arrays of Stoichiometric Coefficients of Reactions and Its Reduction

The arrays respectively constituting of the stoichiometric coefficients of the reactions in Table 3-1 and the reactions on page 52 are shown as follows:

Table A-3. Stoichiometric coefficient array of reactions in Table 3-1.

	(3-7)	(3-8)	(3-9)	(3-10)	(3-11)	(3-12)	(3-13)	(3-14)	(3-15)	(3-16)	(3-17)	(3-18)	(3-19)	(3-20)
H ₂ S(g)	-1	-1	-1	-3	-3	-3	-1	-1	-1	0	0	0	0	-2
H ₂ SO ₄ (l)	-1	0	0	-1	0	0	-3	0	0	-2	0	0	0	0
HSO ₄ ⁻ (a)	0	-1	0	0	-1	0	0	-3	0	0	-2	0	0	0
H ⁺ (a)	0	-1	-2	0	-1	-2	0	-3	-6	0	-2	-4	0	0
SO ₄ ²⁻ (a)	0	0	-1	0	0	-1	0	0	-3	0	0	-2	0	0
S	1	1	1	4	4	4	0	0	0	-1	-1	-1	0	3
H ₂ O(l)	2	2	2	4	4	4	4	4	4	2	2	2	0	2
SO ₂ (g)	1	1	1	0	0	0	4	4	4	3	3	3	-1	0
SO ₂ (a)	0	0	0	0	0	0	0	0	0	0	0	0	1	-1

Table A-4. Stoichiometric coefficient array of reactions on page 52.

	(3-7)	(3-8)	(3-9)	(3-16)	(3-17)	(3-18)	(3-19)	(3-20)
H ₂ S(g)	-1	-1	-1	0	0	0	0	-2
H ₂ SO ₄ (l)	-1	0	0	-2	0	0	0	0
HSO ₄ ⁻ (a)	0	-1	0	0	-2	0	0	0
H ⁺ (a)	0	-1	-2	0	-2	-4	0	0
SO ₄ ²⁻ (a)	0	0	-1	0	0	-2	0	0
S	1	1	1	-1	-1	-1	0	3
H ₂ O(l)	2	2	2	2	2	2	0	2
SO ₂ (g)	1	1	1	3	3	3	-1	0
SO ₂ (a)	0	0	0	0	0	0	1	-1

The four elementary operations upon which the array reduction procedure is based are:

1. Multiplying one of the columns of the array by an arbitrary constant.
2. Interchanging rows of the array.
3. Interchanging columns of the array.
4. Adding a multiple of one column to another column.

These operations render the two arrays the final resulting arrays constituting of the same nonzero vectors, as shown below.

Table A-5. Reduced stoichiometric coefficient array.

H ₂ S(g)	1	0	0	0	0
H ₂ SO ₄ (l)	1	1	0	0	0
HSO ₄ ⁻ (a)	0	-1	1	0	0
H ⁺ (a)	0	-1	-1	4	0
SO ₄ ²⁻ (a)	0	0	-1	2	0
S	-1	0	0	1	0
H ₂ O(l)	-2	0	0	-2	0
SO ₂ (g)	-1	0	0	-3	1
SO ₂ (a)	0	0	0	0	-1